Responses to Reviewer 1

We would like to thank the Reviewer for his/her report which helped us to improve our manuscript.

"*The paper is generally well written. However, taking into account the review of the 1st reviewer, with whom I fully agree, the authors still fail to convince that they have used the MODIS AE-FF data, only over the sea. This is very important to implement.*"

"*Specific comments: The issue of using the MODIS AE-FF data, only over the sea, is not clearly presented in the current version of the manuscript. In the annotated text, this is well noted and the authors should consider it very carefully.*"

We would like to clarify that, as shown in the presented geographical distributions (Figs 2, 3, 9 and 10 in the revised manuscript), in the present analysis the algorithm operates over both land and ocean, making use of the corresponding MODIS retrievals including the Ångström Exponent and Fine Fraction (plus the effective radius product over ocean). Moreover, this is outlined in the algorithm's flowchart, Fig. 1.

"*Technical Comments: In the annotated text several technical corrections have been given. The authors should implement them in their manuscript.*"

We have taken into account all the Reviewer's technical comments annotated in the original manuscript and made the necessary modifications in the revised manuscript.

Responses to Reviewer 2

We would like to thank the Reviewer for his/her comments (in italics) to which responses are provided below.

The main concern of the Reviewer is the absence of clear evidences for the diversification of the present paper and algorithm by those of Gkikas et al. (2009, 2013). Therefore, an effort was made: (i) first to further diversify the existing paper from the previous ones and (ii) to make clearer in the manuscript and to the reader the already existing differences in the original manuscript.

"*The paper is clearly written and previous works on the paper's subject have been accounted for. However, I believe that main paper results have already been reported in Gkikas et al., 2013, as one can observe by comparing the summary of the submitted manuscript with the one of Gkikas et al., 2013. Therefore the paper is not suitable for publication in ACP. Indeed, an updated version of the algorithm introduced in Gkikas et al. (2009, 2013) for the identification of strong and extreme desert dust episodes, over the period March 2000–February 2013, was applied in the submitted manuscript.*"

We acknowledge that there some similarities between the present geographical distributions of desert dust (DD) episodes' frequency and intensity, in sub-section 4.1, and the corresponding ones in the work by Gkikas et al. (2013). However, it should be noted that despite the apparent similarity, there are differences, and more specifically:

(i) In the present study, the satellite-based algorithm is applied over a more extended time period (almost double). We believe that this is important because it confirms the dust episodes regime across the entire Mediterranean basin. Even if this may seem trivial, it is not so, since the work by Gkikas et al. (2013) has been the first, yet the single one to date, which appropriately described this regime, at a complete spatial coverage. Therefore, basically it was not guaranteed that the regime could not change over the time, which is proven by the obtained results in the present paper.

(ii) In the present revised manuscript, apart from the methodology presented by Gkikas et al. (2013), we have also applied another one. This methodology, referring to the identification of dust outbreaks, has been proposed by the Reviewer 4, and the obtained results with the two methodologies are compared to each other. This intercomparison is presented in the revised manuscript and constitutes another novelty.

(iii) In addition, a few other points make the difference between this and our previous works. Thus:

  (a) the evaluation of the satellite-based algorithm is largely improved in terms of robustness by: (1) considering much more, actually all the currently existing AERONET stations within the study region, and (2) using more aerosol optical properties.

  (b) issues related to the MODIS Level 3 AOD sub-grid spatial representativeness and homogeneity, affecting the agreement between MODIS-AERONET AODs, are accounted for and addressed in the present study (Figure 5).

  (c) the comparison of the satellite algorithm's outputs against ground PM_{10} data is more detailed here (e.g. success scores, dust contribution, mean and median levels are reported) than in Gkikas et al. (2013).

  We would like to clarify that the main objective in the work by Gkikas et al. (2013) was the description of the intense Mediterranean desert dust episodes' regime. More specifically,

their main characteristics, namely their frequency of occurrence, intensity and duration, were presented therein at different temporal and spatial scales. On the contrary, the main objective here is the description of the dust outbreaks' vertical structure. This is achieved through the implementation of the CALIOP-CALIPSO lidar profiles.

For all these reasons, we believe that the present revised paper is a significant improvement and extension of that by Gkikas et al. (2013).

"*Moreover, for the identified DD episodes, collocated CALIOP-CALIPSO vertical feature mask and total backscatter coefficient retrievals have also been considered in the submitted manuscript, to describe the annual and seasonal variability of dust outbreaks' vertical extension over the Mediterranean. However, CALIOP-CALIPSO data have not been well exploited. Consequently, the results reported in the manuscript have not added any new scientific result with respect to the ones reported in the many references cited in the manuscript. To my opinion, CALIOP-CALIPSO data could have been used, for example, to understand the weak correlation AOD-PM. Note that quite often dust particles remain confined above the PBL and consequently do not affect the PM at the ground level.*"

Please, note that in the revised version of the manuscript we have added a new section (Section 4.4 and Figures 11, 12, 13) in which the issue raised by the Reviewer is addressed. In this new section, we identified specific desert dust outbreaks of various geometrical characteristics for which our algorithm's outputs, ground PM_{10} concentrations and CALIOP-CALIPSO lidar profiles are all together available concurrently. The objective of this new analysis is to investigate how the dust outbreaks' vertical distribution, i.e. their height and vertical extension, can affect the level of agreement between columnar AOD retrievals (MODIS) and ground PM_{10} concentrations (this was actually suggested by the reviewer, in last paragraph of page C9471 of his Review). There are four such studied dust outbreaks that took place in Censt (southern Sardinia, 26th May 2008), Els Torms (NE Spain, 16th July 2008), San Pablo (central Spain, 12th September 2007) and Agia Marina (Cyprus, 25th February 2007). We believe that describing such dust outbreaks' vertical structure, through the simultaneous implementation of both active and passive satellite retrievals, as done in our analysis, provides essential information, similar to that acquired by ground lidar stations. Nevertheless, the satellite-based approach adopted in our study has the great advantage of extended spatial coverage in contrast to the local-scale ground-based lidar profiles. Even so, such ground-based lidar aerosol profiles are not common, and in the Mediterranean basin come from the EARLINET network which encompasses only a few stations, all of them north of 40^{o} N. Therefore, there is an entire information gap for the southern parts of the Mediterranean basin, i.e. near to the major dust sources, of course not to mention the similar gap in northern areas as well. This gap can only be fulfilled by reliable satellite observations, in the way done in the present analysis (Figures 9 and 10 of the revised manuscript).

Responses to Reviewer 3

We would like to thank the Reviewer for his/her comments which helped us to improve our manuscript. We have modified the text according to the suggestions made and provide below responses to the comments.

General comments

"*This paper aims to provide a description of the vertical structure of the intense Mediterranean dust outbreaks. It is clearly written, the overall presentation is well structured and clear, and the paper addresses scientific questions fully within the scope of ACP/AMT special issue on ChArMEx. Generally the analysis is interesting but it appears that the use of CALIOP-CALIPSO data set to describe the vertical distribution of dust events, with an extended spatial coverage over the Mediterranean area, is the main new contribution of the paper.*
As extensive research has been carried out on Mediterranean dust outbreaks, based on ground-based (AERONET) and satellite observations, the paper should be more focused on what is really new in the data set and associated analysis. For example the analysis presented in Section 4.1. (2-D geographical distributions of desert dust episodes frequency and intensity) is not fully novel as nearly all the conclusions have been already reached in Gkikas et al. (2013). Even if the period of study is extended and the identification of desert dust method slightly improved (use of both MODIS-terra and Aqua, QA-weighted level-3 data, threshold on cloud fraction), the modifications are relatively minor. The main novel aspect of the paper is the analysis of vertical structure of the intense desert dust episodes with CALIOP, so I suggest to emphasize this part of the paper. In the present paper only two figures are related to this aspect."

We agree with the Reviewer that the vertical structure of Mediterranean desert dust (DD) episodes is the main new contribution of the present paper, with respect to the paper by Gkikas et al. (2013), which first introduced the satellite-based identification algorithm. In this context, we also agree with the Reviewer's suggestion to further emphasize this part of the analysis, since the obtained results in Section 4.1 (2-D geographical distributions of desert dust episodes' frequency and intensity) do not reveal remarkable differences compared to the corresponding ones presented by Gkikas et al. (2013). Therefore, also in line with the indications made by Reviewers 2 and 4, we made an effort to strengthen the part of the paper dealing with the vertical structure of DD episodes, while trying to get the manuscript more balanced with respect to the partition of its analysis to the: (i) geographical distribution of DD episodes' features, (ii) evaluation of the satellite algorithm and (iii) description of episodes' vertical structure.
We would just like to note that devoting a considerable part of our analysis to the above mentioned tasks (i) and (ii) was made intentionally for the following reasons:

(a) the satellite-based algorithm is applied in the present study over a more extended time period (almost double) than in Gkikas et al. (2013). We believe that this is important because it confirms the dust episodes regime across the entire Mediterranean basin. Even if this may seem trivial, it is not so, since the work by Gkikas et al. (2013) has been the first, yet the single one to date, which appropriately described this regime, at a complete spatial coverage. Therefore, basically it was not guaranteed that the regime could not change over the time, which is proven by the obtained results in the present paper.

(b) the evaluation of the satellite-based algorithm is largely improved in terms of robustness by: (1) considering much more, actually all the currently existing AERONET stations within the study region, and (2) using more aerosol optical properties.
(c) issues related to the MODIS Level 3 AOD sub-grid spatial representativeness and homogeneity, affecting the agreement between MODIS-AERONET AODs, are accounted for and addressed in the present study (Figure 5).
(d) the comparison of the satellite algorithm's outputs against ground PM_{10} data is more detailed here (e.g. success scores, dust contribution, mean and median levels are reported) than in Gkikas et al. (2013).

Moreover, apart from the previous reasons there is one more, which is the same or even more important. It is that in the present revised manuscript, also based on a relevant comment of Reviewer 4, we applied a second methodology (METHOD-B) for the identification of DD episodes in our algorithm, which does not exist in Gkikas et al. (2013). According to the new methodology, the defined thresholds in the algorithm for the various aerosol optical properties are calculated from the non-dust affected Level 3 retrievals. The results of this methodology and those of the default one are compared and discussed in the revised manuscript, which constitutes a novelty in this paper.
Following, however, the Reviewer's comment, in the revised manuscript more emphasis is given to analyzing the Mediterranean desert dust outbreaks' vertical structure. More specifically, we have identified desert dust outbreaks of different geometrical characteristics for which the satellite algorithm's outputs, PM_{10} concentrations and CALIOP-CALIPSO lidar profiles are all together available concurrently. The obtained results are discussed in the new section 4.4 introduced in the revised manuscript. The scope of this analysis, triggered by the poor-to-moderate agreement between the algorithm outputs and PM_{10} concentrations in the western Mediterranean, is to give a better insight on how dust outbreaks' vertical distribution can affect the level of agreement between columnar AOD retrievals (MODIS) and ground PM_{10} concentrations. This analysis was made by implementing both vertically resolved data retrieved by the CALIOP-CALIPSO, in conjunction with ground PM_{10} measurements (representative for the lowest part of the planetary boundary layer) and MODIS AOD retrievals (representative for the whole atmospheric column).
Finally, another new point in the revised manuscript, giving more emphasis to the vertical structure of Mediterranean dust outbreaks, is that we have reproduced the three dimensional plots of Figure 9, displaying dust outbreaks 3D characteristics (both for dust records and total backscatter coefficient values), but considering all the available CALIOP-CALIPSO dust lidar profiles. The results, presented in Fig S6 of supplementary material, help to investigate the modifications of vertical distribution of CALIOP retrievals under intense desert dust outbreaks. The main findings are discussed in the revised manuscript (lines: 855-882).

"*It is surprising that section 4.2, which is centered on the evaluation of the satellite algorithm (combining MODIS and TOMS/OMI) against AERONET and PM10 measurements represents the longest part of the paper. The analysis and results are interesting but they seem quite disconnected to the main topic and objective of the paper, i.e. vertical structure of intense dust outbreaks, as stated in the abstract. In other words, a lot of effort (and figures) is put in certifying the ability of the satellite algorithm to identify desert dust episodes although it is not clearly announced as a main objective of the paper.*"

We agree with the Reviewer that in the original manuscript, a quite significant part of the manuscript was dedicated to the comparison of the satellite algorithm's outputs against AERONET and PM_{10} data. This was made just for the reasons explained in our previous reply. However, in order to reduce the length of this part of the manuscript we have made some major modifications. More specifically, Figure 6 of the original manuscript was moved to the supplementary material (Figure S3 now) and just a short reference to this figure is made in the main body of the revised text (Lines: 556-563). Also, Figures 8 and 9 (in sect. 4.2 of original manuscript) were moved to the supplementary material (Figs. S4 and S5) while the sections *"Ångström exponent and effective radius"* and *"Single scattering albedo and asymmetry parameter"* of the original manuscript are now merged to a shorter single section entitled *"Size optical properties, single scattering albedo and asymmetry parameter"*. Nevertheless, we would like to point out that some results related to the performance of the satellite algorithm are kept in the revised paper because in our opinion they are critical and have been not presented in Gkikas et al. (2013). For example, the results of Figure 5 deal with the issue of level 3 AOD sub-grid spatial variability, which is essential when attempting comparisons of MODIS satellite against local surface-based AOD data like AERONET ones. Also, the results of Figure 7 (revised manuscript), highlight the validity of the defined thresholds for α, *AI*, *FF* and r_{eff} (green boxes in the flowchart) used in the satellite algorithm for the desert dust aerosols' identification, which is essential since there are not any specific objective and commonly accepted thresholds in literature. Yet, in Figure 8 of revised manuscript, are given the success scores, referring to the performance of the satellite algorithm, the dust contribution as well as the mean and median levels of PM_{10} concentrations, under dust episodes conditions.

"*In order to clearly reflect the contents of the paper, the title should indicate that analysis focus on intense desert dust outbreaks. I suggest: "Mediterranean intense desert dust outbreaks and their vertical structure based on remote sensing data".*"

We agree with the Reviewer's comment and the title has been modified according to his/her suggestion.

"*My recommendation is to publish this paper after some appropriate changes: (i) taking into account the fact that too much conclusions are identical to Gkikas et al. ACP 2013 in sections 4.1 and 4.2 (despite the slight modifications regarding methods, time period, and sensors) and (ii) reinforcing analysis on its main objective and scientific interest, i.e. analysis of CALIOP vertical distributions of intense desert dust events in section 4.3.*"

Done, see our responses to previous comments.

Specific comments

"*1. P 27682, lines 21-22: "The main target of the present study is to describe the Mediterranean desert dust outbreaks' vertical structure over the period from March 2000 to February 2013." This sentence should be reformulated since the analysis of CALIOP retrievals presented in section 4.3. cover the period 2006-2013.*"

Done.

"*2. In section 2.1.2 EP/TOMS and OMI-AURA, the period considered for each satellite data as well as their respective spatial resolution should be provided.*"

Done (Lines: 247-250).

"*3. Figure 1 of the paper has already been published in Gkikas et al., ACP 2013 (figure 2).*"

We prefer to keep Figure 1 in the present manuscript just to avoid making readers to go back and consult the paper by Gkikas et al. (2013).

"*4. Figure 7: it is not necessary to provide results for both MODIS-Terra and Aqua, as they are very similar.*"

We agree and removed Figure 7-ii in the revised manuscript.

"*5. Results presented in Table 2 and page 27701 lines 20-24 are not clearly described.*"

We have modified the relevant part of the manuscript in order to describe more clearly the corresponding results. Please, see lines 647-653.

Responses to Reviewer 4

We would like to thank the Reviewer for his/her detailed review which helped us to essentially improve our manuscript. Point by point responses to the Reviewer's comments (in Italics) are provided below.

"*This manuscript by Gkikas et al. aims at describing the horizontal and vertical distribution of desert dust during 'intense events'. The methods followed to reach this aim include the use of satellite data from passive and active sensors. The work is largely an extension of a previous paper by Gkikas et al. (2013), and this makes it a bit lacking in originality. The manuscript could provide potentially interesting information. However, in its present form it shows some major weaknesses that substantially compromise the validity of the results reached. These weaknesses, as well as some additional comments, are detailed below. For what follows, I cannot recommend the paper for publication until these major weaknesses are properly addressed. I also recommend review of the language as the text is often confusing and difficult to follow.*"

We acknowledge that the present manuscript it is an extension and thus has some similarities with our previous work by Gkikas et al. (2013). Therefore, we can understand the worries of the Referee about its originality. Being aware of this, we had tried to highlight in the original manuscript the differences and steps forward made in the present with respect to our previous work. Nevertheless, obviously this was not achieved entirely, and hence, before presenting our point-by-point responses, we would like to emphasize the differences between the present analysis and Gkikas et al. (2013).

The main objective of the work by Gkikas et al. (2013) was the detailed description of the spatial and temporal variability of Mediterranean desert dust (DD) episodes. The primary focus in the present analysis is to study the vertical structure of the DD episodes, as stated in the title, at an extended spatial and temporal coverage, as not done before. However, we would like to note that in order to attempt this, one should ensure the quality of the utilized tool and derived DD episodes. It should be reminded that the episodes are identified with a satellite-based algorithm, thus having limitations and being constrained by the input satellite retrieved products. Such limitations were revealed in Gkikas et al. (2013) where a rather preliminary evaluation of the algorithm was made. For this reason, in the present study we emphasize the evaluation of the satellite algorithm through extensive and detailed comparisons against surface-based measurements from AERONET and PM_{10} stations. This is why a considerable part of the manuscript is devoted to this aim. On the other hand, the very short extent of section 4.1, dealing with the spatio-temporal regime of DD episodes, i.e. the main goal in Gkikas et al. (2013), shows the low priority given to this in the present paper.

Of course, one may consider that even this relatively short reference to the episodes' regime could be avoided here, as it was given in Gkikas et al. (2013). Nevertheless, we have chosen to include it for two reasons: (i) the temporal coverage of the episodes regime in Gkikas et al. (2013) was relatively short, namely from 2000 to 2007. Note that it was the first time that the Mediterranean DD episodes regime has been described at a complete spatial coverage in Gkikas et al. (2013) whereas no other study to date has done something similar. It is not given in any way that this regime remains unchanged with time, therefore it is valuable to re-assess it over longer time periods, and this is made in the present study where the period is almost double (2000-2013). (ii) obtaining the regime over the longer period, 2000-2013, is necessary in this study also in order to overlap with the period to which the examined vertical structure of episodes refers to. Note that the anyhow scarce available vertically resolved information is taken from CALIOP-CALIPSO, which is not available for years before 2006.

Finally, we would like to note that apart from what it has been reported above, we acknowledge that the part of the analysis dealing with the vertical structure of the DD episodes could, indeed, be a bit strengthened. In this view, an effort was made to further extend the relevant analysis in the revised manuscript, which is now enriched by the detailed study of specific dust outbreaks in the Mediterranean, also giving insight to the level of agreement between the algorithm outputs and surface-based measurements.

Major weaknesses of the work:

1) Methodological Problems.

"*Although the study follows a methodology almost identical to the one already published in Gkikas et al. (2013), in my view this methodology builds on assumptions that should AT LEAST be further commented and 'tested' to make the reader understand how reliable the derived results are. In particular a key point of the work is the identification of 'intense dust events' ant their separation into 'strong dust episodes' and 'extreme dust episodes' by the so-defined 'objective and dynamic satellite algorithm'. This selection is basically fully dependent on the AOD threshold chosen, defined as 'AOD Mean' in the text. Unfortunately I could not find any definition of this 'AOD Mean' in the text other that 'the mean (Mean) and the associated standard deviation (SD) are calculated for the whole study period' (page 27688, lines 18-20).*"

1.1) What does this 'Mean' mean?

"You use over 10 years of AOD data, so: are you getting a 1x1-resolved 'AOD Mean' by simply averaging the 1x1-resolved AOD time series corresponding to each pixel? (This is what I understood reading Gikaks et al. (2013), but this is not clarified in this manuscript)."

Yes, the mean AOD value is calculated for each grid cell over the whole study period, namely by averaging all the available daily AOD retrievals. In the revised manuscript we have modified the relevant text (lines 333-335) while in the caption of Figure 1 we have clarified that the methodology is applied to 1° x 1° grid each grid cell.

"What's the total number of AOD data points you have in each pixel? Are all years within the record equally represented? Are all seasons (or even months) in each year equally represented? You should show this is the case, otherwise the 'Mean' AOD value you get might be meaningless. In fact, given the inter-annual variability of AOD, and, above all, given its marked seasonal variability, an unequal data coverage of the different years/seasons could lead to a 'biased' Mean AOD. More explicitly: if, for example, the number of data points in winter is 50-60% of those in summer (this is likely due to enhanced cloud cover in winter) you derive a summer-biased 'Mean' AOD which alters all the subsequent analysis. Therefore, please provide a clear indication of the number of data points you are including in your statistics (for example with maps in an Appendix), and of their inter- and intra-annual distribution. If the monthly-resolved data coverage is not uniform (as I suspect), and if you still prefer to perform the whole analysis using a single, pixel-resolved 'AOD Mean' threshold value, then you should rather obtain it as an average of monthly-mean AODs. A map of the derived AOD Mean values would also be of help to better interpret the final results.

Although we see the point raised by the Referee, we would like to note that in our opinion, an unequal distribution of available AOD data to the various months and seasons is not a problem in our methodology. We think that the AOD thresholds should be simply determined/computed from the entire dataset, since any climatic, health or other effect of aerosols is not dependent on season or month. Nevertheless, in order to dispel concerns of the Referee about this issue, we have investigated the AOD data's availability, in terms of percentages, at different temporal scales, namely monthly, seasonal, and yearly, and we have reproduced the corresponding geographical distributions. For brevity reasons, the analysis is made only for the period March 2000 – February 2013 using the MODIS-Terra AOD data. The results are presented and discussed below.

MONTHS

According to our results (Figure R1) the temporal dependence of AOD availability, i.e. its month by month variation, is dependent on the area of interest, if we except the desert areas of North Africa and Middle East, where retrievals of AOD are restricted by highly reflecting surfaces (note that Dark Target MODIS products are

used in the present analysis). Apart from these areas, it is apparent a reduced data availability in winter months, especially in the northern continental parts of the study region, e.g. Balkans. The reduced availability of AOD in winter, compared to other months, can really affect the representativeness (in temporal terms) of the calculated AOD mean value for the whole study period, as stated by the Reviewer. Even if, as stated before, this should not be a problem, we further like to note that its consequences for our analysis are minimized by the fact that due to the prevailing atmospheric circulation and the higher precipitation amounts (wet deposition) in this season, the probability for a desert dust outbreak to reach the areas with low AOD availability is rather small. In the revised manuscript (lines 350 - 360) we addressed the specific issue of month to month variation of AOD data availability raised by the Referee by adding a short paragraph.

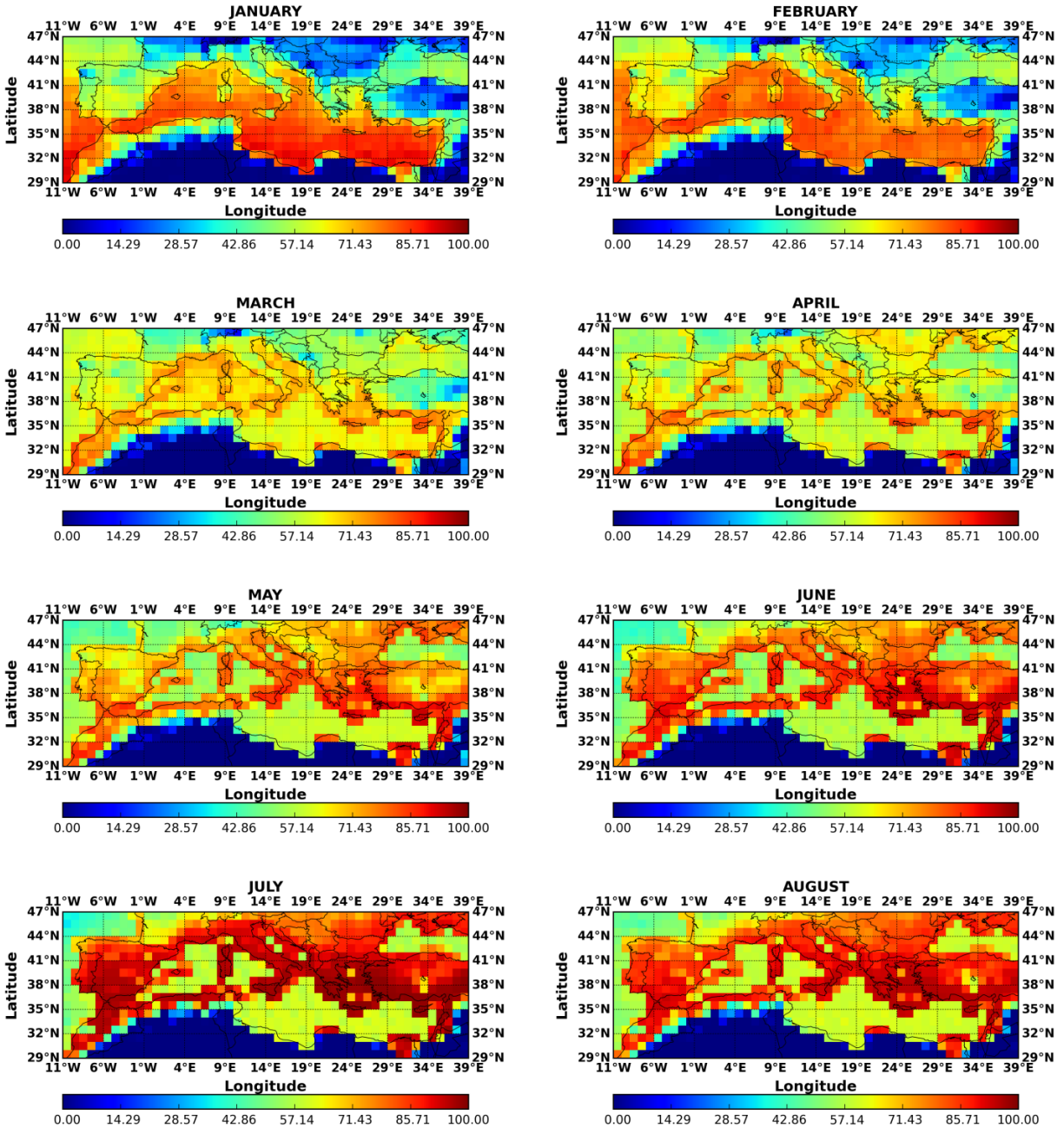

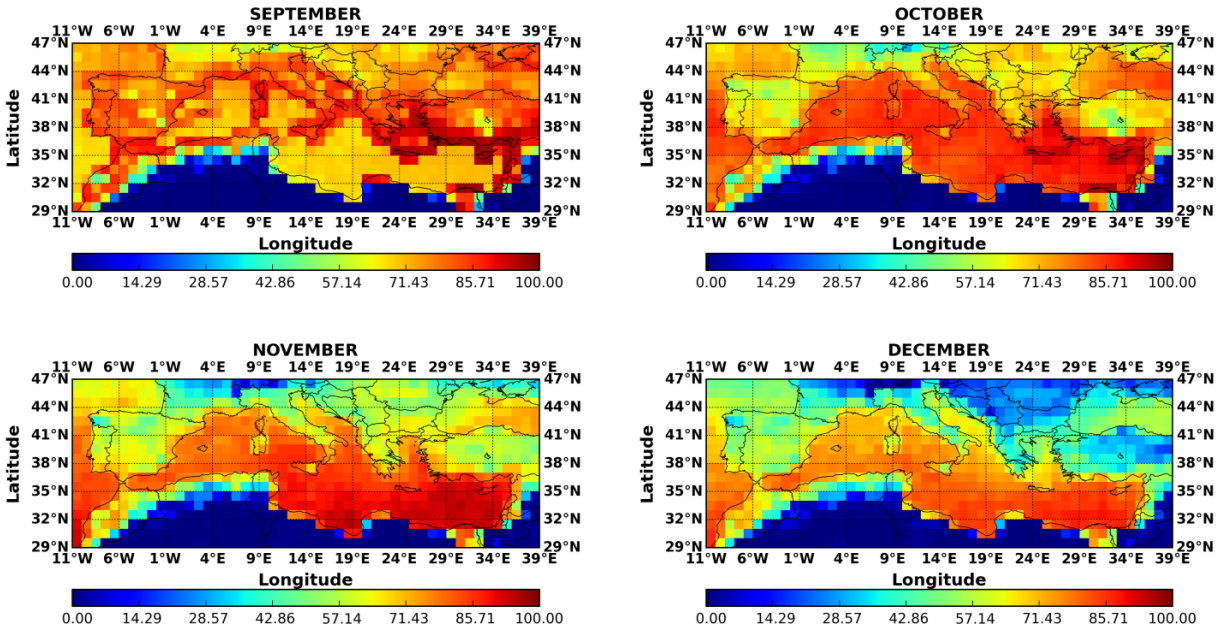

Figure R1: Monthly geographical distributions of the MODIS-Terra AOD_{550nm} retrievals availability (expressed in percentages), over the broader Mediterranean basin, for the period Mar. 2000 - Feb. 2013.

SEASONS

The geographical distributions of AOD data availability have been also reproduced on a seasonal basis, i.e. for winter, spring, summer and autumn, over the period 2000-2013. The results of Fig. R2 summarize those in Fig. R1 (monthly basis), namely that if we except the North Africa and Middle East deserts, where a low AOD availability is observed throughout the year, unequal seasonal low AOD availability is observed in the northernmost parts of the study region (e.g. Balkans), with numbers ranging from < 30% in winter to more than 80% in summer. For a discussion of possible consequences of this the Reviewer is referred to the discussion of monthly statistics above.

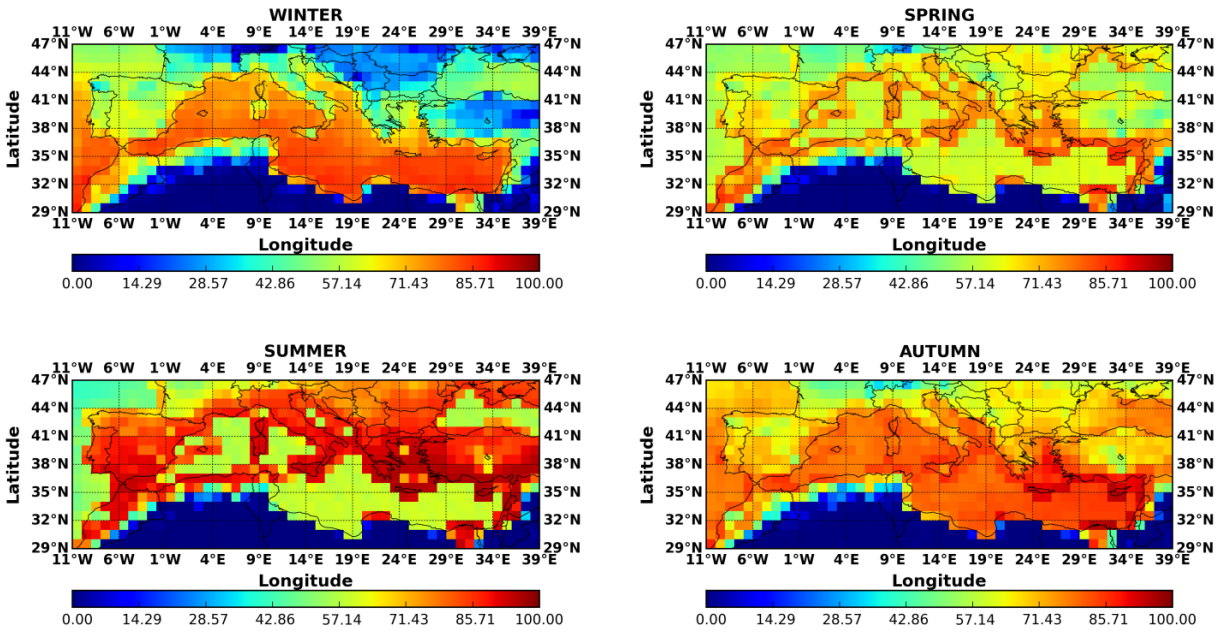

Figure R2: Seasonal geographical distributions of the MODIS-Terra AOD_{550nm} retrievals availability (expressed in percentages), over the broader Mediterranean basin, for the period Mar. 2000 - Feb. 2013.

ANNUAL

For the whole study period (2000-2013), the lowest percentages (about 40%) are observed across the northern parts of the study region. On the contrary, the highest percentages (75 - 95%) are recorded mainly across the coastlines and closed seas (e.g. Aegean and Adriatica). In all other areas, the AOD availability is satisfactory ranging between 65 and 80%.

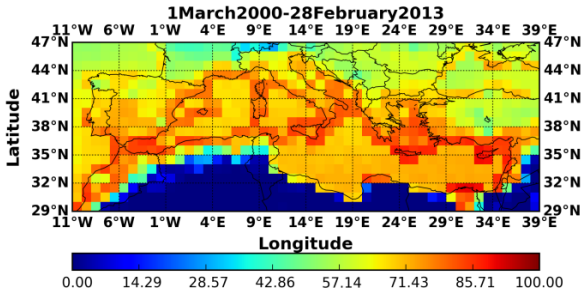

Figure R3: Geographical distribution of the MODIS-Terra AOD_{550nm} retrievals availability (expressed in percentages), over the broader Mediterranean basin, for the period Mar. 2000 - Feb. 2013.

YEAR BY YEAR

Finally, we have reproduced the corresponding geographical distributions of MODIS-Terra AOD retrievals' availability for each year (from March to February of next year) of the study period (2000-2013). It is evident, that the spatial patterns remain constant throughout the years revealing a stable regime in terms of aerosol optical depth data availability.

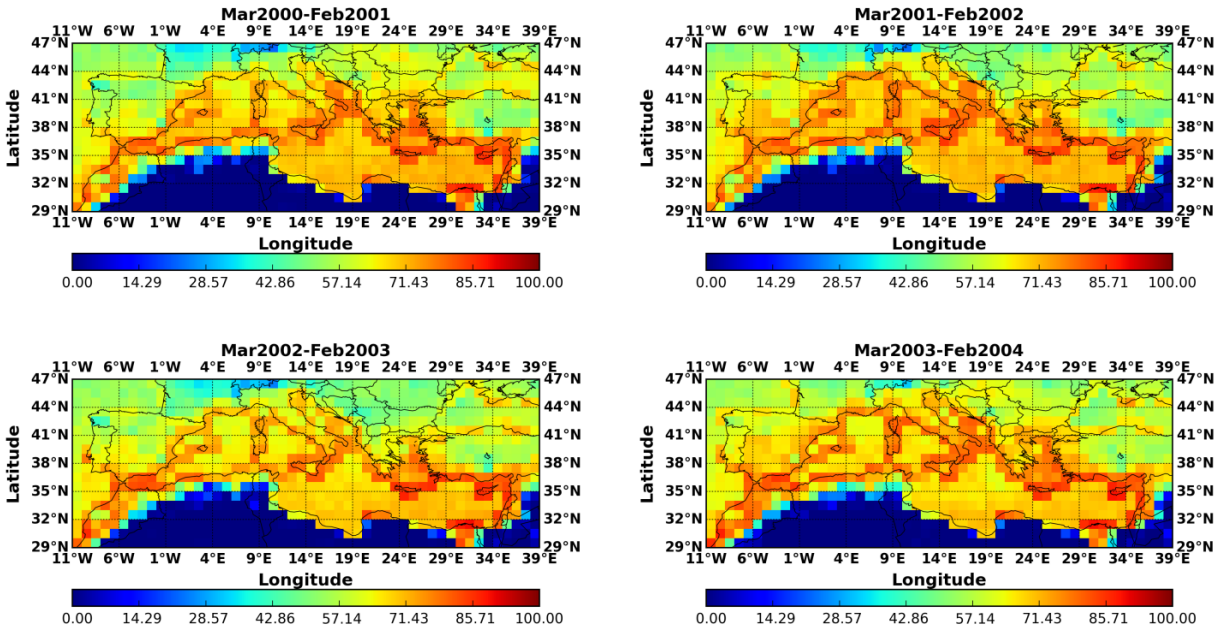

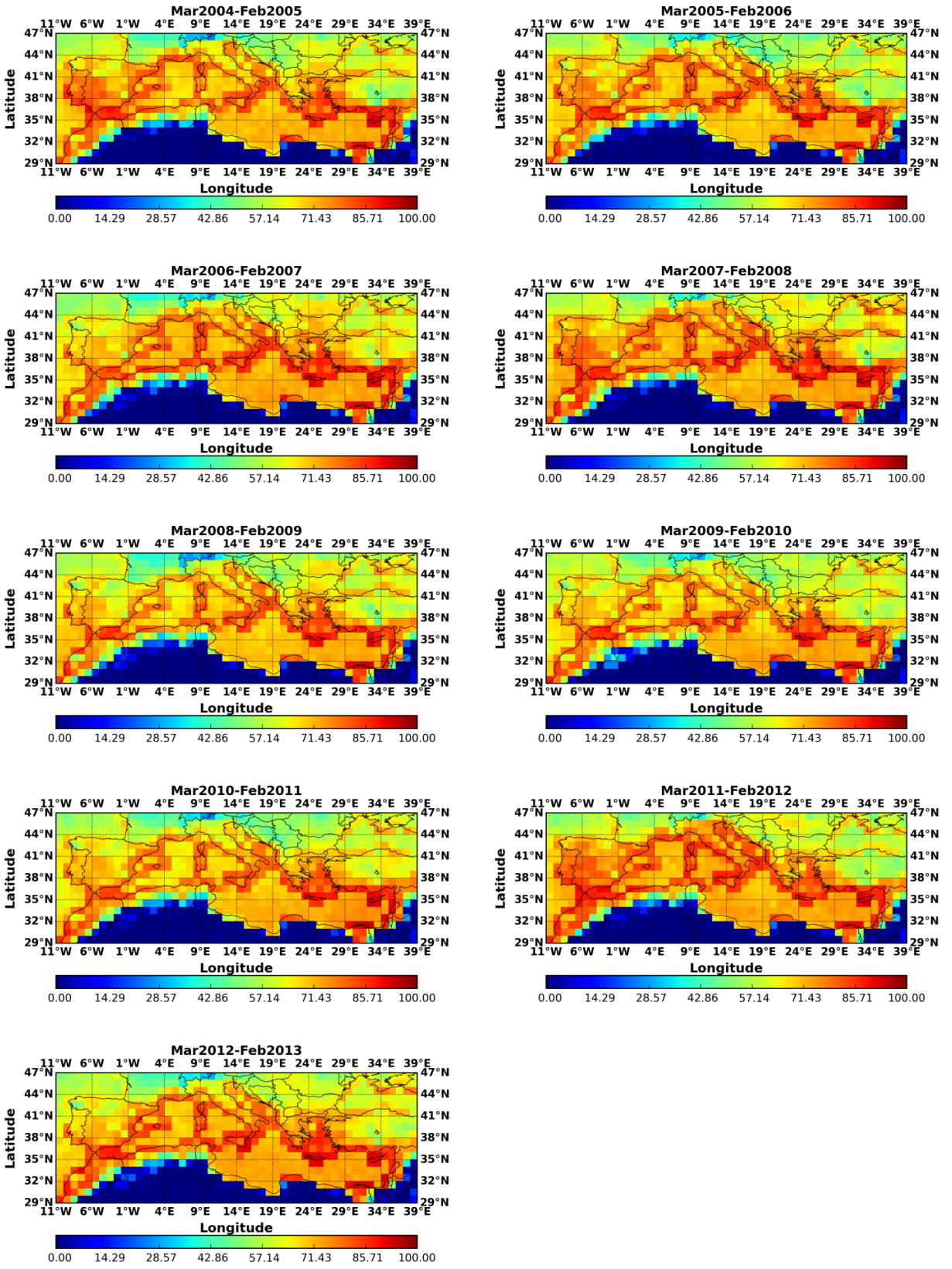

Figure R4: Annual geographical distributions of the MODIS-Terra AOD_{550nm} retrievals availability (expressed in percentages), over the broader Mediterranean basin, for each year of the period Mar. 2000 - Feb. 2013.

As suggested by the Reviewer, we show in Figure R5 the geographical distribution of the long-term averaged MODIS-TERRA (i) and MODIS-AQUA (ii) AOD at 550 nm, over the periods March 2000-February 2013 and 2003-2012, respectively.

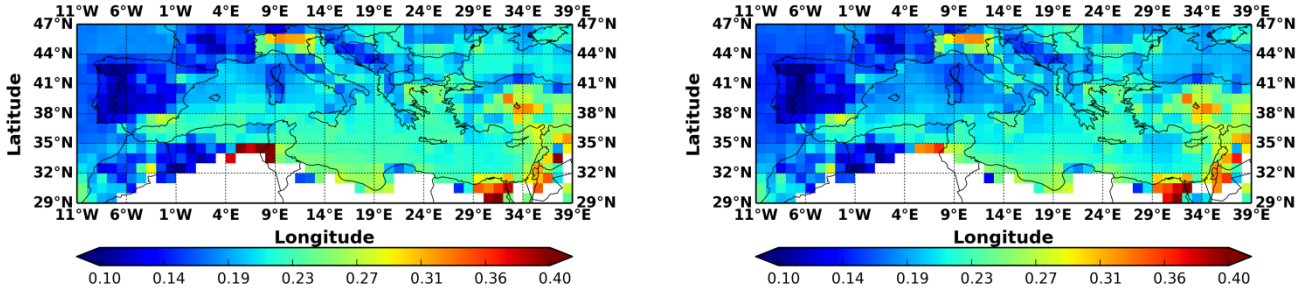

(i) (ii)

Figure R5: Geographical distributions of the long-term averaged AOD at 550, over the broader Mediterranean basin, for the periods: (i) 1 Mar. 2000 - 28 Feb. 2013 (MODIS-Terra) and (ii) 2003 – 2012 (MODIS-Aqua).

1.2) *"I also see another problem in the computation of the 'Mean AOD'. Your algorithm firstly performs selection of the 'strong dust episodes' and of 'extreme dust episodes' based on the 'Mean AOD' threshold and AFTERWARDS uses the AI and FF information to exclude possible 'not-dust' cases. However, this means that if, by paradox, all the days of the time series are 'dust-affected', and assuming for simplicity a normal distribution of those AOD values around their mean, following your approach only a very limited fraction of them would be classified as 'strong' dust (the 2.2%) or 'extreme dust' (the 0.003%) (this is because in a normal distribution the 2.2% and the 0.003% of data exceed respectively the 'Mean + 2 s. d.' and 'Mean + 4 s. d.' thresholds you fixed). This is to say that, in my view, dust events should be firstly filtered out of the record to compute a sort of 'dust-free' mean AOD; otherwise, again, you get a biased 'Mean AOD' to which to compare the 'dust-affected' record. The way to do this could be based on a combined analysis including the other parameters you consider in your analysis (Angstrom, AI and FF). Obviously, this problem mostly affects those regions with higher dust-events frequency. Can you comment on that?"*

In order to answer to the Reviewer's comment we have applied our algorithm according to his/her suggestion followed a new methodology, so-called METHOD-B. According to this, from the raw AOD retrievals we have excluded the 'pure' DD cases, defined based on the defined thresholds for Ångström exponent, Fine Fraction, Aerosol Index and Effective radius (available only over sea). From the remaining non-DD AOD retrievals we have calculated the mean and the associated standard deviation values for the whole study period as well as the defined thresholds, in each grid cell.

The obtained results for the frequency of occurrence and the intensity of strong and extreme DD episodes, over the period 2000-2013, based on METHOD-B, are depicted in Figure R6. The spatial patterns, both for strong and extreme DD episodes, are quite similar with those displayed in Figures 2 i-a and 2 ii-a of the manuscript. The main difference, between the two methods, is that the frequencies are higher, both for strong

(up to 13.3 episodes year^{-1}) and extreme (up to 8.1 episodes year^{-1}) DD episodes, when the algorithm operates based on METHOD-B. This is expected since omitting dust-affected cases in the computation of long-term mean AOD values results in lower AOD mean and thresholds. As it concerns the intensity, the AOD levels for the strong and extreme DD episodes are lower than the corresponding levels computed in our primary methodology (Figures 3 i-a and 3 ii-a). This is again expected, because the determined DD episodes with METHOD-B include cases with smaller AODs, which can result in loss of a "clear signal" of DD episodes determined with the new method. Indeed, the consequence of this can be seen in Fig. R6, 2ii-a, for the strong DD episodes, where there are not so distinct geographical patterns as in Fig. 3i-a (original manuscript, basic methodology). On the contrary, for the extreme DD episodes (stronger signal), the differences between the two applied methodologies are less remarkable in terms of spatial variability. Summarizing, when the algorithm operates based on METHOD-B the frequency of occurrence and the intensity of DD episodes increases and decreases, respectively, without revealing remarkable differences, in spatial terms, with regards to the default methodology. Both facts can be explained by the reduction of the defined thresholds. Since there is not a single commonly accepted methodology in literature for the determination of DD episodes, and given that when applying the alternative suggested methodology the results do not change essentially, we prefer to keep the original methodology. However, the obtained results with METHOD-B are now provided in the supplementary material (Figs. S1 and S2) whereas the differences with the default methodology are discussed in the manuscript (lines 472-488).

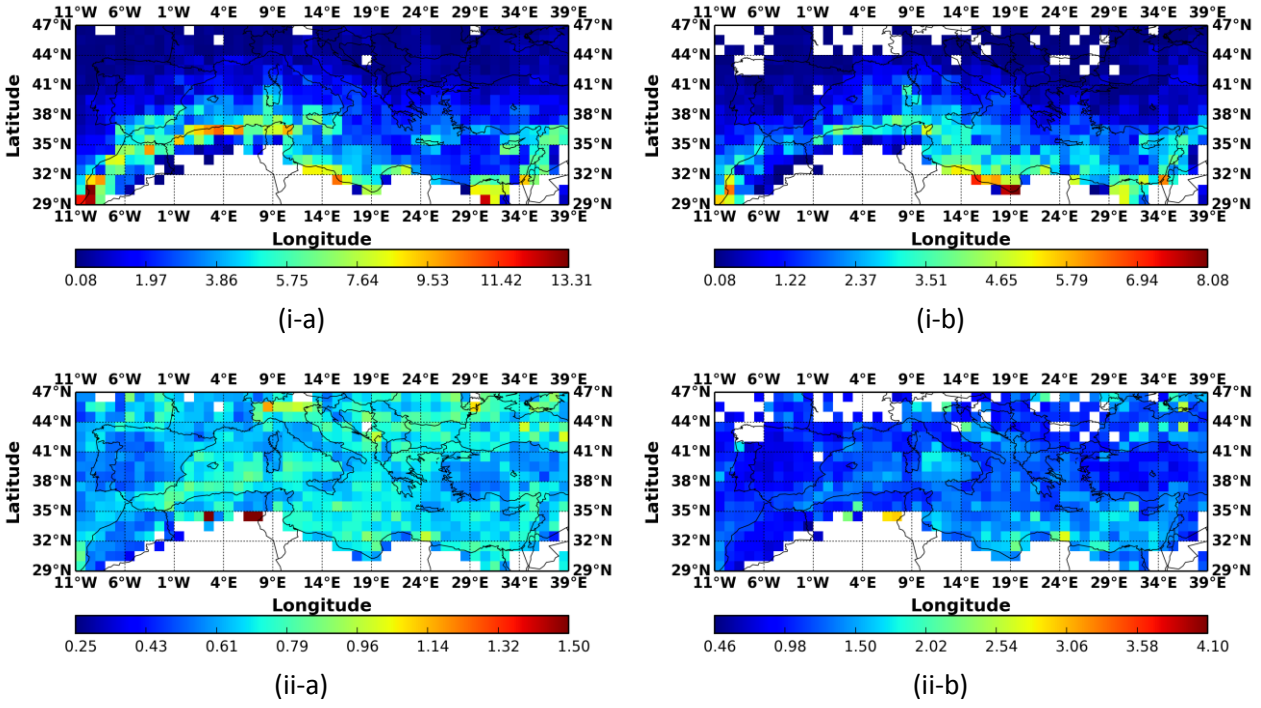

Figure R6: Geographical distributions of the: (i) frequency of occurrence (episodes/year) and (ii) intensity (in terms of AOD_{550nm}) for the: (a) strong and (b) extreme desert dust episodes, for the period Mar. 2000 – Feb. 2013 (MODIS-Terra), over the broader area of the Mediterranean basin. Both episodes' characteristics have been calculated based on METHOD-B.

2) Dataset problems

"2.1) You make several efforts in the text to highlight the differences of this work with respect to the previous one (Gkikas et al., 2013) which, as mentioned above, is very similar to this in terms of methodology and structure. In fact, one of the differences with that paper is the extension in time and the use of the additional similar datasets from Modis-AQUA. So, one of the potentially interesting points of the study

relates to the differences found between the TERRA and the AQUA-based results. Unfortunately, at the present stage, the validity of this comparison is completely jeopardized by the different time-periods used in the manuscript for the two Modis sensors. In those cases in which differences between the two outcomes are found and commented in the text, there is always the ambiguity whether those differences are due to a 'real' aerosol (mostly desert-dust in this case) diurnal variability, or rather to the different time-period covered by the two datasets (note that this point is also connected to my point 1). It is well know that AQUA has a shorter time-coverage with respect to TERRA, but I do not see the reason not to limit the analysis to the period 2003-2012, which is common to both sensors."

In order to answer to the Reviewer's comment, we are presenting here the geographical distributions for the DD episodes' frequency of occurrence (episodes/year) and intensity (in terms of AOD_{550nm}), in Figures R7 and R8, respectively, over the period 2003-2012 based on MODIS-Terra retrievals. It is evident a great similarity, both for frequency and intensity, between the satellite algorithm's outputs when it operates with MODIS-Terra retrievals over the periods 2000-2013 (Figs 2 i-a, 2 ii-a of the revised paper) and 2003-2012 (Figs R7 and R8). This means that the "direct" comparison between MODIS-Terra and MODIS-Aqua, as it is described in the submitted manuscript, can be done even though the study periods are different. We agree with the Reviewer that a more detailed analysis it is required in order to highlight the differences (if any) between the two MODIS sensors, however this is not our primary scientific target in this paper. We have decided to present the results for the period 2000-2013 (MODIS-Terra) and not for 2003-2012 (MODIS-Aqua) for the following reasons:

1. MODIS-Terra provides data for 13 years instead of 10, which are available from MODIS-Aqua. The three extra years allow us to have more coincident measurements between the satellite algorithm's outputs and AERONET retrievals. Please, keep in mind that our algorithm requires satellite retrievals from different sensors (MODIS, OMI, TOMS) to be available concurrently and moreover in many AERONET stations there are gaps in data availability. Both facts can reduce the number of coincident observations and for this reason we prefer to keep the more extended study period (2000-2013) in order to have a larger sample of dust episodes.
2. The PM_{10} measurements are available from 2001 to 2011 (11 years). Through the implementation of MODIS-Terra retrievals (2000-2013), we can have more data (two years, 2001-2002) compared to MODIS-Aqua measurements, which are available since 2003. This means that the common period between MODIS-Terra/PM is 11 years (2001-2011) while between MODIS-Aqua/PM is 9 years (2003-2011).
3. As it concerns the part of the analysis referring to the satellite algorithm's outputs and CALIOP lidar profiles, we have found more coincident data between MODIS-Terra/CALIOP in comparison to MODIS-Aqua/CALIOP. Even though the main findings are similar, in the case of MODIS-Aqua/CALIOP the 3D plots are not so distinct, mainly for the latitudinal projections, as in MODIS-Terra/CALIOP (Figs 9 and 10 in the revised manuscript).

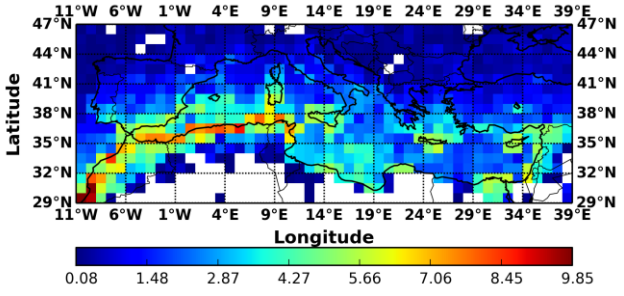

(i)

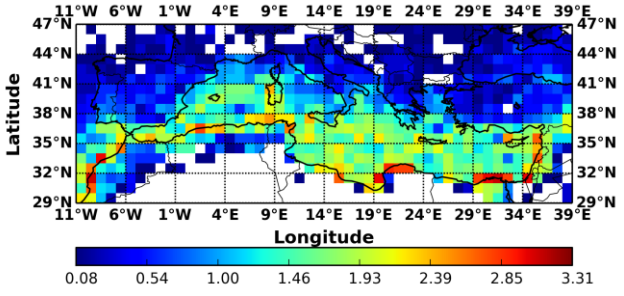

(ii)

Figure R7: Geographical distributions of the frequency of occurrence (episodes/year) of: (i) strong and (ii) extreme desert dust episodes, for the period 2003 – 2012 (MODIS-Terra), over the broader area of the Mediterranean basin.

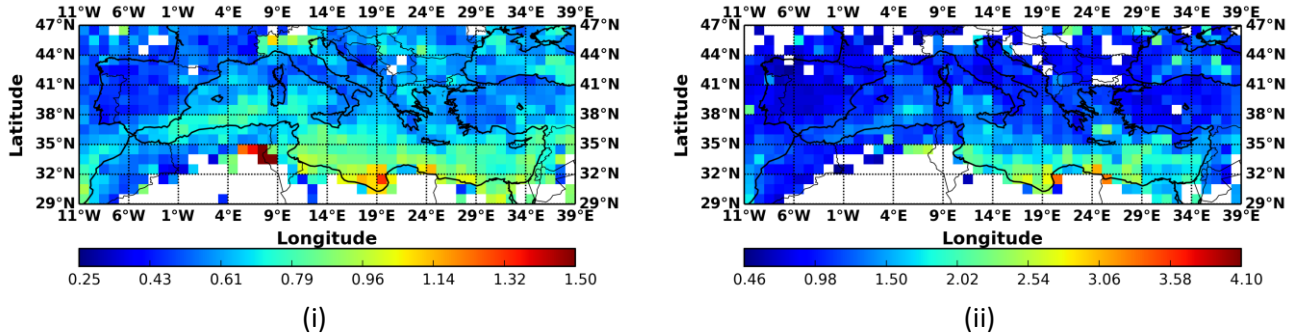

(i) (ii)

Figure R8: Geographical distributions of the intensity (in terms of AOD_{550nm}) of: (i) strong and (ii) extreme desert dust episodes, for the period 2003 – 2012 (MODIS-Terra), over the broader area of the Mediterranean basin.

"*In this respect, in Section 4 (page 27691) you specify that: 'In order to investigate this difference in detail we have also applied the satellite algorithm, over the period 2003–2012, i.e. that of Aqua, using MODIS-Terra retrievals as inputs. Through this analysis (results not shown here), it is evident that there is a very good agreement between the satellite algorithm's outputs, for the periods March 2000–February 2013 and 2003–2012, revealing a constant dust episodes' regime. Therefore, the discrepancy appeared between MODIS-Terra and MODIS-Aqua spatial distributions in Fig. 2, is attributed to the diurnal variation of factors regulating the emission and transport of dust particles from the sources areas.' Apart from the fact that you decide not to show in the text an element that would be fundamental in your analysis, in my view this sentence is by no means sufficient to justify the use of a different time-period coverage of the AQUA and TERRA Modis data in your study. I think the same period for both sensors should be used to strengthen the results reached.*"

We think that our previous answer explains adequately why we have decided to present the results for the extended period (2000-2013). Moreover, the fundamental element and main target of our analysis is to describe the annual and seasonal variation of the Mediterranean dust outbreaks' three dimensional structure and not to discuss in detail the possible inconsistencies between Terra and Aqua retrievals.

"*2.2) In the present form, description of the datasets used and of the way the different variables are matched is lacking. Description of the single datasets does not allow to get all the necessary information to understand their advantages and limits. I found some more details in Gkikas et al. (2013), but it is a bit annoying to always go to that paper to better understand the current one. Please provide more details to your Section 2 (e.g., 1- resolution of the AI from TOMS and OMI is a bit different, can you specify this? How do you match these values with the MODIS derived ones? 2- What's the exact meaning of 'Quality assurance-weighted' data?).*"

The satellite data which we have been used in our analysis have been thoroughly described and presented in numerous studies related to aerosol research in the past. For this reason, we believe that it is better to keep the existing information provided in our text without extending our manuscript with many technical details. Nevertheless, we have added the required information about the spatial resolution of the EP-TOMS and OMI satellite retrievals, which was missing in the submitted paper, and a better explanation of the term "Quality assurance-weighted" is given in the final version of the manuscript. More specifically, the MODIS and OMI satellite retrievals are provided at 1^{o}x1^{o} spatial resolution while the coordinates are provided at the center of each grid cell. EP-TOMS data are provided at 1^{o}x1.25^{o} (lat x lon) spatial resolution and they have been converted in order to match, in terms of spatial resolution and colocation, with the other two databases

(MODIS, OMI). After regridding the EP-TOMS data, all the satellite retrievals have common spatial resolution and geolocation information (coordinates).

MODIS data are available at Levels, apart from Collections, corresponding to different spatial (from meters to degrees) and temporal (from minutes to months) scales. Here, we are using the daily Level 3 data provided at 1^{o}x1^{o} spatial resolution. The MODIS team produces the aforementioned measurements from the Level 2 data (swaths of 5-min intervals at 10km x 10km spatial resolution). Each Level 2 retrieval, is flagged with a bit value (from 0 to 3) corresponding to confidence levels (No confidence: 0, Marginal: 1, Good: 2 and Very Good: 3). Based on this, the Level 3 QA-weighted spatial means are obtained by the corresponding Level 2 retrievals considering as weight their confidence level (bit value). In order to avoid any misunderstanding from our side we are providing the relevant part from the MODIS documentation (http://modis-atmos.gsfc.nasa.gov/_docs/QA_Plan_2007_04_12.pdf, at the bottom of Page 4):

"The MODIS Atmosphere L3 processing software makes use of the L2 Usefulness and Confidence flags by creating L3 QA-weighted mean and standard deviation statistics. The QA weighting is performed by weighting each L2 input pixel by its Confidence flag, so that non-fill no confidence data has a weight of 0x, marginal data has a weight of 1x, good data has a weight of 2x, and very good data has a weight of 3x in the statistical computation within the L3 one-degree grid box."

The web link is already provided in our manuscript, for those who want to find more details about the methodology, which is applied by the MODIS Team for the calculation of Level 3 grid cells spatial averages from the corresponding Level 2 retrievals. In the updated version of our manuscript, we have added a sentence explaining briefly the term "Quality assurance-weighted" as it has been asked by the Reviewer (lines 214-220).

"*In Section 2.1.1 you only give the expected accuracy of the AOD data used. Which is the accuracy of the other MODIS-derived parameters employed in the study? How does this accuracy change above land and ocean? Is it sufficient to make this products suitable to be employed for scientific purposes?*"

To our knowledge, we don't have enough information about the FF, Ångström exponent (or alpha), and effective radius retrievals' accuracies since those quantities have not been evaluated to the same extent that AOD has. FF and alpha data are derived from spectral information and their accuracy is determined by very sensitive spectral dependent factors such as errors in the surface model or sensor calibration changes. Over land, these factors play an important role and for this reason the accuracy of the aforementioned observations is lower compared to the corresponding ones over maritime regions. Over sea, the size parameters (FF and alpha) are strongly dependent on wind conditions. According to our analysis, it seems that for strong AOD signals, such as the case of intense desert dust outbreaks, the results reveal a satisfactory agreement between satellite and ground measurements.

"*The algorithm uses the information on Angstrom Exponent (AE), AI and FF (plus reff over sea) to select 'strong' dust and 'extreme' dust events. However, there is very little information in the text on HOW the matching between AOD, AE, FF (plus reff) and AI is operatively done at the pixel level. In particular the manuscript lacks in describing the statistics of the coincident multi-parameter dataset. I guess you do not always have ALL the parameters a vailable at the same time. What happens in case you do not have coincident datasets? How frequent these cases are? What's the impact of this on the final outcome of your study?*"

All the aerosol optical properties retrievals have common spatial and temporal resolution. Therefore, it is straightforward how the collocation, in spatial and temporal terms, is done. Following the Reviewer's comment, we have added in our manuscript that all the defined criteria must be fulfilled concurrently in order to be clear to the reader (lines: 364-366).

As to what happens with the algorithm when there are not coincident data, that is when the criterion for a dust episode is not fulfilled, we would like to note that the applied algorithm in the present analysis is a branch of a unified algorithm which identifies and characterizes not only DD episodes, but also four other types of aerosol episodes, namely biomass-urban (BU), dust/sea-salt (DSS), mixed (MX) and undetermined (UN). The relevant results, for the period 2000-2007, over the Mediterranean Sea, are discussed thoroughly in Gkikas et al. 2016 (http://www.sciencedirect.com/science/article/pii/S135223101530563X). Here, we are presenting the results for the whole study region, as they have been described in Gkikas et al. (2016):

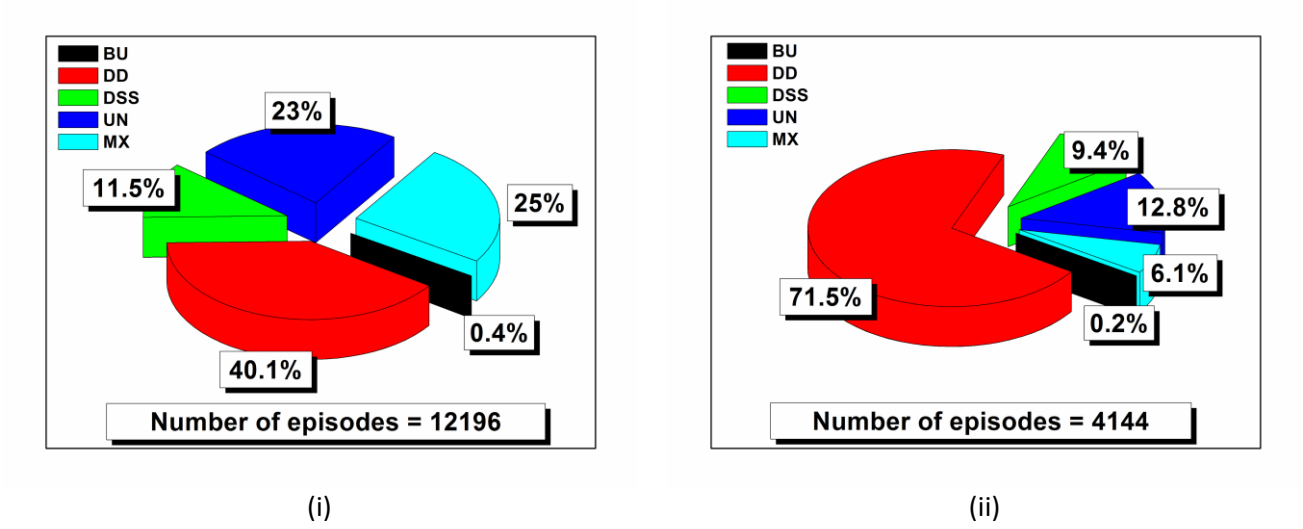

(i) (ii)

Figure R9: Percent contribution of BU (in black color), DD (in red), DSS (green), UN (in blue) and MX episodes (in cyan) to the total number of aerosol episodes over the sea surfaces of the broader Mediterranean basin as well as of its western, central and eastern parts. Results are separately given for: (i) strong and (ii) extreme aerosol episodes.

According to our results, 40.1% and 71.5% of the overall strong and extreme Mediterranean episodes, respectively, has been classified as DD episodes. Note, that desert dust aerosols can participate in MX and DSS categories, however in the present analysis we are keeping only the "pure" DD episodes. Moreover, the satellite retrievals which we are using are representative for the whole atmospheric column making thus impossible to quantify the contribution of mineral particles to the MX and DSS episodes. The performance of the algorithm with respect to the number of identified aerosol episodes is relatively satisfactory, since 77 and 87.2% of all strong and extreme episodes, respectively, have been classified. Nevertheless, 23% and 12.8% of the strong and extreme episodes, respectively, is unclassified (UN) mainly due to missing AI data. Our algorithm has been constructed in such way that makes possible the identification and classification of the aerosol episodes when all the satellite retrievals are available (coincident), trying to avoid any "guess" (UN episodes) which can be ambiguous.

3) Presentation of Results.

"*3.1) Results are reported in Section 4 which however includes a large body of material intended to provide a sort of 'validation' of the method followed (comparison with AERONET and in situ PM10 data). This is a bit confusing as, in my view, the logical sequence would be to present the methodology, then check/demonstrate its validity, and only at that point present the results obtained by that methodology. I would therefore rename the relevant sections accordingly.*"

We strongly believe that it is better to keep the existing paper's structure since it helps the reader to follow our approach without going back and forth on the text. In Section 3, it is described how the satellite algorithm operates. Then, depending on the analysis phase, the reader can easily follow our methodology, at each stage, about the comparison of satellite algorithm against AERONET/PM_{10} measurements (Section 4.2), how the CALIOP lidar profiles are used in order to describe the Mediterranean desert dust outbreaks' vertical structure (Section 4.3) and how the dust outbreaks' vertical distribution can affect the level of agreement between columnar AOD retrievals and ground PM_{10} concentrations (Section 4.4).

"*Additionally, for its contents, the evaluation of the Method (Section 4.2) within Section 4 does not represent a real 'validation' but rather a 'comparison' with other datasets. Just to mention an example: the comparison of the AERONET AOD to the MODIS one (Figure 5) does not represent a validation of your 'objective and dynamic satellite algorithm' but rather a 'validation' of the Modis-AOD-retrieval algorithm. Therefore, I would avoid using expressions as 'the performances of the satellite algorithm are evaluated', widely used throughout the text, and rather refer to this material as: 'the results of the satellite algorithm are compared to...', which is completely different.*"

We agree with the Reviewer's comment. In the updated version of our algorithm the relevant parts have been modified accordingly.

"*3.2) In the same Section, I also believe the comparison with PM10 measurements has little validity in the context of this work. You want to report on the vertical structure of desert dust events, as clearly highlighted in the title of the manuscript. Your results show that several dust events do not reach the ground (see for example Figure 12), so: what do you expect to derive from the straightforward comparison of (columnar) AOD to (ground-level) PM10? I think this topic is of potential interest in general, but not in the form it is presented here. I would remove this part from the manuscript, as it does not add much to the text and rather makes it more confusing and weak.*"

In the revised manuscript, we have added a new section related to the investigation of specific dust events where satellite algorithm's outputs, ground PM_{10} measurements and CALIOP profiles are available concurrently providing an insight of possible factors which can lead to agreement or disagreement between MODIS AOD and ground PM_{10} concentrations. For this reason, to our view, it is required to sustain the part of the analysis related to in-situ measurements. Moreover, in the present analysis is provided information about the success score (a measure related to the performance of the satellite algorithm, Fig. 8-iii), dust contribution to the total PM_{10} (Fig. 8-iv) as well as the mean (Fig. 8-v) and median (Fig. 8-vi) PM_{10} concentrations. All the aforementioned results were not presented in Gkikas et al. (2013).

Other general comments

"*- Title: I would suggest to modify it as 'Mediterranean Intense Desert Dust Outbreaks from columnar and vertically–resolved remote sensing data'*"

We have changed the title to "Mediterranean intense desert dust outbreaks and their vertical structure based on remote sensing data" according to the suggestion of the Reviewer 3.

"*- Please define somewhere at the beginning of the manuscript the term 'intense dust events' you often refer to in the text and use the acronym IDD to refer to it. Specify clearly that, according to your classification, IDD events are divided into 'strong dust events' and 'extreme dust events' (and use respectively the acronyms SDD and EDD to indicate them throughout the text). This will improve its readability.*"

In order to sustain our terminology consistent with Gkikas et al. (2013) we prefer not to change the terms "strong" or "extreme" DD episodes to IDD and EDD, respectively, as it has been proposed by the Reviewer. The term "intense" is just a generic term trying to highlight that emphasis is given to intense dust outbreaks. It is repeated many times in the manuscript just to remind to the reader which dust outbreaks are considered in the present analysis.

"*- Please define somewhere at the beginning the exact study region considered.*"

Done (Lines: 332-333).

Minor Comments

"There are several minor revisions the manuscript would need. However, as major revisions are requested and the text will probably change a lot in its revised version, a not exhaustive list of minor comments is given below."

Section 2

"*Section 2.1.1. The ocean and land Angstrom exponents are computed using different wavelengths. Please explain why you use the same threshold for them in your algorithm.*"

The difference between Ångström exponents calculated in the spectral ranges where MODIS provides data over land (470-660 nm) and sea (550-865 nm) is very small (almost negligible). This is confirmed by the findings in Basart et al. (2009), who classified aerosols according to their type based on ground observations derived by AERONET stations located in northern Africa, Middle East and Mediterranean (http://www.atmos-chem-phys.net/9/8265/2009/acp-9-8265-2009.pdf). The authors reported that in the most dust affected Mediterranean sites δα (δα=α(440,675)–α(675,870)) values are almost equal to zero. Note that the wavelength pairs used for the calculation of Ångström exponent by MODIS sensor over land and sea are similar with those used in Basart et al. (2009). This indicates that common Ångström exponent thresholds over land and sea surfaces can be used in the satellite algorithm.

"*Page 27686, Lines 8-13. Confusing, please explain better*"

The CAD scores are bit values indicating the presence of aerosols (negative CAD scores) or clouds (positive CAD scores). As the CAD scores are getting higher, in absolute terms, the retrieval algorithm is more reliable either for aerosols or clouds. In our study we are using only the total backscatter retrievals associated with CAD scores between -100 and -20, as it has been proposed by Winker et al. (2013). Moreover, we are providing the weblink where the reader can find the relevant information in the CALIOP documentation. We have rephrased the relevant part in order to be clear to the reader (Lines: 271-272).

Section 2.2.2

"*Please specify better which data from AirBase and/or EUSAAR are you using (if this part will be kept in the revised version, which I discourage).*"

The data for the stations Montseny and Finokalia have been taken from the EUSAAR database while the corresponding data for the other stations have been downloaded from the Airbase database. Both have been added in the final version of the manuscript (Lines: 323-326).

Section 3

"*Page 27689 Line 22: It is not the quality of results to be improved but rather the quality of input data. Please rephrase.*"

We have rephrased the relevant part according to the Reviewer's comment.

"*Lines 25-28: '...in the present version of the algorithm are not implemented temporal filters, concerning the availability (masking out of AOD grid cells with less than 50% available data of the time-series) of raw AOD data, in contrast to Gkikas et al. (2009, 2013)'. This sentence is not clear to me. Do you mean in this work L3 pixels having less than 50% of L2 data are included? If so, do you consider this as an improvement of the methodology?*"

This sentence refers to the temporal availability of the L3 retrievals (i.e. the number of days over the period 2000-2013 or 2003-2012 where AOD data are available) and not in the number of L2 counts which are used for the calculation of the L3 retrieval. In order to avoid any misunderstandings we have removed it from the text since our analysis clearly shows that only few grid cells in the north parts of the study region have less than 50% available observations (Please, see our answer in comment 1.1).

"*Line 29 to the next page: Rephrase as this sentence is confusing. At the beginning I understood you performed the analysis only considering CF < 0.8, but then in Section 4 you mention (Page 27692, Lines 9-12): '...The analysis has been repeated (results not shown here) considering only AODs associated with cloud fractions lower/equal than 0.8,...' . I think you should restrict the analysis JUST to the cases with CF < 0.8, as AOD is not reliable above this threshold.*"

We have reproduced and show below the obtained geographical distributions of frequency of occurrence for the strong (Figure R10-i) and extreme (Figure R10-ii) DD episodes, when applying the same satellite algorithm but using only daily AOD values associated with cloud fractions (CF) lower than 0.8. The analysis has been accomplished for the period March 2000 – February 2013 using MODIS-Terra retrievals. For the strong DD episodes, it is evident that the spatial distribution reveals many similarities with the corresponding distribution obtained without applying the cloud filter (Figure 2 i-a of the revised manuscript). The main differences are encountered in the central parts of the Mediterranean Sea while the maximum frequency can reach up 11.9 episodes year^{-1}. On the contrary, for the extreme DD episodes the "zone" of maximum frequencies is restricted across the northern African coasts instead of the central Mediterranean Sea (Figure 2 ii-a of the manuscript).

The cloud filtration leads to the exclusion of possibly overestimated AODs retrievals, due to cloud contamination, from the dataset. Nevertheless, in the majority of the identified DD episodes without cloud filtering DD episodes the collocated AERONET AODs are relatively high indicating thus the occurrence of a dust outbreak (Figs 7-iii-a and 7-iii-b in the revised manuscript). This adds confidence to the general results (without applying the cloud filter). Taking also into account that cloud filtering diminishes the dataset (number) of DD episodes, we think that is better to use the raw AOD data (without cloud filtration).

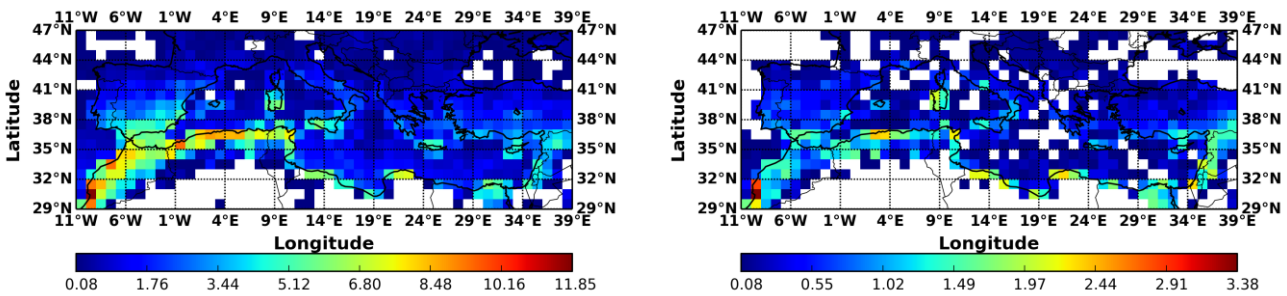

(i) (ii)

Figure R10: Geographical distributions of the occurrence frequency (episodes/year) of: (i) strong and (ii) extreme desert dust episodes, averaged for the period Mar 2000 – Feb 2013 (MODIS-Terra), over the broader area of the Mediterranean basin, when the satellite algorithm operates with AODs associated with cloud fractions lower than 0.8.

Section 4

"*Page 27690, Line 21-22: '..The obtained patterns are in a very good agreement with those presented by Gkikas et al. (2013),..'. This is just an example of similar comments you often insert in the text to comment your results. However my suggestion is to avoid repetition of this concept as it is rather obvious that results comparable to those presented in Gkikas et al. (2013) are obtained in this study, which follows a very similar methodology.*"

We have tried to reduce the number of similar statements in our manuscript as it has been proposed by the Reviewer. However, we would like to mention that it is reasonable to refer to Gkikas et al. (2013), only in the parts which are common but few, since the two different versions of the satellite algorithm (mainly different periods) are applied in each study. Moreover, these statements in the initial document are restricted only in Section 4.1 (geographical distributions) and in the part of the manuscript where the structure of the satellite algorithm is presented.

"*Page 27692, Lines 9-12: '...The analysis has been repeated (results not shown here) considering only AODs associated with cloud fractions lower/equal than 0.8,... ' . You are commenting something which is not shown and provide no explanation of the differences found. As already commented above for the same sentence, I think your study should be limited to the cases with CF < 0.8, avoiding most of the comments at the end of Section 4.1.*"

We think that we have already answered satisfactorily in our previous answer (two comments above).

"*Page 27693, Section 4.2: The title of this section is inappropriate for the reasons explained in my general comments 3.1 and 3.2.*"

The title has been modified according to the Reviewer's comment.

Page 27694

"*Lines 5-7: Do you mean you '...found at least one strong or extreme dust episode' over the whole period considered?*"

In each grid cell (1^{o} x 1^{o}), where an AERONET station is located within its geographical limits, it is found the number of DD episodes (strong or extreme) with coincident optical properties from the ground. It is clear that these calculations are done for each AERONET station at a pixel level and the number of coincident measurements depends on the availability both of satellite and ground-based retrievals.

"*Lines 5-19: This part is quite confusing. What's your aim here and how are you pursuing it? How do you define a 'clim' value? (what does it mean 'calculated from all the available retrievals'? how many data-points are used? Do these data cover the same period of your satellite dataset?). Additionally, when you refer to AERONET data please use 'ground-based' instead of 'ground' as this latter can be confused with 'in situ'.*"

We think that the relevant part of the document provides satisfactorily the information that we want to give to the reader. The climatological value is calculated from all the available AERONET retrievals, collected from all sites, during the period 2000-2013. Of course, this period is not common for each AERONET station individually

since the availability of the AERONET data varies depending on the station. Here, the mean value is calculated from all these available retrievals derived by all AERONET stations located into the geographical limits of the study region (Mediterranean). Please note that the number of AERONET retrievals is provided in the caption of Figure S3 as well as in the legend of Figure 6 (revised manuscript). For 7 AERONET stations (depicted with cyan circles in Figure 4) we have identified the DD episodes based on ground-based observations and we are comparing the outputs versus the satellite retrievals (Figure 7) for the time period where AERONET observations are available (see Table 1). However, we have rephrased a little bit the relevant part of the document in order to be clearer to the reader (Lines: 510-521). As it concerns the term "ground" we have changed it to "ground-based" according to the reviewer's suggestion.

Section 4.2.1

"*Subsections of Section 4.2.1 should be numbered. If I understand correctly, you are comparing the 1x1 degree satellite data with the AERONET data (measured in a specific site). Please at least comment on the expected spatial variability of AOD with in a 1x1 cell, and therefore on the validity of such an approach.*"

In the initial version of the paper, submitted to the ACPD, the subsections were numbered according to the Reviewer's suggestion (i.e. 4.2.1.x) but the Journal didn't accept it (not supported) due to its typesetting rules. As it concerns the second comment of the Reviewer, we would like to point out that the Figures 5 ii-a and 5 ii-b, and the relevant discussion in the text, address the issue of the sub-grid spatial representativeness and homogeneity, respectively, inside the Level 3 grid cells (1^{o}x1^{o} spatial resolution).

"*Page 27694, Line 22: '...346 pixel level intense DD episodes'. To understand the relevance of this number it would be important to mention somewhere how many pixels you have in your domain, how many of these are classified as intense DD (IDD).*"

Our study region consists of 900 Level 3 grid cells of 1^{o} x 1^{o} spatial resolution. At about 200-250 grid cells, located in the desert parts of the study region, AOD retrievals are not possible since we are using the MODIS Dark Target Algorithm products. Moreover, the number of grid cells with available AOD retrievals varies day by day, since many factors (e.g. clouds) can prohibit the satellite observations. During the period 2000-2013, the number of grid cells with available AOD data is equal to 2426303. Based on our algorithm, we have identified 22016 strong and 10619 extreme DD episodes, respectively, at pixel level, while the overall (strong+extreme) sample comprises 32635 DD episodes. The number (346) of coincident satellite algorithm's outputs and available AERONET retrievals corresponds to 1.06% of all DD episodes which have been identified based on our methodology. At a first glance, this percentage it seems quite low but can be easily explained. First, most of the identified DD episodes occur over maritime areas where there are not available AERONET observations. Furthermore, the station-by-station AERONET data availability varies a lot with regards to the satellite period (2000-2013) and also it is well know that there are gaps in the timeseries.

Section 4.3

"*How much do the Calipso-based result change if you use the overall calipso database and its aerosol type discrimination to investigate desert dust, not limiting only to those cases previously classified as IDD in your scheme?*"

In order to answer to the Reviewer's comment, we have reproduced the Figures 9-i and 9-ii considering only the dust and polluted dust records of the CALIOP-CALIPSO aerosol classification scheme without taking into account the satellite algorithm's outputs. The obtained results are available in the supplementary material (Fig. S6-ii and S6-ii) while in the last paragraph of Section 4.3.1 are discussed briefly the differences between average dust and intense dust outbreaks' conditions.

Figures:

Figure 1

"*The scheme of the work is exactly the same of Figure 2 in Gkikas et al. (2013), which is quite inconvenient, please modify highlighting differences from that work or remove the Figure.*"

We prefer to keep Figure 1 in our manuscript since it helps the reader to understand our methodology just reading this paper without going back to Gkikas et al. (2013).

Figure 2

"*- It should be enlarged as it is not very readable at the moment.*"
"*- As commented above, it should refer to the same period for Aqua and Terra.*"
"*- There is a clear discontinuity between land and ocean, can you comment?*"
"*- Change the color scale to more clear numbers (e.g. 0-10, top, 0 – 3 bottom)*"

-We have enlarged the size of the figures.
-We have already explained the reasons that we prefer to keep the MODIS-Terra period.
-As it has been addressed in our previous answers, the retrievals above land are less reliable compared to the corresponding ones over sea surfaces. This can affect the identification of DD episodes as well as their intensity. However, we don't think that this discontinuity is so pronounced as it has been stated by the Reviewer, particularly for the strong DD episodes.
-Done. For the strong and extreme DD episodes the ranges are 0-10 and 0-3.5, respectively.

Figure 3
"*- It should be enlarged as it is not very readable at the moment.*"
"*- In the i-plots, I see a problem of misclassification over the Po valley in Italy. Can you comment on that?*"

-Done
-Please note that the high intensities over the Po Valley are associated with relative small frequencies. This means that the intensity over the northern parts of the study region is computed from a small sample of DD episodes. In such a case, few relative high AODs, associated with long-ranged dust outbreaks, can exceed the defined thresholds in the aforementioned locations resulting thus to high intensity values. However, we must always keep in mind that possible misclassifications, especially over land, by the satellite retrievals or cloud contamination can affect the identification ability of the satellite algorithm.

Figure 12
"*- It should be enlarged as it is not very readable at the moment.*"
"*- Please specify the units of the backscatter values.*"

-We have enlarged furthermore the size of the figure.
-We have added the backscatter units in the captions of Figures 9 and 10.

Mediterranean intense desert dust outbreaks and their vertical structure based on remote sensing data

A. Gkikas[1], S. Basart[1], N. Hatzianastassiou[2], E. Marinou[3,9], V. Amiridis[3], S. Kazadzis[4,5], J. Pey[6], X. Querol[7], O. Jorba[1], S. Gassó[8] and J.M. Baldasano[1,8]

[1]Earth Sciences Department, Barcelona Supercomputing Center, Barcelona, Spain
[2]Laboratory of Meteorology, Department of Physics, University of Ioannina, Ioannina, Greece
[3]Institute for Astronomy, Astrophysics, Space Applications and Remote Sensing, National Observatory of Athens, Athens, 15236, Greece
[4]Physikalisch-Meteorologisches Observatorium Davos, World Radiation Center, Switzerland
[5]Institute of Environmental Research and Sustainable Development, National Observatory of Athens, Athens, Greece
[6]Spanish Geological Survey. Zaragoza IGME Unit, Zaragoza, Spain
[7]Institute of Environmental Assessment and Water Research, IDÆA-CSIC C/Jordi Girona, 18–26, 08034 Barcelona, Spain
[8]Environmental Modelling Laboratory, Technical University of Catalonia, Barcelona, Spain
[9]Laboratory of Atmospheric Physics, Department of Physics, Aristotle University of Thessaloniki, Thessaloniki, Greece

Corresponding author: Antonis Gkikas (antonis.gkikas@bsc.es)

Abstract

The main aim of the present study is to describe the vertical structure of the intense Mediterranean dust outbreaks, based on the use of satellite and surface-based retrievals/measurements. Strong and extreme desert dust (DD) episodes are identified at 1° x 1° spatial resolution, over the period Mar. 2000 – Feb. 2013, through the implementation of an updated objective and dynamic algorithm. According to the algorithm, strong DD episodes occurring at a specific place correspond to cases in which the daily aerosol optical depth at 550nm (AOD_{550nm}) exceeds or equals the long-term mean AOD_{550nm} (Mean) plus two standard deviations (Std) value being smaller than *Mean+4*Std*. Extreme DD episodes correspond to cases in which the daily AOD_{550nm} value equals or exceeds *Mean+4*Std*. For the identification of DD episodes additional optical properties (Ångström exponent, fine fraction, effective radius and Aerosol Index) derived by the MODIS-Terra & Aqua (also AOD retrievals), OMI-Aura and EP-TOMS databases are used as inputs. According to the algorithm using MODIS-Terra data, over the period Mar. 2000 – Feb. 2013, strong DD episodes occur more frequently (up to 9.9 episodes yr^{-1}) over

the western Mediterranean while the corresponding frequencies for the extreme ones are smaller (up to 3.3 episodes yr^{-1}, central Mediterranean Sea). In contrast to their frequency, dust episodes are more intense (AODs up to 4.1), over the central and eastern Mediterranean Sea, off the northern African coasts. Slightly lower frequencies and higher intensities are found when the satellite algorithm operates based on MODIS-Aqua retrievals, for the period 2003–2012. The consistence of the algorithm is successfully tested through the application of an alternative methodology for the determination of DD episodes, which produced similar features of the episodes' frequency and intensity, with just slightly higher frequencies and lower intensities. The performance of the satellite algorithm is assessed against surface-based daily data from 109 sun-photometric (AERONET) and 22 PM_{10} stations. The agreement between AERONET and MODIS *AOD* is satisfactory (R=0.505-0.750) improving considerably when MODIS level 3 retrievals with higher sub-grid spatial representativeness and homogeneity are considered. The CALIOP vertical profiles of pure and polluted dust observations and the associated total backscatter coefficient at 532 nm (β_{532nm}), indicate that dust particles are mainly detected between 0.5 and 6 km, though they can reach 8 km between the parallels 32º N and 38º N in warm seasons, while an increased number of CALIOP dust records at higher altitudes is observed with increased latitude, northwards to 40° N, revealing an ascending mode of the dust transport. However, the overall intensity of DD episodes is maximum (up to 0.006 km^{-1} sr^{-1}) below 2 km and at the southern parts of the study region (30° N - 34° N). Additionally, the average thickness of dust layers gradually decreases from 4 to 2 km moving from south to north. In spring, dust layers of moderate-to-high β_{532nm} values (~ 0.004 km^{-1} sr^{-1}) are detected over the Mediterranean (35° N - 42° N), extending from 2 to 4 km. Over the western Mediterranean, dust layers are observed between 2 and 6 km, while their base height is decreased down to 0.5 km for increasing longitudes underlying the role of topography and thermal convection. The vertical profiles of CALIOP β_{532nm} confirm the multilayered structure of the Mediterranean desert dust outbreaks on both annual and seasonal basis, with several dust layers of variable geometrical characteristics and intensities. A detailed analysis of the vertical structure of specific DD episodes using CALIOP profiles reveals that consideration of the dust vertical structure is necessary when attempting comparisons between columnar MODIS AOD retrievals and ground PM_{10} concentrations.

1. Introduction

The Mediterranean basin, due to its proximity to the major dust source arid areas of Northern Africa and Middle East (Middleton and Goudie, 2001; Prospero et al., 2002; Ginoux et al., 2012) is frequently affected by transported high dust loads referred to as episodes or events. The suspension and

accumulation of mineral particles into the atmosphere over the Saharan and Arabian Peninsula's deserts are determined by various factors such as the enhanced turbulence, soil conditions (reduced vegetation cover and soil moisture), reduced precipitation amounts, latitudinal shift of the Intertropical Convergence Zone (ITCZ) as well as by small scale meteorological processes (e.g. haboobs). However, dust particles can be transported far away from their sources, mainly towards the Atlantic Ocean (e.g. Prospero and Lamb, 2003; Ben-Ami et al., 2010; Huang et al., 2010) and Europe (e.g. Mona et al., 2006; Mona et al., 2012; Papayannis et al., 2008; Basart et al., 2012; Bègue et al., 2012; Pey et al, 2013), favored by the prevailing atmospheric circulation patterns, from planetary to synoptic scales. Due to their frequent transport in the Mediterranean, mineral dust particles, constitute the predominant aerosol type there (Barnaba and Gobbi, 2004; Basart et al., 2012), as shown by the good agreement, in spatial terms, between the geographical distributions of dust episodes' *AOD* (Gkikas et al., 2013) and average *AOD* conditions (Papadimas et al., 2008).

Dust particles play an important role for the shortwave (SW) and longwave (LW) radiation budget (e.g. Kaufman et al., 2002; Tegen et al., 2003; Heinold et al., 2008) and climate (IPCC, 2013). They affect atmospheric heating/cooling rates (e.g. Mallet et al., 2009) while they can also result in a modification of atmospheric dynamics and large atmospheric circulations like monsoons (e.g. Lau et al., 2006; Bollasina et al., 2011), cloud properties and precipitation (e.g. Huang et al., 2006; Solmon et al., 2008). Moreover, it has been shown that the consideration of their radiative impacts in numerical simulations can improve the forecasting accuracy of weather models (Pérez et al., 2006). Dust particles also affect air quality in urban areas (Basart et al., 2012) causing adverse health effects (Díaz et al., 2012; Karanasiou et al., 2012; Pérez García-Pando et al., 2014). All these consequences of dust aerosol are relevant and maximize under maximum dust loads, namely dust episodes, highlighting thus the significance of analyzing the spatial and temporal characteristics of such events. To this aim, many studies have been carried out using either surface (e.g. Cachorro et al., 2006) or satellite (e.g. Moulin et al., 1998) observations, as well as modelling techniques (e.g. Heinold et al., 2007) focusing on the broader Mediterranean area. These studies have been done either for specific cases (e.g. Kubilay et al., 2003; Balis et al., 2006) or for extended periods at specific locations (e.g. Meloni et al., 2007; Toledano et al., 2007a; Gobbi et al., 2013; Mona et al., 2014). Recently, Gkikas et al. (2013) developed an objective and dynamic algorithm relying on satellite retrievals, which enabled an overall view of dust episodes over the entire Mediterranean and the characterization of their regime.

Extensive research has been also carried out on the mechanisms of Mediterranean dust outbreaks. Therefore, several mechanisms and processes of transport, apart from dust emissions in source areas,

have been proposed as controlling factors. Moulin et al. (1997) showed that the exported dust loads from Northern Africa towards the Atlantic Ocean and the Mediterranean are controlled by the phase of the North Atlantic Oscillation (NAO). Other studies, focused on the description of atmospheric circulation characteristics favoring the occurrence of desert dust outbreaks over the central (Barkan et al., 2005; Meloni et al., 2008) or western (Querol et al., 1998; Rodriguez et al., 2001; Salvador et al., 2014) Mediterranean, but on a synoptic scale. An objective classification, based on multivariate statistical methods, of the atmospheric circulation patterns related to dust intrusions over the Mediterranean, has been presented by Gkikas et al. (2015) and Varga et al. (2014).

The concentration of dust aerosols in the Mediterranean is characterized by strong spatial and temporal variability, associated with the seasonal variability of cyclones dominating or affecting the broader Mediterranean basin (Trigo et al., 2002). According to Moulin et al. (1998), dust *AOD* levels are higher in spring and summer compared to the wet seasons of the year. Moreover, dust intrusions are mainly recorded over the southeastern Mediterranean in spring and winter, over the western parts in summer and over the central ones in autumn (Gkikas et al., 2013).

Dust transport over the Mediterranean is characterized by a multi-layered structure (Hamonou et al., 1999; Papayannis et al., 2008) in contrast to the Atlantic Ocean, which is well confined to the Saharan Air Layer (SAL, Karyampudi et al., 1999). The vertical distribution of dust load into the troposphere as well as the profile of dust aerosols' optical properties at different altitudes, control the impacts on atmospheric dynamics induced by the mineral particles (Zhang et al., 2013). In order to describe the geometrical features of dust transport, many researchers have used ground lidar measurements, model simulations (Alpert et al., 2004; Kishcha et al. 2005) or they have relied on a synergistic use of satellite observations and ground lidar profiles (Berthier et al., 2006). The vertical extension of the Saharan dust intrusions over Europe, during the period 2000-2002, was the subject of a comprehensive study by Papayannis et al. (2008), who used lidar measurements from the EARLINET (European Aerosol Research Lidar Network, Bösenberg et al., 2003). Over the Mediterranean stations, the mean base, top and thickness of dust layers was found to vary from 1356 to 2980 m, 3600 to 5900 m and 726 to 3340 m, respectively. According to the obtained results, tracers of dust particles can be detected up to 10 km, as also reported by Gobbi et al. (2000), who studied a Saharan dust event in Crete (south Greece) during spring of 1999.

Several similar studies have been also performed for specific Mediterranean locations based on EARLINET lidar measurements. For example, Mona et al. (2006) analyzed the vertical structure of 112

Saharan intrusions that occurred over Potenza (Italy), from May 2000 to April 2003. The authors found that these outbreaks are confined between 1.8 and 9 km while their mass center is located at 3.5 km above sea level (a.s.l.). A similar analysis for Athens and Thessaloniki over the period 2000-2002, was conducted by Papayannis et al. (2005) who demonstrated that dust layers are recorded mainly between 2 and 5 km while their thicknesses vary from 0.2 to 3 km. The geometrical characteristics of dust layers over Athens, during the period 2004 – 2006, have been also presented by Papayannis et al. (2009), who pointed out that the center of mass of dust layers is located at 2.9 km being in a very good agreement with Kalivitis et al. (2007) findings (around 3 km) for the eastern Mediterranean. Additionally, the authors reported that the dust layers mainly extend from 1.6 to 5.8 km while mineral particles can be detected, at very low concentrations, up to 8 km a.s.l.. Gobbi et al. (2013) found that dust plumes, over Rome, mainly extend from 0 to 6 km while their center of mass is located at around 3 km. In the southern parts of Italy (Potenza), dust layers' base is found between 2 and 3 km, their geometrical height extends from 2.5 to 4 km while tracers of dust particles can be detected up to 10 km, based on a dataset of 310 dust events analyzed by Mona et al. (2014). Finally, Pisani et al. (2011) stated that the mean base and top of dust layers is found at 1.5 km and 4.6 km a.s.l., respectively, while their mean thickness is equal to 3.1 km, based on a statistical analysis of 45 desert dust episodes observed over Naples (Italy), from May 2000 to August 2003.

Surface-based lidar measurements like those used in the aforementioned studies provide useful information about the geometrical and optical properties of dust layers, but they are representative only for specific locations. Yet, a more complete knowledge about the vertical structure of dust outbreaks is necessary in order to adequately understand and determine their possible effects. The limitation imposed by the use of surface-based lidar observations can be overcome by utilizing accurate satellite retrievals, as a complementary tool, which provide extended spatial coverage. Since 2006, vertical resolved observations of aerosols and clouds from space were made possible thanks to the CALIOP (Cloud-Aerosol Lidar with Orthogonal Polarization) lidar flying onboard the CALIPSO (Cloud-Aerosol Lidar and Infrared Pathfinder Satellite Observations) satellite (Winker et al., 2009). Based on CALIOP observations, Liu et al. (2008) analyzed the global vertical distribution of aerosols for one year, while other studies focused on the vertical structure of dust outflows towards the Atlantic Ocean (e.g. Ben-Ami et al., 2009; Adams et al., 2012; Tsamalis et al., 2013) and the Pacific Ocean (e.g. Eguchi et al., 2009; Hara et al., 2009). On the contrary, over the broader Mediterranean area, only a small number of studies has been made aiming at describing the vertical distribution of dust aerosols (Amiridis et al., 2013) or specifying the vertical structure of dust events (Amiridis et al., 2009).

Nevertheless, they only dealt with a single dust event (18-23 May 2008, Amiridis et al., 2009) and thus cannot satisfy the need to know the general vertical structure of Mediterranean dust episodes.

The main target of the present study is to describe the Mediterranean desert dust outbreaks' vertical structure. For this purpose, satellite retrievals derived by the MODIS-Terra/Aqua, Earth Probe-TOMS, OMI-Aura and CALIOP-CALIPSO databases (Section 2) are used in a synergistic way. The dust outbreaks are identified with an objective and dynamic algorithm, which uses appropriate aerosol optical properties representative of suspended particles' load, size and nature (Section 3). Based on its outputs, the primary characteristics of the intense Mediterranean desert dust (DD) episodes, namely their frequency and intensity, are described in Section 4.1. Just in order to assess the consistency of the algorithm' concept, an alternative methodology for the determination of DD episodes is also applied and the obtained results are inter-compared with the basic methodology. The outputs of the default version of the satellite algorithm are compared versus surface measurements provided by AERONET or PM_{10} stations, located within the study region (Section 4.2). Additionally, useful information about various optical and physical properties under intense dust episodes conditions is also derived from the aforementioned analysis. For the identified DD episodes, collocated CALIOP-CALIPSO vertical feature mask and total backscatter coefficient at 532 nm retrievals are used in order to describe the annual and seasonal variability of dust outbreaks' vertical extension over the Mediterranean (Section 4.3). Moreover, in Section 4.4, a thorough analysis of few specific Mediterranean DD episodes is made, in order to examine how the vertical distribution of desert dust outbreaks can affect the agreement between MODIS AOD and PM_{10} data. Finally, the summary and conclusions are drawn in Section 5.

2. Satellite and surface-based data

The different types of satellite retrievals that have been used as inputs to the objective and dynamic satellite algorithm are described below, namely the MODIS (Section 2.1.1), EP-TOMS and OMI-Aura (Section 2.1.2) databases. Also, CALIOP-CALIPSO vertically resolved satellite data, coincident with the identified desert dust outbreaks by the satellite algorithm, are described in Section 2.1.3. Finally, surface-based sun-photometric AERONET retrievals and PM_{10} concentrations, both used for the comparison against the satellite algorithm's outputs, are described in Sections 2.2.1 and 2.2.2, respectively.

2.1 Satellite data

2.1.1 MODIS

MODerate resolution Imaging Spectroradiometer (MODIS) onboard the Terra and Aqua satellites – with daytime local equator crossing time at 10:30 and 13:30 UTC, respectively, and 2330 km viewing swath – acquires measurements at 36 spectral bands between 0.415 and 14.235 μm with varying spatial resolution of 250, 500 and 1000 m. Observations from Terra and Aqua are made continuously since February 2000 and July 2002, respectively, and are available from the LAADS website (ftp://ladsweb.nascom.nasa.gov/). Aerosol optical properties are retrieved through the Dark Target (DT) algorithm (see e.g. Kaufman et al., 1997, 2001; Tanré et al., 1997; Levy et al., 2003; Remer et al., 2005) where different assumptions are considered depending on the underlying surface type (land or ocean). Several evaluation studies (e.g. Remer et al., 2008; Papadimas et al., 2009; Levy et al., 2010; Nabat et al., 2013) have shown that aerosol optical depth (*AOD*) can be retrieved satisfactorily by MODIS, nevertheless its performance is better over sea (uncertainty equal to ± 0.03 ± 0.05 × *AOD*, Remer et al., 2002) than over land (± 0.05 ± 0.15 × *AOD*, Levy et al., 2010).

The following daily MODIS-Terra and MODIS-Aqua Collection 051 (C051) level 3 satellite data (MOD08_D3 and MYD08_D3 files) provided at 1° × 1° latitude-longitude spatial resolution are used: (i) AOD_{550nm}, (ii) Ångström exponent over land ($\alpha_{470-660nm}$), (iii) Ångström exponent over ocean ($\alpha_{550-865nm}$), (iv) fine-mode fraction (*FF*) of *AOD* over land and ocean and (v) Effective radius over ocean (r_{eff}). It must be mentioned that the size parameters (α, *FF*) over land are less reliable compared to the corresponding ones over sea, since they are highly sensitive to spectral dependent factors such as errors in the surface model or sensor calibration changes. Over sea, the accuracy of size parameters is strongly dependent on wind conditions. Similar data have been used by Gkikas et al. (2013), however, in the present study we have improved data quality by using the quality assurance-weighted (QA) level 3 data (http://modis-atmos.gsfc.nasa.gov/_docs/QA_Plan_2007_04_12.pdf) derived from the level 2 retrievals (10 km x 10 km spatial resolution). Each level 2 retrieval, is flagged with a bit value (from 0 to 3) corresponding to confidence levels (No confidence: 0, Marginal: 1, Good: 2 and Very Good: 3). Based on this, the level 3 QA-weighted spatial means are obtained by the corresponding level 2 retrievals considering as weight their confidence level (bit value). In addition, the day cloud fraction as well as the number of level 2 counts, which are both relevant to the performance of the satellite

algorithm, are also used in this study. The time series of daily MODIS aerosol data cover the 13-yr period March 2000-February 2013 (Terra) and the 10-yr period January 2003-December 2012 (Aqua).

2.1.2 EP/TOMS and OMI-Aura

The selected retrievals from MODIS provide information about particles' load (*AOD*) and size (α, *FF*, r_{eff}), which are both necessary to identify dust episodes. However, since dust is not the only coarse aerosol, for example sea-salt can be so as well, another optical property indicative of particle absorption efficiency is also required by the algorithm. To address this issue, the Absorption Aerosol Index (*AI*) daily data were also used, derived from measurements taken by the Total Ozone Mapping Spectrometer (TOMS) instrument onboard the NASA's Earth-Probe satellite (2000-2004) and the Ozone Monitoring Instrument (OMI) onboard the NASA's Aura satellite (2005-2013). *AI* is the primary TOMS aerosol product (Herman et al., 1997) based on a spectral contrast method in a UV region (331-360 nm) where ozone absorption is very small and can be used for the distinction between scattering (e.g. sea-salt) and absorbing (e.g. desert dust, smoke) aerosols. The retrieval algorithm (fully described by Torres et al., 1998; 2002; 2005) takes advantage of the low surface albedo in the UV spectrum range, even in arid and semi-arid areas, making thus possible the estimation of the *AOD* over highly reflecting desert surfaces, where the major dust sources are located. Since the late 70's, the TOMS sensor onboard Nimbus-7 (1978 – 1993) and Earth Probe (1996 – 2005) has been providing global aerosol measurements. With the deployment of the EOS-Aura OMI (Ozone Monitoring Instrument) in mid-2004 (Torres et al., 2007) the near UV aerosol record continues to be extended into the foreseeable future. OMI is a hyperspectral sensor, covering the 270-500 nm range, launched onboard the EOS-Aura satellite on July 15, 2004 (1:38 pm equator crossing time, ascending mode) providing almost daily global coverage thanks to its wide viewing swath (2600 km with 13 km x 24 km nadir resolution). Apart from *AI* measurements, OMI aerosol products include also the total and absorption *AOD* and the single scattering albedo at 388 and 500 nm (Torres et al., 2007). Both EP-TOMS and OMI-Aura retrievals are available via the Mirador ftp server (http://mirador.gsfc.nasa.gov/) of the Goddard Earth Sciences Data and Information Services Center (GES DISC). OMI-Aura data, as MODIS, are provided at 1° x 1° spatial resolution while the EP-TOMS retrievals have been regridded from their raw spatial resolution (1° x 1.25°) in order to match with the other two datasets (OMI, MODIS).

2.1.3 CALIOP-CALIPSO

The Cloud-Aerosol Lidar with Orthogonal Polarization (CALIOP) onboard the NASA's satellite CALIPSO (Cloud-Aerosol Lidar and Infrared Pathfinder Satellite Observations), launched in April 2006, provides vertical resolved aerosol and cloud observations (Winker et al., 2009) since June 2006. CALIPSO is flying in the A-Train constellation (Stephens et al., 2002; http://atrain.nasa.gov/) in a sun-synchronous polar orbit at 705 km over the surface, with a 16-day repeat cycle, crossing the equatorial plane at about 13:30 local solar time (Winker et al., 2009). CALIOP is an active sensor measuring the backscatter signal at 532 nm and 1064 nm as well as the polarization at 532 nm (Winker et al., 2009). These level 1 retrievals are further processed (calibration and range corrections) passing to Level 2 in order to retrieve the backscatter and extinction coefficients, at 532 nm and 1064 nm, for aerosol and cloud layers. The identification of cloud and aerosol layers within the atmosphere (Vaughan et al., 2009) is made through the cloud aerosol discrimination (*CAD*) algorithm (Liu et al., 2009), which is based on the probability distribution functions (PDFs) of altitude-and-latitude-dependent parameters (integrated color ratio, layer-integrated volume depolarization ratio, mean attenuated backscatter coefficient). *CAD* scores vary mainly from -100 to 100 indicating the presence of aerosols and clouds when are negative and positive, respectively, while bins of confidence levels, both for aerosols and clouds, are defined based on their absolute values (https://eosweb.larc.nasa.gov/sites/default/files/project/calipso/quality_summaries/CALIOP_L2VFMProducts_3.01.pdf). More specifically, the performance of the classification scheme in the VFM algorithm, either for aerosols or clouds, is more reliable for increasing CAD scores in absolute terms. Aerosols are categorized in 6 primary types namely: (i) clean marine, (ii) dust, (iii) polluted continental, (iv) clean continental, (v) polluted dust and (vi) smoke (Omar et al., 2009).

In the present analysis, we use the Version 3 (3.01 and 3.02) of the Level 2 Vertical Feature Mask (VFM) and Aerosol Profile Products (APro) files, available from June 2006 to February 2013, both derived from the NASA's Earth Observing System Data and Information System (http://reverb.echo.nasa.gov/). The aerosol profile products are generated at a uniform horizontal resolution of 5 km (http://www-calipso.larc.nasa.gov/products/CALIPSO_DPC_Rev3x6.pdf), while the vertical resolution varies from 60 to 180 m depending on the altitude range and the parameter. The scientific data sets which have been analyzed are the following: (i) aerosol subtype, (ii) *CAD* score and

(iii) Total Backscatter Coefficient at 532 nm (β_{532nm}), reported at several tropospheric and stratospheric levels above mean sea level (Hunt et al., 2009).

2.2 Surface-based data

2.2.1 AERONET

The AErosol RObotic NETwork (AERONET, Holben et al., 1998) is a worldwide network of installed CIMEL sun-sky radiometers obtaining sun-photometric observations in more than 1000 locations of the planet (http://aeronet.gsfc.nasa.gov). The solar irradiances received by the photometer are inversed to columnar aerosol optical and microphysical properties through the implementation of retrieval algorithms (e.g. Dubovik and King, 2000; O' Neill et al., 2003). The followed standardized methods concerning instrument maintenance, calibration, cloud screening and data processing allow aerosol monitoring and comparison between different study periods and areas (Smirnov et al., 2000). From the global AERONET stations, 109 are located within the geographical limits of our study region. For each station, the daily averages of cloud-screened and quality assured data (Level 2.0) of direct sun and almucantar retrievals are used for: (i) *AOD* at 7 wavelengths from 340 to 1020 nm, (ii) size distribution retrieved for 22 logarithmically equidistant discrete points (r_i) in the range of sizes 0.05 μm ≤ r ≤ 15 μm, (iii) Ångström exponent between 440 and 870 nm ($\alpha_{440\text{-}870nm}$), (iv) total effective radius (r_{eff}), and (v) single scattering albedo (*SSA*) and asymmetry parameter (g_{aer}) both retrieved at 440 nm, 675 nm, 870 nm and 1020 nm. The uncertainty in the estimation of *AOD* depends on technical (e.g. calibration method) factors and inversion assumptions, both described in detail in Holben et al. (1998). Moreover, the accuracy of the retrieved *AOD* by the CIMEL radiometer is spectrally dependent, being higher (<±0.01) for wavelengths longer than 440 nm and lower (<±0.02) for the UV wavelengths (Eck et al., 1999). It should be also noted that the AERONET Level 2.0 inversion products (e.g. SSA) are provided when AOD at 440 nm is higher than 0.4 ensuring the minimization of the inversion uncertainties, which are also determined by other factors (e.g. scattering angle, particles' sphericity) as stated in detail by Dubovik et al. (2000).

2.2.2 PM_{10}

Daily total and dust surface PM_{10} concentrations, over the period 2001-2011 from 22 regional background and suburban background sites were used in this study. The monitoring sites are distributed

as follows: 10 in Spain; 2 in southern France; 5 in Italy; 3 in Greece; 1 in southern Bulgaria and 1 in Cyprus. PM_{10} concentrations were obtained in most cases from gravimetric determinations on filters, whereas in few cases they were determined by real time instruments (Querol et al., 2009b; Pey et al., 2013) but corrected against gravimetric measurements carried out in annual field campaigns. The disaggregation of the dust component to the total amount is made based on a statistical approach which has been applied in several past studies (e.g. Rodríguez et al., 2001; Escudero et al., 2007; Querol et al., 2009b; Pey et al., 2013). A full description of the methodology which is followed for the calculation of dust particles' contribution to the total PM_{10} is presented in Escudero et al. (2007). Briefly, the net dust PM_{10} amount is calculated through the subtraction of the regional background PM_{10}, which is obtained by applying a monthly moving 30^{th} percentile to the PM_{10} timeseries excluding days of dust transport, from the corresponding values of the total PM_{10} concentrations. Most of the derived data were obtained from the AirBase (http://acm.eionet.europa.eu/databases/airbase/) database, while for the stations Finokalia (Crete) and Montseny (NE Spain) the relevant measurements have been acquired from the EUSAAR (http://www.eusaar.net/) database.

3. Identification of desert dust episodes

Following the methodology proposed by Gkikas et al. (2013), desert dust (DD) episodes are identified based on an objective and dynamic algorithm, which is depicted in the flowchart of Figure 1. The algorithm operates in three steps and is applied in each individual 1° x 1° geographical cell within the geographical limits of the study domain (29° N - 47° N and 11^{o} W - 39^{o} E. First (Fig. 1, yellow box), the mean (*Mean*) and the associated standard deviation (*Std*) from the available AOD_{550nm} retrievals are calculated for the whole study period. These primary statistics are used for the definition of two threshold levels, which are equal to *Mean+2*Std* and *Mean+4*Std*. At the next step, the algorithm analyzes the daily AOD_{550nm} timeseries and classifies an episode as a strong one when *AOD* is between the two defined thresholds ($Mean+2*Std \leq AOD_{550nm} < Mean+4*Std$) and as an extreme one when *AOD* is higher/equal than *Mean+4*Std* (cyan boxes). The same approach was undertaken by Gkikas et al. (2009) who classified the Mediterranean aerosol episodes over the period 2000-2007 according to their strength and described their frequency and intensity. It must be clarified that according to our methodology in areas frequently affected by dust episodes, both mean and standard deviation values are expected to be high resulting to high thresholds which means that cases with moderate-to-high *AODs*, also possibly relevant to radiative and health effects, are masked out from the

dataset. In order to investigate the possible impact of this, "unbiased" mean, standard deviation and thresholds of AOD are also computed based on another methodology and the results are discussed comparatively to those of the primary methodology in a separate paragraph. Moreover, it must be mentioned that the satellite algorithm identifies only intense desert dust episodes since their *AOD* must be higher than *Mean+2*Std* which is considered as a high threshold level.

It should be noted that the representativeness of the calculated mean levels is possibly affected by the availability of the AOD retrievals and particularly by the way these data are distributed at different temporal scales. To this aim, we have calculated the percentage availability of AOD retrievals on a monthly, seasonal and year by year basis, over the period 2000-2013 (results not shown here). Seasonal differences of AOD availability are mainly encountered in the northern parts of the study region, with lower values (20 to 40 %) from December to February against 50-85% for the rest of the year. This is attributed to the enhanced cloud coverage prohibiting the satellite observations. Nevertheless, this does not essentially affect the algorithm outputs since these regions, being far away from the dust sources, are not so frequently affected by dust outbreaks, especially given the significant wet removal of aerosols during this most rainy season of the year. On a year by year basis, the differences of the AOD data's availability are almost negligible.

In a further step of the methodology, the strong and extreme DD episodes are identified separately over land and sea surfaces of the study region. This is achieved through the usage of specific aerosol optical properties, namely the Ångström exponent, effective radius, fine fraction and aerosol index, which provide information about particles' size and nature (black box, Figure 1). For each optical property, appropriate upper or lower thresholds have been set up (green boxes, Figure 1) which must be valid concurrently in order to certify the presence of dust particles in the atmosphere. These cut-off levels have been selected according to the literature findings, availability of raw data and several sensitivity tests (more details are provided in Gkikas et al., 2013). The validity of these thresholds is further evaluated against AERONET measurements and the corresponding results are discussed in Section 4.2.1.4.

In order to address the issue of possible overestimation of the defined threshold levels, particularly in the most dust affected areas as it has been mentioned above, we have also applied the satellite algorithm using an alternative methodology (METHOD-B) in which dust-affected grid cells were excluded. In this case, from the raw AOD retrievals we have masked out the "pure" desert dust grid cells, which were identified based on the concurrent fulfillment of the defined criteria for dust occurrence in the algorithm (for Ångström exponent, fine fraction, aerosol index and effective radius,

green boxes of Figure 1). Then, from the remaining data (non-dust AOD retrievals), the mean, the associated standard deviation as well as the defined thresholds of AOD are computed for the whole study period, for each pixel, as also done in the primary methodology. Finally, also similarly to the way done in the primary methodology, the DD episodes were classified into strong and extreme ones. The frequency of occurrence and intensity of DD episodes determined with METHOD-B are provided in the supplementary material (Figures S1 and S2) while their differences with regards to the primary methodology are discussed in Section 4.1.

As explained, a similar methodology and data were used in the study by Gkikas et al. (2013). Nevertheless, the present one is a significant extension mainly for five reasons: (i) DD episodes are identified here over an extended period of study and for both MODIS platforms, i.e. Mar. 2000 – Feb. 2013 for MODIS-Terra and 2003-2012 for MODIS-Aqua, (ii) a second methodology (METHOD-B) for the identification of DD episodes is tested, (iii) the quality of the input data is improved by using QA-weighted level-3 data produced by weighting level-2 data based on their confidence flag instead of regular ones (QA≥1), (iv) emphasis is given to the vertical structure of the intense DD episodes and (v) the role of the detailed dust outbreaks' vertical structure for the level of agreement between columnar MODIS AOD and ground PM_{10} concentrations is investigated. Moreover, an improvement of the methodology consists in the application of our satellite algorithm also using only *AODs* associated with cloud fractions (*CF*) lower/equal than 0.8, in order to investigate possible modifications of our results due to the cloud contamination effects on MODIS *AODs*. The critical value of 0.8 for *CF* has been defined according to Zhang et al. (2005) and Remer et al. (2008), who stated that under extended cloud coverage conditions *AOD* levels can be increased substantially.

4. Results

Before dealing with the vertical structure of dust outbreaks (sub-sections 4.3 and 4.4), it is very important to describe their horizontal patterns (sub-section 4.1) and also to compare the algorithm's outputs against quality AERONET and PM_{10} observations (sub-section 4.2) in order to ensure an accurate three-dimensional view of the intense Mediterranean DD episodes. It must be clarified, that the comparison of the satellite algorithm's outputs versus AERONET/PM_{10} is made only for its default version and not for the METHOD-B, since between the two methodologies are not found remarkable differences, as it will be presented in Section 4.1. Accordingly, the synergistic implementation of the CALIOP-CALIPSO lidar profiles is done only when the DD episodes are identified based on the

primary methodology. The present section has been organized accordingly and the results are given below.

4.1 2D geographical distributions of desert dust episodes' frequency and intensity

The mean geographical distributions of strong and extreme DD episodes' frequency of occurrence (episodes yr^{-1}) are presented in Figure 2. Results are given separately as obtained from MODIS-Terra and Aqua for the periods Mar. 2000 – Feb. 2013 and 2003 – 2012, corresponding to local late morning-to-noon (Terra) and afternoon (Aqua) conditions, respectively. It is evident a gradual reduction of frequencies from south to north, while for the strong DD episodes also appears a west to east decreasing gradient. The decreasing south-to-north gradient of intense DD episodes' frequency, which is also in agreement with previous studies based on ground PM measurements (Querol et al., 2009b; Pey et al., 2013), model simulations (Papayannis et al., 2008; 2014) and AERONET *AOD* retrievals (Basart et al., 2009), can be attributed to the increasing distance from the major dust sources and to the higher precipitation amounts at the northern parts of the basin (e.g. Marrioti et al., 2002; Mehta and Yang, 2008).

The maximum frequencies (9.9 episodes yr^{-1}) of strong DD episodes are observed in the western parts of the study region, for both periods and datasets, while the corresponding values for the extreme ones (3.3 episodes yr^{-1}) are observed over the central Mediterranean Sea for MODIS-Terra (Mar. 2000 – Feb. 2013). In general, there is similar spatial variability between Terra and Aqua, though slightly lower maximum frequencies are found for Aqua. Although dust episodes occur rarely across the northern parts of the study region (<1 and 0.5 episode yr^{-1} for strong and extreme episodes), their occurrence proves that dust particles can be transported far away from their sources, up to the central (e.g. Klein et al., 2010) or even northern (e.g. Bègue et al., 2012) European areas under favorable meteorological conditions. A noticeable difference between the two study periods and platforms is that relatively high frequencies of extreme DD episodes are recorded in more northern latitudes in the Mediterranean Sea, i.e. up to 43° N, according to MODIS-Terra over Mar. 2000 – Feb. 2013, while they are restricted south of 40° N parallel for MODIS-Aqua during 2003-2012. In order to investigate this difference in detail we have also applied the satellite algorithm, over the period 2003–2012, i.e. that of Aqua, using MODIS-Terra retrievals as inputs. Through this analysis (results not shown here), it is evident that there is a very good agreement between the satellite algorithm's outputs, for the periods Mar. 2000 – Feb. 2013 and 2003-2012, revealing a constant dust episodes' regime. Therefore, the

discrepancy appeared between MODIS-Terra and MODIS-Aqua spatial distributions, is attributed to the diurnal variation of factors regulating the emission and transport of dust particles from the sources areas. Schepanski et al. (2009), analyzed the variation of the Saharan dust source activation throughout the day, based on MSG-SEVIRI satellite retrievals, reporting that dust mobilization is more intense in the local early morning hours after sunrise. Note, that desert dust episodes over the period Mar. 2000 – Feb. 2013 have been identified based on observations retrieved by the Terra satellite, which flies over the study region around noon in contrast to Aqua which provides aerosol measurements at early afternoon hours.

The analysis has been also repeated (results not shown here) considering as inputs to the satellite algorithm only *AODs* associated with cloud fractions lower/equal than 0.8, in order to investigate possible modifications to our results (Figs 2 and 3) due to the cloud contamination effect. As it concerns the strong DD episodes, the geographical distributions are similar with those of Fig. 2, but the maximum frequencies (recorded in Morocco) are higher by up to 2 episodes yr^{-1} and 0.3 episodes yr^{-1} for the MODIS-Terra (Mar. 2000 – Feb. 2013) and MODIS-Aqua (2003-2012) data set, respectively. On the contrary, in the case of extreme DD episodes the maximum frequencies decrease to 2.5 episodes yr^{-1} for the period 2003-2012 and they shift southwards, namely over the northern coasts of Africa, while over the central parts of the Mediterranean Sea are lower than 1 episode yr^{-1}.

The maps of intensities (in terms of AOD_{550nm}) of DD episodes (Figure 3), show that for both study periods and satellite platforms, the maximum intensities are over the Gulf of Sidra and the Libyan Sea, along the northern African coasts. These intensities reach *AODs* up to about 1.5 for strong and 4.1 for extreme episodes, while the minimum ones (values down to 0.25-0.46) are recorded in the northern and western Mediterranean parts. Note that dissimilar spatial patterns appear between the geographical distributions of DD episodes' frequency and intensity, indicating that these two features are determined by different factors (e.g. tracks or strength of depressions). Finally, when the cloud contamination is minimized using only *AODs* associated with *CF* lower than 0.8, then the maximum intensities are shifted southwards, across the northern Africa and eastern coasts of the Mediterranean, being lower than 1 and 2 for strong and extreme DD episodes, respectively. Through the rejection of possibly overestimated *AODs* from the dataset, it is found that the threshold levels are decreased (mainly over the most frequently dust affected areas) since both mean and standard deviation values are lower (results not shown here). Nevertheless, even though these *AODs* can be overestimated, in the majority of the cases the collocated AERONET *AODs* are high (but lower than the satellite observations) indicating the occurrence of desert dust outbreaks as it will be shown in Section 4.2.1.4.

The analysis has been also repeated applying the alternative METHOD-B described in Section 3. Just to ensure a longer temporal coverage, this analysis was done for the period Mar. 2000-Feb. 2013 using MODIS-Terra data. The obtained results for the frequency of occurrence as well as for the intensity of DD episodes are depicted in Figures S1 and S2, respectively, in the supplementary material. The geographical patterns for the frequency of occurrence between the two methodologies are similar; however, the maximum values for the strong and extreme DD episodes can reach up to 13.3 episodes $year^{-1}$ (Fig. S1-i) and 8.1 episodes $year^{-1}$ (Fig. S1-ii), respectively. As it concerns the intensity, the geographical patterns, particularly for the strong DD episodes, are dissimilar and less distinct compared to the corresponding ones obtained with the primary methodology. This difference is attributed to the inclusion of more dust episodes with variable intensity, which leads to a not so clear "signal" when all these episodes are averaged. Based on METHOD-B, the maximum intensities (in terms of AOD_{550nm}) of strong DD episodes can reach up to 1 (Fig. S2-i) while for the extreme episodes (Fig. S2-ii) it can be as large as 3. The main finding, based on the intercomparison of the two methodologies for the identification of DD episodes, is that the frequency of the episodes is higher for the METHOD-B with respect to the primary methodology, while the intensity is decreased. Both facts are expected and can be explained by the lower calculated AOD thresholds with METHOD-B thus yielding more DD episodes of lower intensity.

This introductory analysis was conducted in order to specify the locations where the Mediterranean dust outbreaks occur more frequently and are more intense. Nevertheless, this paper is orientated to the description of the intense Mediterranean dust outbreaks' vertical structure as well as to the detailed assessment of the applied satellite algorithm for the identification of DD episodes in order to consolidate our methodology, and not to emphasize on their regime, which has been thoroughly analyzed in Gkikas et al. (2013).

4.2 Comparison of the satellite algorithm's outputs against AERONET and PM_{10} measurements

The ability of the satellite algorithm to identify satisfactorily DD episodes, is tested against ground measurements from 109 AERONET (Fig. 4, orange squares) and 22 PM_{10} (Fig. 4, green triangles) stations located in the broader Mediterranean area. This is an extended and thorough comparison which exceeds largely a similar one done for the outputs of the previous version of satellite algorithm (2000-2007, Gkikas et al., 2013), but only relying on 9 AERONET stations and using *AOD* and volume size distribution data. Here, the comparison is repeated for the improved algorithm, being extended over a

longer time period, for a much larger number of AERONET stations, and an analysis of more optical properties, namely the Ångström exponent, effective radius, single scattering albedo and asymmetry parameter is made. The comparison is performed for both study periods and satellite platforms (Mar. 2000 – Feb. 2013 for Terra and 2003-2012 for Aqua) while the issue of possible cloud contamination is also considered. However, since the obtained results revealed a very similar performance of the algorithm for both periods and platforms, only the results for the period Mar. 2000 – Feb. 2013 are given here.

In 46 out of 109 AERONET stations, depicted with yellow triangles in Figure 4, we have found at least one strong or extreme dust episode, for which coincident satellite and ground measurements are available. For the specific AERONET stations and episode days, the mean values of the selected AERONET aerosol optical properties have been calculated separately for strong, extreme and all (both strong and extreme) DD episodes identified by the satellite algorithm. Subsequently, these values were compared to the corresponding ones calculated from all the available retrievals (climatological conditions, clim) collected from the 109 Mediterranean AERONET stations, during the period Mar. 2000 – Feb. 2013, aiming at highlighting the effect of episodes on these optical properties. Additionally, in 7 AERONET stations (cyan circles in Figure 4) the intense DD episodes have been identified from ground (AERONET) and the corresponding results are compared with the satellite algorithm outputs (Section 4.2.1.4). Finally, the performance of the algorithm is also tested against surface PM_{10} measurements from 22 stations (Section 4.2.2).

4.2.1 AERONET

4.2.1.1 Aerosol optical depth

During the period Mar. 2000 – Feb. 2013, 346 pixel level intense DD episodes have been identified by the satellite-based algorithm, in which coincident MODIS-Terra and AERONET retrievals are available. It should be noted that AERONET AOD_{550nm} values have been calculated from available AERONET AOD_{870nm} and Ångström exponent data ($\alpha_{440\text{-}870nm}$) by applying the Ångström equation (Ångström, 1929) to match the MODIS AOD_{550nm}. For these intense DD episodes, the comparison between the satellite and ground aerosol optical depths at 550 nm is given in Figure 5. Two similar scatterplots with matched MODIS-AERONET data pairs are given. The first one (Fig. 5 i-a) is resolved by the number of level 2 (L2) measurements of 10 km x 10 km spatial resolution from which the

compared 1^o x 1^o level 3 (L3) *AODs* in the figure are derived. The second scatterplot (Fig. 5 i-b) is resolved by the spatial standard deviation inside the 1^o x 1^o geographical cell (level 3 AODs). Both scatterplots address the issue of level 3 *AOD* sub-grid spatial variability, which is essential when attempting comparisons against local surface-based *AOD* data like the AERONET.

The overall correlation coefficient (R) between MODIS and AERONET *AODs* is equal to 0.505, with the satellite *AODs* being overestimated (bias=0.143). From the overall scatterplots, it is evident the existence of outliers associated with small number of level 2 retrievals (<20, blue color Fig. 5 i-a) and/or high standard deviations (>0.5, yellowish-reddish points, Fig. 5 i-b) inside the L3 grid cell. This finding underlines the role of homogeneity and representativeness of L3 retrievals for the comparison of MODIS *AODs* against AERONET. This role is better visualized in Fig. 5 ii-a, where are presented the computed R values between MODIS level-3 and AERONET *AODs* depending on the number of L2 retrievals from which the L3 products were derived. In general, it is known that the L2 pixel counts range from 0 to 121 while in polar regions (typically around 82° latitude) the maximum count numbers can be even higher due to overlapping orbits and near nadir views intersect (Hubanks et al., 2008). It is clear from our results that the correlation coefficients are gradually and essentially improved, from 0.49 to 0.75, with increasing representativeness of MODIS *AODs*, i.e. increasing counts of L2 retrievals attributed. A similar improvement has been reported by Amiridis et al. (2013) who found a better agreement between MODIS/AERONET and CALIOP aerosol optical depths applying similar spatial criteria. The agreement between MODIS and AERONET also improves when the former *AOD* products are more spatially homogeneous, i.e. when they are characterized by smaller *AOD* standard deviations at the grid-level (from <0.25 down to <0.05, Fig. 5 ii-b). However, our results also indicate that apart from increasing correlation coefficients (up to 0.7-0.8) with increasing level-2 counts and decreasing standard deviations, the number of intense DD episodes is decreased dramatically (about 40-50 for more than 50 counts and standard deviation smaller than 0.05).

In addition, the spectral variation of the AERONET AODs at 7 wavelengths, from 340 to 1020 nm, in climatological and dust episodes conditions has been investigated (results given in Figure S3, supplementary material). The AOD boxplots produced for all the available daily AERONET measurements (orange) and for the corresponding retrievals during strong (cyan), extreme (red) and all DD (green) episodes identified by the satellite algorithm show that the spectral variation of aerosol optical depth decreases in cases of dust episodes, with respect to the "climatological" conditions. This is mainly attributed to the further increasing AOD levels at wavelengths longer than 500 nm (by about 6 times) than in (or near) the visible.

565

566 *4.2.1.2 Aerosol volume size distribution*

567 In Figure 6, are presented the mean aerosol volume size distributions (*AVSDs*) calculated from all
568 available AERONET data (orange curve) as well as under strong (cyan curve), extreme (red curve) and
569 all (green curve) DD episodes conditions. The results are given for Mar. 2000 – Feb. 2013 using
570 MODIS-Terra (346 intense DD episodes) retrievals as inputs to the satellite algorithm. In the
571 climatological curve, two modes are distinct centered at 0.15 μm for the fine mode and 2.24 μm for the
572 coarse mode. There is an about equal contribution of both modes, indicating the coexistence of fine
573 (e.g. urban aerosols) and coarse (e.g. dust aerosols) particles over the broader Mediterranean area. This
574 result is in agreement with previous studies for the Mediterranean (e.g. Fotiadi et al., 2006; Mallet et
575 al., 2013). However, under dust episode conditions, although the *AVSD* still has two modes, there is a
576 dramatic increase of the coarse mode, which strongly dominates. More specifically, the peak of the
577 coarse mode (radius between 1.7 and 2.24 μm) is increased by factors of about 10, 15 and 11 for the
578 strong, extreme and all DD episodes. The differences between the strong and extreme AVSDs are
579 statistically significant (confidence level at 95 %) for almost all size bins (18 out of 22) except bin 1
580 (0.050 μm), 2 (0.065 μm), 6 (0.194 μm) and 7 (0.255 μm). Moreover, it should be noted that the
581 increment factors are slightly decreased when the algorithm operates only with *AODs* associated with
582 cloud fractions less than 0.8 which is reasonable since possible "overestimated" retrievals are masked
583 out from the analysis. Similar modifications in the shape of *AVSD* during dust outbreaks have been
584 pointed out by several studies in the past, either for the Mediterranean region (e.g. Kubilay et al., 2003;
585 Lyamani et al., 2005; Córdoba-Jabonero et al., 2011) or for other dust affected areas of the planet (e.g.
586 Alam et al., 2014; Cao et al., 2014).

587 *4.2.1.3 Size optical properties, single scattering albedo and asymmetry parameter*

588 The accuracy of the DD episodes identification method was further assessed by also using other
589 AERONET aerosol optical properties than *AOD*, namely the Ångström exponent (α) and the effective
590 radius (r_{eff}), able to provide information about particles' size. For both aerosol optical properties, the
591 boxplots for all the available AERONET retrievals as well as for the corresponding data during strong,
592 extreme and all DD episodes, have been produced and depicted in Figure S4 (supplementary material).

593 Based on our results, the appropriateness of the applied methodology is confirmed by the drastic
594 reduction of α and increase of r_{eff} values when dust outbreaks occur. When all available AERONET
595 retrievals are considered (clim), the majority (>75%) of α values is higher than 1.04 indicating the

strong presence of fine particles in the study domain. On the contrary, during intense dust episodes the majority of the corresponding values for all and strong DD episodes are lower than 0.54 while for the extreme ones are lower than 0.36. Such low Ångström exponent values, attributed to transported mineral particles from the northern African deserts (Pace et al., 2006), have been reported also in previous studies (e.g. Tafuro et al. 2006; Basart et al., 2009). The existence of coarse aerosols is also confirmed by the increase of r_{eff} values under intense DD conditions compared to the climatological levels. For all DD episodes, the 75% of r_{eff} values is higher than 0.55 μm reaching up to 1.4 μm, while the mean and the median values are equal to about 0.73, compared to about 0.37 for the climatological conditions. These values are even higher when extreme DD episodes are concerned.

Moreover, the spectral variations of the averaged AERONET single scattering albedo (*SSA*) and the asymmetry parameter (g_{aer}) are also studied. During intense dust outbreaks the shape and magnitude of spectral *SSA* (Figure S5-i) and g_{aer} (Figure S5-ii) are modified compared to the climatological conditions. The spectral curves of both parameters become less and more flattened during dust episodes for *SSA* and g_{aer}, respectively. For *SSA*, the steepening results from decreasing values in the visible and increasing values in the near-infrared (by up to 0.04, reaching 0.97 at 1020 nm). The flattening for g_{aer} arises from smaller and larger increments in visible and near-infrared values, by up to 0.04 and 0.07, respectively. The differences between strong and extreme DD episodes SSA spectral curves are statistically significant at 95 % confidence level only at 870 and 1020 nm. On the contrary, the corresponding differences for the g_{aer} are statistically significant in all wavelengths. Our results are in agreement with those presented for *SSA* by Mallet et al. (2013) in the Mediterranean and for g_{aer} by Alados-Arboledas et al. (2008) during a dust episode over the southeastern parts of Spain.

4.2.1.4 Intercomparison of surface-based and satellite algorithms used for the identification of the desert dust episodes

Despite their great usefulness, satellite aerosol retrievals still suffer from uncertainties, and generally are considered as inferior to surface-based similar products, which are taken as the reference. In order to examine this degree of uncertainty and to verify the successful performance of the algorithm, we also tested using it along with AERONET retrievals. This has been made for 7 Mediterranean AERONET stations, depicted with cyan circles in Figure 4, during the periods for which ground retrievals are available (Table 1). The selection of the AERONET stations was based on: (i) data availability (see last column of Table 1), (ii) their location (i.e. near to the Northern African and

627 Middle East deserts) and (iii) the inclusion of sites where the aerosols' regime is complex (e.g. El
628 Arenosillo, FORTH Crete). The intense DD episodes were identified following the methodology
629 described in section 3, but using only *AOD* at 870 nm, $\alpha_{440\text{-}870nm}$ (lower/equal than 0.7) and r_{eff} (higher
630 than 0.6) as criteria, based upon their availability from AERONET. Subsequently, the algorithm was
631 also operated again using satellite (MODIS-Terra, OMI-Aura, EP-TOMS) input data for the days with
632 available data in each of the 7 AERONET stations.

633 In Figure 7, we present the overall scatterplots between satellite and ground *AODs* when intense
634 DD episodes have been identified based on the ground (left column) and the satellite (right column)
635 algorithm. Colors in Figs. 7 i-a, 7 ii-a, 7 iii-a represent the associated MODIS-Terra Ångström
636 exponent, effective radius and day cloud fraction (CFD) retrievals, respectively. In Figs. 7 i-b and 7 ii-b
637 colors represent the AERONET Ångström exponent and effective radius, respectively, while in Figure
638 7 iii-b represent the day cloud fraction observations derived by MODIS-Terra. Through this approach it
639 is feasible to assess furthermore the performance of the satellite algorithm, specify its drawbacks and
640 check the validity of the defined thresholds (green boxes in Figure 1).

641 It is apparent that the agreement between MODIS-Terra and AERONET *AODs* is better when DD
642 episodes are identified from the ground, as shown by the increased correlation coefficients (from 0.521
643 to 0.704), increased slopes (from 0.6 to 0.9-1.0) and decreased biases (from 0.16 to -0.03). In
644 particular, when DD episodes are identified from space, the MODIS-Terra *AOD* retrievals are
645 overestimated (bias=0.163) with regards to AERONET, particularly at low *AOD* values (<0.5). In both
646 algorithms, the highest overestimations are associated with cloud fractions higher than 0.7 due to the
647 possible contamination of the satellite *AODs* by clouds (Figure 7 iii-a, iii-b). Given that DD episodes'
648 identification based on AERONET retrievals is more efficient, we have used these results in order to
649 check the validity of the defined thresholds for α, *AI*, *FF* and r_{eff} (green boxes in Figure 1) used in the
650 satellite algorithm. For each aerosol optical property, it has been calculated the percentage of intense
651 DD episodes for which the corresponding satellite observations are below or above the defined
652 thresholds, depending on the parameter. The results given in Table 2 are satisfactory, since the
653 percentages range from 87 to 99%, and confirm the validity of the defined thresholds.

654 The scatterplots in Figs. 7 i-b and ii-b also reveal some weaknesses of the satellite-based algorithm.
655 More specifically, it is found that for few DD episodes identified by the satellite algorithm the
656 corresponding AERONET Ångström exponent and effective radius values are higher than 1 and
657 smaller than 0.4, respectively. These values indicate a predominance of fine particles instead of coarse

ones as it would be expected for desert dust aerosols. In order to quantify the number of misclassified pixel level intense DD episodes by the satellite algorithm, we have computed the percentage of cases for which the AERONET α values are higher than 1 (15%) and r_{eff} values are lower than 0.4 (17.7%). Also, we have repeated these calculations for all DD episodes (Section 4.2.1.1) and the corresponding percentages were found to be equal to 11.8% and 14.5%, respectively. These misclassifications of the satellite algorithm occur in AERONET stations (e.g. Thessaloniki, Rome, Avignon) with a strong presence of anthropogenic aerosols (Kazadzis et al., 2007; Gobbi et al., 2007; Querol et al., 2009a; Yoon et al., 2012). Some misclassifications also occur in AERONET stations (e.g. Evora, El Arenosillo, FORTH CRETE) with mixed (natural plus anthropogenic) aerosol loads (Fotiadi et al., 2006; Toledano et al., 2007b; Hatzianastassiou et al., 2009; Pereira et al., 2011). Over these areas, there are converging air masses carrying particles of different origin, as shown by performed back-trajectories analyses (results are not shown here) using the HYSPLIT (HYbrid Single-Particle Lagrangian Integrated Trajectory) model (Draxler and Rolph, 2015). Nevertheless, it must be mentioned that DD episodes' misclassifications can be attributed to the lower accuracy of MODIS aerosol size retrievals over land (Section 2.1.1).

4.2.2 PM_{10} and dust contribution

The satellite algorithm's outputs, apart from AERONET retrievals, have been also compared against ground PM_{10} concentrations ($\mu g\ m^{-3}$) measured in 22 Mediterranean stations (green triangles in Figure 4).

First, for each station, the number of intense DD episodes was calculated, for which coincident satellite and ground measurements (total PM_{10}) are available (Figure 8-i). The number of concurrent DD episodes varies from 3 to 53, being in general decreasing from southern to northern stations. For 14 out of 22 stations, where at least 10 intense DD episodes were identified by the satellite-based algorithm, we have computed the correlation coefficients between satellite *AODs* and surface total PM_{10} concentrations (Fig. 8-ii). The highest R values (up to 0.8) are recorded in the central and eastern parts of the Mediterranean while the lowest ones are found in the western stations. It must be noted that the correlation coefficients are affected by outliers, because of the limited number of DD episodes in each station, highlighting the sensitiveness of the intercomparison. Such outliers can be expected when satellite-based columnar *AODs* and surface-based PM_{10} data are compared, since satellite *AODs* are representative for the whole atmospheric column in contrast to in-situ PM measurements which are

689 more representative for the lowest part of the planetary boundary layer affected also by local factors.
690 Therefore, the vertical distribution of desert dust load, as it will be presented in the next sections, can
691 determine the level of agreement between satellite *AODs* and surface PM concentrations. Another
692 influencing factor can be cloud contamination of MODIS *AOD*.

693 The identification method by the satellite algorithm can be considered as correct when dust PM_{10}
694 concentrations are higher than zero (i.e. dust has been recorded at the station). According to this, the
695 ratio between the number of non-zero dust PM observations and the number of DD episodes
696 (coincident satellite-derived DD episodes and total PM_{10} measurements) for each station is defined as
697 success score. The calculated success scores (Figure 8-iii) vary from 68% (Monagrega, northeastern
698 Spain, 28 episodes) to 97% (Boccadifalco, Sicily, 33 episodes) confirming the appropriateness of the
699 DD episodes' identification. In the majority of stations, the contribution of dust particles to the total
700 burden (Figure 8-iv) is above 50%, ranging from 44% (Zarra, Spain) to 86.8% (Ayia Marina, Cyprus).
701 In order to complete our analysis we have also calculated the mean (Figure 8-v) and the median (Figure
702 8-vi) dust PM_{10} concentrations for the identified intense DD episodes in each station. The mean PM_{10}
703 concentrations mainly vary between 20 and 50 μg m^{-3}, being higher in the southern stations, as
704 expected. The minimum mean value (17 μg m^{-3}) was recorded in Censt (Sardinia) and the maximum
705 one (223 μg m^{-3}) in Ayia Marina (Cyprus). Our values are much higher than the corresponding ones in
706 Querol et al. (2009b), who obtained that the mean levels of mineral matter in PM_{10} during dusty days
707 range from 8 to 23 μg m^{-3} based on ground concentrations derived by 21 Mediterranean stations. These
708 differences are reasonable since here only intense desert dust outbreaks associated with high aerosol
709 optical depths are considered. Finally, the median PM_{10} concentrations are lower compared to the
710 average ones, indicating that outliers (cases with extremely high *AOD* or PM_{10}) can alter the results,
711 attributed to the fact that both parameters' (*AOD* and PM_{10}) distributions are not Gaussians. For this
712 reason the highest differences are found in Finokalia (Crete) and Agia Marina (Cyprus), where the
713 maximum daily PM_{10} concentrations, equal to 690 and 1291 μgm^{-3}, respectively, were recorded during
714 an intense dust outbreak affected the eastern Mediterranean on 24 and 25 February 2006.

715

716 4.3 Vertical structure of the Mediterranean desert dust outbreaks

717 The ability of the developed satellite algorithm to detect intense dust episodes has been proved
718 adequate through the comparison analysis against AERONET retrievals and PM_{10} concentrations.
719 Nevertheless, its main limitation is that it uses columnar satellite retrievals and not vertical resolved

data prohibiting thus the description of the vertical structure of these dust outbreaks. In order to address this issue, the CALIOP-CALIPSO retrievals are used as a complementary tool to the satellite algorithm's outputs. First, for the identified dust episodes by the satellite algorithm, the spatially and temporally collocated vertically resolved CALIOP lidar observations are selected. For these cases and for each 1° x 1° grid cell, we have divided the lower troposphere, up to 8 km, in 16 layers of 500 meters height. In this way, 14400 boxes of 1° x 1° surface area and 500 meters height have been produced. Then, for each one of them, we have calculated the overall number of dust and polluted dust observations (hereafter named as dust) according to the aerosol subtyping scheme of the CALIOP Vertical Feature Mask (VFM). Note that dust and polluted dust were chosen because in previous studies (Mielonen et al., 2009) they were shown to be the best two defined aerosol types among the other ones classified by the CALIOP VFM. Nevertheless, in case of polluted dust, Burton et al. (2013) reported that dust particles can be mixed with marine aerosols instead of smoke or pollution as assumed by the VFM retrieval algorithm. In our study, more than 95% of the aerosol type records were pure dust, for the collocated cases between the satellite algorithm and CALIPSO observations. In addition, in the majority of the defined boxes, the percentage of dust from the overall observations is higher than 70%, confirming furthermore the validity of the algorithm DD episodes' identification procedure. This is an excellent proof of the successful identification of DD episodes by the satellite algorithm, since CALIOP-CALIPSO is an independent and vertically resolved platform and database. Thereby, CALIOP vertical observations were subsequently used to examine the vertical structure of dust outbreaks.

In order to analyze the intensity of desert dust outbreaks at different altitudes in the troposphere, the CALIOP data of the total backscatter coefficient at 532 nm (β_{532nm}) have been also acquired. For each box, the average β_{532nm} values have been calculated from all the available CALIOP measurements (day and night), for the identified intense dust episodes by the satellite algorithm. More specifically, the average β_{532nm} values were calculated for the dust observations based on the CALIOP VFM associated with CAD scores ranging from -100 to -20, as it has been proposed by Winker et al. (2013) for discriminating aerosol from clouds. The selection of β_{532nm} values instead of extinction coefficients ensures that incorrect lidar ratio assumptions in the CALIOP retrieval algorithm do not affect our results. In the literature, it has been documented that the CALIOP lidar ratio is underestimated over the northern African deserts and the surrounding areas affected by Saharan dust particles, leading to an underestimation of the columnar *AOD* compared to MODIS and AERONET retrievals (Redemann et al., 2012; Schuster et al., 2012). Amiridis et al. (2013) stated that an increase of the lidar ratio from 40

752 to 58 sr, along with a series of post-corrections in the CALIOP retrievals and the implementation of
753 several criteria concerning the cloud coverage and the spatial representativeness, can improve
754 substantially the agreement between MODIS-Aqua/AERONET and CALIOP observations.

755 It should be noted that in the present work, we have analyzed all the available CALIOP overpasses
756 (~ 10000) over the study region, during the period Jun. 2006 – Feb. 2013. For brevity reasons,
757 however, only the obtained results based on MODIS-Terra retrievals are presented here, since similar
758 findings are drawn for MODIS-Aqua (Jun. 2006 – Dec. 2012). Moreover, the analysis (results are not
759 shown here) has been made separately for the identified strong and extreme DD episodes without
760 revealing remarkable differences in the geometrical characteristics of dust outbreaks. Nevertheless, the
761 β_{532nm} values are higher for the extreme DD episodes being consistent with the discrimination of dust
762 episodes' intensity (in terms of *AOD*) which is applied to the satellite algorithm. In order to facilitate
763 the visualization of our results, for each column (1° x 1° spatial resolution) and latitudinal/longitudinal
764 zone (1° degree), we have calculated the overall number of dust observations and the associated
765 weighted averages of β_{532nm}, depending on the projection plane (latitudinal, longitudinal and columnar),
766 according to dust observations in each box. For both parameters, the analysis has been made on an
767 annual and seasonal basis and the corresponding results are discussed in Sections 4.3.1 and 4.3.2,
768 respectively.

769

770 *4.3.1 Annual characteristics*

771 In Figure 9, are presented the three dimensional structures of the CALIOP overall dust observations
772 (Fig. 9-i) and the associated total backscatter coefficients at 532 nm (Fig. 9-ii), during intense dust
773 episodes conditions, over the broader Mediterranean area, for the period Jun. 2006 – Feb. 2013. From
774 the latitudinal projection in Fig. 9-i, it is evident that dust particles are mainly detected between 0.5 and
775 6 km, and more rarely up to 8 km, between the parallels 32° N and 38° N. The number of dust
776 observations is increased at higher altitudes with increasing latitudes, up to 40° N, while the altitude
777 range (thickness) where these records are detected is gradually reduced from 4 to 2 km. At northern
778 latitudes, the CALIPSO dust records are drastically reduced and are mainly observed between 1 and 4
779 km. The ascending mode of the transported mineral particles over the Mediterranean is attributed to the
780 prevailing low pressure systems, which mobilize and uplift dust particles from the source areas across
781 the Sahara Desert and the Arabian Peninsula. Dust aerosols are transported over the planetary boundary
782 layer (Hamonou et al., 1999) due to the upward movement of dry and turbid air masses (Dulac et al.,

783 1992), while the prevailing synoptic conditions determine also the spatial and temporal characteristics
784 of desert dust outbreaks over the Mediterranean (Gkikas et al., 2014).

785 In general, our results are in agreement with previous studies, based on lidar profiles, which have
786 been made in several Mediterranean sites. More specifically, Papayannis et al. (2008) found that dust
787 layers, over the EARLINET Mediterranean stations, extend from 0.5 to 10 km above mean sea level,
788 their center of mass is located between 2.5 and 3.5 km and their thickness ranges from 2.1 to 3.3 km.
789 Hamonou et al. (1999) reported that dust layers are mainly detected between 1.5 and 5 km based on
790 lidar measurements in the northwestern and northeastern Mediterranean. According to di Sarra et al.
791 (2001), who studied the Saharan dust intrusions in Lampedusa (central Mediterranean) for the period
792 May-June 1999, dust particles can be detected up to 7-8 km, which is in line with our findings for the
793 corresponding latitudinal zones (35° N - 36 ° N). Balis (2012), analyzed 33 Raman/lidar profiles of
794 Saharan dust intrusions over Thessaloniki (northern Greece), and found that the mean base and top of
795 dust layers were equal to 2.5±0.9 and 4.2±1.5 km, respectively.

796 As to the variation of vertical extension with longitude (Fig. 9-i), it is revealed that the base height
797 of dust layers is decreased towards the eastern parts of the study region. In the western Mediterranean,
798 the mineral particles are mainly detected between 2 and 6 km while over the central and eastern
799 Mediterranean the corresponding altitudes are equal to 0.5 and 6 km, respectively. It is well known,
800 that dust is transported over the western Mediterranean mainly in summer (e.g. Moulin et al., 1998)
801 favored by low pressure systems located over the northwestern Africa (Gkikas et al., 2014) and the
802 enhanced thermal convection, uplifting effectively dust aerosols at high altitudes in the troposphere.
803 Moreover, air masses carrying dust particles are "convected" towards higher altitudes due to the
804 existence of the Atlas Mountains Range. Therefore, the combination of strong convective processes
805 over North Africa along with topography can explain the identification of dust aerosols at higher
806 tropospheric levels over the western Mediterranean. It is the presence of mineral particles at high
807 altitudes in western Mediterranean that can explain the poor-to-moderate agreement between PM_{10}
808 concentrations and MODIS *AODs* found in the Iberian Peninsula (Fig. 8-ii). In order to give a better
809 insight to how the dust outbreaks' vertical extension can affect the level of agreement between
810 columnar AOD satellite retrievals and ground PM_{10} concentrations, emphasis is given at specific dust
811 events and the relevant findings will be discussed in section 4.4. In the central and eastern parts of the
812 Mediterranean basin, air masses carrying African dust aerosols travel at lower altitudes over Africa
813 because of absence of significant topographical objects on their route, as suggested by Pey et al.
814 (2013).

Previous studies have shown that dust layers over the Mediterranean are characterized by a multilayered structure (e.g. Hamonou et al., 1999; Mona et al., 2006; Papayannis et al., 2008). This is also depicted in the longitudinal projection of Figure 9-i, where several dust layers of different base/top altitudes and geometrical thicknesses are detected. In general, the base heights vary from 0.5 to 2 km, the top heights from 4 to 6 km and the thicknesses from 1 to 4 km. The majority of common observations between the CALIOP profiles and the identified intense DD episodes by the satellite algorithm are recorded over the maritime parts of the study region (bottom map of Fig. 9-i). The maximum number of CALIOP dust observations (~ 19000) is recorded along the Atlantic coasts of Morocco, but high numbers (about 10000 – 15000) are also found across the northern African coasts.

Apart from the CALIOP dust observations, we have also analyzed the associated β_{532nm} values at the defined altitude ranges in order to describe the variation of intensity of the desert dust episodes with height over the Mediterranean (Fig. 9-ii). The maximum backscatter coefficients (up to 0.006 km^{-1} sr^{-1}) are observed below 2 km, being increased towards the southern edges (30° N - 34° N) of the study region, where their source areas are found. This is explained by the fact that dust particles due to their coarse size and large mass, are efficiently deposited and for this reason they are recorded at higher concentrations near to the source areas and at low altitudes. Nevertheless, the decreasing intensity with height towards the north is not so evident. Thus, high β_{532nm} values (~ 0.004 km^{-1} sr^{-1}) are observed between 2 and 4 km in the latitudinal zone extending from 35° N to 42° N. Though, the uppermost altitudes where relatively high β_{532nm} values gradually decrease from 6 to 4 km, moving from south to north. Any differences in the latitudinal patterns of dust observations and backscatter values (Figs 9-i and 9-ii) can be explained by the fact that β_{532nm} values take into account only the dust records and not the overall observations (all aerosol types).

The decrease of backscatter values at higher altitudes has been pointed out in previous studies where lidar profiles have been analyzed over specific Mediterranean locations (e.g. Mona et al., 2006; Papayannis et al., 2008). Nevertheless, it must be considered that in the aforementioned studies the lidar measurements are valid above the retrieved planetary boundary layer (Matthias et al., 2004) which varies depending on the location and the season (McGrath-Spangler et al., 2013). Despite the good agreement, as it concerns the vertical shape of the β_{532nm} curves, between our findings and the corresponding ones based on ground retrievals, in the present analysis the calculated backscatter coefficients are in general higher, which is reasonable since are considered only cases of intense desert dust outbreaks.

The longitudinal pattern of β_{532nm} profiles (Fig. 9-ii) is less distinct compared to the corresponding one resulted from the latitudinal projection. Relatively high β_{532nm} values (~ 0.004 km^{-1} sr^{-1}) are found between 1 and 5 km over the western Mediterranean, while over the central and eastern parts of the study region the desert dust outbreaks' intensity (~ 0.006 km^{-1} sr^{-1}) is higher below 1.5 km. Among the sub-regions, the backscatter coefficients are higher in the central and eastern Mediterranean, which is also depicted in the bottom map of Fig. 9-ii. It is reminded that higher intensities of dust episodes over the central and eastern Mediterranean have also been noticed based on MODIS retrievals (Figure 3). From the obtained longitudinal projection, it is evident a patchy structure of the total backscatter coefficient profiles, especially in the central and eastern parts, indicating the existence of several dust layers of varying intensities at different altitudes into the atmosphere.

The three dimensional plots of Figures 9-i and 9-ii, have been also reproduced considering all the available dust and polluted dust CALIOP-CALIPSO records, without taking into account the satellite algorithm's outputs (for intense dust outbreaks). The obtained results for the number of observations and β_{532nm} are presented in Figures S6-i and S6-ii, respectively. Note, that for each studied parameter the colorbar scales in Figure 9 and S6 are not identical because the number of observations for dust average conditions (Fig. 6-i) is extremely larger than the corresponding one during intense dust outbreaks (Fig. 9-i) while the opposite is found for the β_{532nm} values (Fig. 9-ii and Fig. 6-i). It is apparent that the latitudinal projections calculated for the intense dust outbreaks (Fig. 9-i) and for all the available CALIOP dust records (Fig. S6-i) reveal different patterns. More specifically, when all available CALIOP dust records are considered, it is found that dust aerosols are mainly confined between 1 and 3 km in the southernmost parts of the study region while the number of observations gradually decreases at higher altitudes and towards northern latitudes (Fig. S6-i). On the contrary, during dust outbreaks, mineral particles are transported over the Mediterranean following an ascending path, as it is depicted in the latitudinal projection of Figure 9-i. Nevertheless, it must be mentioned that over the desert areas there is a full coverage (see bottom map in Fig. S6-i) when all dust CALIOP records are considered in contrast to intense dust outbreaks (see bottom map in Fig. 9-i) attributed to the absence of DT retrievals, used as inputs to the satellite algorithm, over desert areas. The comparison between the longitudinal projections during intense dust outbreaks (Figure 9-i) and during average dust conditions (Fig. S6-i) reveals less remarkable differences than for the latitudinal projections. According to the longitudinal projection of Figure S6-i, in the western Mediterranean, dust layers are confined between 1 and 6 km, while their base and top altitude both decrease down to 0.5 and 4.5 km, respectively, for increasing longitudes. In the easternmost part of the study region, dust

878 layers are mainly confined between 1 and 3 km, while its top height can reach up to 5 km. The intensity
879 of dust loads (in terms of β_{532nm}) is lower than 0.003 km^{-1} sr^{-1} regardless the projection plane for
880 average dust conditions based on CALIOP-CALIPSO lidar profiles (Fig. S6-ii). Moreover, the intensity
881 of dust loads decreases gradually with height as well as from south to north revealing a distinct pattern
882 in all projection planes in contrast to the corresponding ones found during desert dust outbreaks (Fig. 9-
883 ii).

884

885 *4.3.2 Seasonal characteristics*

886 The vertical structure of the Mediterranean desert dust outbreaks has also been analyzed separately
887 for winter (DJF), spring (MAM), summer (JJA) and autumn (SON). The seasonal three dimensional
888 representations of the CALIOP overall dust observations and the associated total backscatter
889 coefficients are depicted in the left and right column of Figure 10, respectively. It must be noted, that
890 for β_{532nm} the colorbars' ranges are common, depending on the projection plane. More specifically, the
891 maximum limits have been set to 0.012 km^{-1} sr^{-1}, 0.014 km^{-1} sr^{-1} and 0.021 km^{-1} sr^{-1} for the latitudinal,
892 longitudinal and bottom map projections, respectively. It should be mentioned that β_{532nm} values can
893 reach up to 0.045 km^{-1} sr^{-1}, but are associated with a very small number of dust observations.

894 The majority (85%) of dust observations is recorded in spring and summer, attributed to the
895 enhanced production rates of mineral particles and the prevailing atmospheric circulation over the
896 source areas and the Mediterranean. According to the latitudinal projections, it is evident a seasonal
897 variability of the intense Mediterranean desert dust outbreaks' geometrical characteristics. Dust
898 particles are detected at higher altitudes (6-7 km) during warm seasons of the year while in winter are
899 mainly detected below 3 km and in autumn are recorded between 2 and 5 km. Nevertheless, it should
900 be mentioned that during these seasons only a small number of pixels (see bottom maps in Figs. 10 i-a,
901 iv-a) is available considering also that clouds prohibit the satellite observations. Note that in spring,
902 dust can be found at low tropospheric levels while in summer it is mainly observed above 1 km
903 highlighting thus the role of topography and the enhanced thermal convection. During the first half of
904 the year, the maximum dust observations are confined between the parallels 31° N and 37° N while
905 during the second one, are shifted northwards in the latitudinal zone extending from 34° N to 40° N.
906 Similar latitudinal projections were also presented by Luo et al. (2015), for the same zonal areas of the
907 study region, who developed a new algorithm to improve CALIOP's ability to detect optically thin dust
908 layers. From the longitudinal projections as well as from the bottom maps, it is evident that the

maximum dust records are found in different Mediterranean sub-regions, depending on the season. The geometrical characteristics, in longitudinal terms, of intense DD episodes affecting the western, central and eastern parts of the Mediterranean are similar to those presented in the annual three dimensional structure (Fig. 9-i) being more frequent in the eastern and central Mediterranean in winter, spring and autumn and in the western and central Mediterranean in summer.

The seasonal patterns of β_{532nm} latitudinal projections are different than those for the dust observations, while they also differ among the four seasons. The intensity of winter DD episodes is stronger (up to 0.012 km^{-1} sr^{-1}) below 2 km and at the southern parts of the study region. According to the longitudinal and bottom map projections, these episodes take place over the central and eastern Mediterranean Sea but the number of grid cells with coincident CALIOP observations and DD episodes is limited. In spring, the highest β_{532nm} values (up to 0.006 km^{-1} sr^{-1}) are recorded between the parallels 31° N and 35° N and below 2 km, although, relatively high β_{532nm} values (up to 0.004 km^{-1} sr^{-1}) are found up to 6 km (Fig. 10 ii-b). Moving northwards, over the Mediterranean, dust layers are mainly confined between 2 and 4 km, associated with high β_{532nm} values (up to 0.004 km^{-1} sr^{-1}) in the latitudinal zone extending from 35° N to 43° N. The existence of these elevated dust layers, has been also confirmed by model simulations through specific (Papayannis et al., 2008; 2014) or averaged (Alpert et al., 2004) cross sections of dust concentrations in the central sector of the Mediterranean. This is in accordance with our longitudinal projection (Fig. 10 ii-b), where β_{532nm} is high varying from 0.004 to 0.008 km^{-1} sr^{-1} at these altitude ranges.

In summer, the intensity of dust episodes is smoothly decreased at higher altitudes, where dust layers of considerable β_{532nm} values are also found. More specifically, the highest backscatter coefficients (up to 0.008 km^{-1} sr^{-1}) are recorded near to the surface but also moderate values (up to 0.006 km^{-1} sr^{-1}) are observed between 2 and 5 km, particularly over the southern parts of the study region (Fig. 10 iii-b). Most of these intense DD episodes occur in the western Mediterranean, where the highest β_{532nm} values (up to 0.005 km^{-1} sr^{-1}) are recorded between 2 and 5 km. Over the central and eastern Mediterranean, even higher β_{532nm} values are found (up to 0.014 km^{-1} sr^{-1}) but at lower altitudes (< 1 km). In autumn, the majority of the grid cells of coincident CALIOP profiles and DD episodes identified by the satellite algorithm are located between the parallels 33° N and 41° N. In this latitudinal zone, CALIOP profiles are available over the interior parts of the Iberian Peninsula and over western and central parts of the Mediterranean Sea, near to the northern African coasts. According to the latitudinal projection, β_{532nm} values mainly vary from 0.002 to 0.009 km^{-1} sr^{-1}, revealing an increasing tendency for increasing heights. On the contrary, the total backscatter coefficients do not

show a distinct spatial pattern on the longitudinal projection, due to the limited number of grid cells participating in the calculations. Throughout the year, based on the CALIOP β_{532nm} retrievals, the DD episodes are more intense (up to 0.018 km^{-1} sr^{-1}) in spring, when massive dust loads are transported from the Sahara desert towards the central and eastern parts of the Mediterranean Sea (bottom map in Fig. 10 ii-b).

4.4. Intercomparison of satellite AOD and PM_{10} concentrations for specific desert dust outbreaks

In Section 4.2.2, it has been shown that the agreement between the satellite algorithm's outputs and PM_{10} concentrations is better in the central and eastern Mediterranean with regards to the western parts (Figure 8-ii). This discrepancy has been mainly attributed to the higher altitude of dust layers' base over the western sector of the study domain (Figure 9-i), in relation to the existing areal orography. Here, aiming at addressing how dust layers' geometrical characteristics influence the agreement between columnar AOD satellite and ground PM_{10} measurements, specific desert dust outbreaks that took place over the PM_{10} stations are analyzed. These outbreaks were selected based on concurrent fulfillment of the following criteria: (i) a DD episode must be identified by the satellite algorithm at pixel level (at 1° x 1° gridded cell), (ii) total PM_{10} measurement must be available at the station which lies into the geographical limits of the corresponding grid cell and (iii) CALIPSO flies across the grid cell. These criteria were met for 13 desert dust outbreaks, which took place over 9 PM_{10} stations during the period 2000-2013. Similarities were found among the identified cases and therefore only the results for four desert dust outbreaks of different geometrical characteristics are discussed in the present section. For each case, we have produced the cross sections of the β_{532nm} vertical profiles up to 8 km above sea level (a.s.l.) along the CALIOP-CALIPSO track when the satellite flies near the PM_{10} site (Figures 11-13). Moreover, the corresponding aerosol subtype profiles, acquired from the CALIOP website (http://www-calipso.larc.nasa.gov/products/lidar/browse_images/production/), are provided in the supplementary material (Figures S7-S9). Since the PM_{10} concentrations are available only as daily averages, the optimum solution would be to have the maximum number (2) of CALIOP overpasses near PM_{10} site throughout the day, in order to reduce the temporal inconsistencies between satellite vertical resolved retrievals and ground data. However, in 8 out of 13 desert dust outbreaks this was not feasible.

971 *4.4.1 Case 1: Censt (26th May 2008)*

972 The first study case refers to a desert dust outbreak that took place on 26th May 2008 and affected
973 the station Censt (Lat: 39.064, Lon: 8.457) located in southern Sardinia. At the ground, the measured
974 mean daily total PM_{10} concentration was 19 μg m^{-3} whereas 68% (or 13 μg m^{-3}) of the load consisted of
975 dust particles indicating thus their strong presence in the lowest troposphere. Based on MODIS-Terra
976 retrievals, representative for the whole atmospheric column and grid cell, the aerosol optical depth at
977 550 nm was equal to 0.81. In order to investigate the vertical distribution of the dust outbreak, the cross
978 sections of the β_{532nm} vertical profiles along CALIOP track, near the station, during daytime and
979 nighttime have been reproduced and depicted in Figures 11-i and 11-ii, respectively. In addition, the
980 corresponding aerosol subtype profiles are provided in Figures S7-i and S7-ii in the supplementary
981 material. During night, it is evident the predominance of a well-developed dust layer mixed with
982 polluted aerosols (Figure S7-i) extending from surface up to 5 km a.s.l. between the parallels 33° N and
983 38° N, while near the station its top is lowered down to 3 km (left side of Figure 11-i). Moreover, the
984 β_{532nm} values range mainly from 0.002 to 0.003 km^{-1} sr^{-1} without revealing remarkable variations, thus
985 indicating a rather compact dust layer. According to the daytime CALIOP overpass (Figure 11-ii), a
986 pure dust layer (Figure S7-ii) is confined between surface and 4 km, affecting the surrounding area of
987 the station, while its intensity (in terms of β_{532nm}) varies slightly from 0.0015 to 0.002 km^{-1} sr^{-1}.
988 Nevertheless, due to the background solar illumination, leading thus to a lower signal-to-noise ratio
989 (Nowottnick et al., 2015), the "borders" of the dust plume during daytime are not so distinct in contrast
990 to nighttime. According to the obtained results, the ground-based measurements are able to capture
991 satisfactorily the dust event when its load is equally distributed in the lowest tropospheric levels,
992 resulting thus to a good agreement between MODIS and PM_{10} observations.

993

994 *4.4.2 Case 2 and 3: Els Torms (16th July 2008) and San Pablo (12th September 2007)*

995 Two dust events that affected Els Torms (NE Spain, Lat: 41.395, Lon: 0.721) and San Pablo
996 (central Spain, Lat: 39.525, Lon: -4.353) on 16th July 2008 and 12th September 2007, respectively, are
997 studied here. The daily averages of the total PM_{10} concentrations were equal to 16 and 30 μg m^{-3},
998 respectively, whereas the dust particles' contribution (dust PM_{10}) to the total amount was zero in Els
999 Torms and 33 % in San Pablo. On the contrary, the MODIS-Terra level 3 AOD retrievals were high
1000 and equal to 0.56 (Els Torms) and 0.64 (San Pablo), indicating the existence of dust aerosols according
1001 to the satellite algorithm's classification method. In order to give a better insight, aiming at describing

the discrepancies between MODIS-Terra AOD and PM_{10} concentrations, we have reproduced the cross sections of the total backscatter at 532 nm when CALIPSO flies, during daytime, near Els Torms (Figure 12-i) and San Pablo (Figure 12-ii). The corresponding profiles of the CALIOP aerosol classification scheme are also available in Figures S8-i and S8-ii. In Els Torms, where the dust PM_{10} concentration was zero, a dust layer (Figure S8-i) with its base at 3.5 km a.s.l. and its top at 5 km a.s.l., is recorded by the CALIOP lidar between the parallels 41° N and 43° N. The intensity of the elevated dust layer, in terms of β_{532nm}, varies from 0.002 to 0.004 km^{-1} sr^{-1} (Figure 12-i). Through CALIOP lidar profiles, it is confirmed the existence of a dust layer aloft, which cannot be captured by the PM_{10} measurements in contrast to the MODIS spectroradiometer. In San Pablo, where the dust particles' contribution to the total PM_{10} load was equal to 33 %, a dust layer abuts the ground extending up to 5-6 km ASL, whereas the dust plume covers a wide range, in latitudinal terms, from the sub-Sahel to the Celtic Sea, affecting the Iberian Peninsula (Figure S8-ii). Nevertheless, the intensity of the dust layer, over the surrounding area of the station, differs with altitude being higher between 2.5 and 5 km a.s.l. (0.004 to 0.007 km^{-1} sr^{-1}) and lower between ground and 2 km a.s.l. (<0.003 km^{-1} sr^{-1}), as it is depicted in the middle of Figure 12-ii. The two studied cases here differ from Case 1 (Section 4.4.1) either with regards to the position of the elevated dust layer (Els Torms) or to its vertical distribution (San Pablo), which explains the poor agreement between satellite columnar AOD retrievals (MODIS) and ground PM_{10} concentrations.

4.4.3 Case 4: Agia Marina (25th February 2007)

The case studied here, namely the desert dust outbreak recorded in Agia Marina (Cyprus, Lat: 35.039, Lon: 33.058) on 25th February 2007, is the strongest one among the selected cases. More specifically, the daily average of the dust PM_{10} concentration was equal to 134 μg m^{-3} accounting for the 92 % of the total PM_{10} measured amount at the station, which is indicative of the strong predominance of dust particles in the lowest troposphere. The MODIS-Terra level 3 AOD value for the grid cell to which the station it is found, is high and equal to 1.04. According to the CALIOP aerosol classification scheme, during nighttime, a shallow low-elevated dust layer mixed with polluted or marine aerosols is heading towards the station, whereas above the PM_{10} site (Agia Marina) extends from close to the ground up to 9 km a.s.l., comprising only pure dust aerosols (Figure S9). The main part of the dust layer, in the surrounding area of the station, is confined between 2.5 and 4 km a.s.l.

where the maximum β_{532nm} values (up to 0.006 km^{-1} sr^{-1}) are observed (Figure 13). Also, similar β_{532nm} values are recorded below 1 km a.s.l.; however, the dust layer is not well represented in the cross section of the CALIOP β_{532nm} vertical profiles due to the total attenuation of the lidar beam by clouds (located between 3 and 4 km a.s.l.) superimposed to the low-elevated dust layer.

5. Summary and conclusions

This study aims at describing the vertical structure of intense desert dust outbreaks affecting the broader Mediterranean basin. To achieve this target, an updated version of an objective and dynamic algorithm, which has been introduced by Gkikas et al. (2009; 2013), has been applied for the identification of strong and extreme desert dust episodes, over the period Mar. 2000 – Feb. 2013. For its operation, a group of optical properties, retrieved by satellite sensors (MODIS-Terra/Aqua, EP-TOMS and OMI-Aura) on a daily basis, is used, providing information about aerosols' load, size and nature. Briefly, the satellite algorithm consists of three parts; at the first one are computed the mean *AOD* value (*Mean*) and the associated standard deviation (*Std*) for the whole study period in each grid cell of 1° x 1° spatial resolution, at the second one the identified aerosol episodes are classified based on their intensity to strong and extreme ones. Finally, at the third part the identified aerosol episodes are categorized as desert dust episodes, separately over land and sea. Through this approach the selected dataset consists only of intense desert dust episodes since their intensity (expressed in terms of AOD_{550nm}) is higher/equal than *Mean + 2*Std*. The DD episodes have also been determined by applying an alternative second methodology (METHOD-B) which excludes dust-affected cases identified based on the criteria set concerning the aerosol size related optical properties.

Based on the satellite algorithm's outputs, an overall view about the regime of Mediterranean desert dust outbreaks is presented for the periods Mar. 2000 – Feb. 2013 (MODIS-Terra) and 2003-2012 (MODIS-Aqua). The main findings concerning the intense DD episodes' frequency (in terms of episodes yr^{-1}) and intensity (in terms of *AOD* at 550nm) are the following:

- Strong DD episodes occur more frequently (up to 9.9 episodes yr^{-1}) in the western Mediterranean while the extreme ones occur more frequently (up to 3.3 episodes yr^{-1}) over the central parts of the Mediterranean Sea, when the satellite algorithm operates with MODIS-Terra retrievals.

- The intensity of strong and extreme DD episodes, in AOD terms, can reach to 1.5 and 3-4, respectively, over the central and eastern parts of the Mediterranean Sea, near off the northern African coasts.
- Slightly lower frequencies and higher intensities are found for the period 2003-2012, when the satellite algorithm operates with MODIS-Aqua retrievals.
- Through the intercomparison between the two applied methodologies, it is revealed that the geographical patterns of frequency of occurrence are similar both for strong and extreme DD episodes; however, higher frequencies are found based on METHOD-B.
- Based on METHOD-B, the DD episodes' intensities are decreased whereas the geographical patterns for the strong DD episodes are not so distinct compared to the corresponding results obtained by the default version of the satellite algorithm.
- The similarity between the outputs of the algorithm using the two methodologies shows the consistency of the algorithm and the validity of its concept.

Through the comparison of the satellite algorithm against surface measurements derived from 109 AERONET and 22 PM_{10} stations, it is found that:

AERONET

- The correlation coefficient between MODIS and AERONET *AODs* is increased from 0.505 to 0.750 when level 3 grid cells with higher sub-grid spatial representativeness and homogeneity are considered.
- According to the AERONET volume size distributions, it is evident the predominance of the coarse mode with a peak (~ 0.25 $\mu m^3\ \mu m^{-2}$) for particles radii between 1.70 and 2.24 μm, in case of intense DD episodes.
- The appropriateness of DD episodes' identification method applied to the satellite algorithm is confirmed since the majority (>75%) of AERONET $\alpha_{440\text{-}870nm}$ and r_{eff} values are lower than 0.54 and higher than 0.55 μm, respectively.
- About 15% of the pixel level intense DD episodes are misclassified by the satellite algorithm and these drawbacks are encountered in AERONET stations where the aerosol load is dominated either by fine particles or by complex aerosol types.

PM_{10} and dust contribution

- The agreement between surface and satellite measurements is better over the central and eastern Mediterranean stations.
- On a station level, the percentage of the intense DD episodes, for which a dust contribution to PM_{10} surface concentration has been recorded, varies from 68% (Monagrega, northeastern Spain) to 97% (Boccadifalco, Sicily).
- In the majority of stations, dust particles contribute more than 50% of the total amount reaching up to 86.8% (Ayia Marina, Cyprus).
- The mean PM_{10} concentration levels mainly vary from 20 to 50 μg m^{-3} reaching up to 223 μg m^{-3} in Ayia Marina (Cyprus).

In order to describe the vertical structure of the intense Mediterranean dust outbreaks, the CALIOP vertical profiles of aerosol subtyping and total backscatter coefficient at 532 nm, are used as a complementary tool to the identified intense DD episodes by the satellite algorithm. Through this synergistic approach it is found that:

- Dust particles are mainly detected between 0.5 and 6 km, following an ascending mode, up to 40º N, leaving from the source areas and transported towards the Mediterranean.
- Over the western Mediterranean, the dust layers are mainly observed between 2 and 6 km while their base height is decreased down to 0.5 km for increasing longitudes.
- During the warm period of the year, dust particles are uplifted at higher altitudes (up to 8 km).
- In summer, the transported dust loads over the western Mediterranean are recorded above 1 km and in spring at lower altitudes over the central and eastern parts of the study region. This behavior underlies the role of topography (e.g. Atlas Mountains) and the enhanced thermal convection.
- The intensity of dust outbreaks, in terms of β_{532nm}, is maximized (up to 0.006 km^{-1} sr^{-1}) below 2 km and at the southern parts (30° N - 34° N) of the study region.
- In spring, considerably high β_{532nm} values (~ 0.004 km^{-1} sr^{-1}) are observed between 2 and 4 km in the latitudinal zone extending from 35° N to 42° N.
- Moderate-to-high β_{532nm} values are observed up to 6 km, near to the source areas, while the top of dust layers is gradually decreased down to 4 km towards northern latitudes.
- From the longitudinal projection of β_{532nm}, it is evident that DD episodes are more intense (~ 0.004 km^{-1} sr^{-1}) between 1 and 5 km in the western Mediterranean, while over the central and eastern sectors, the maximum intensities (~ 0.006 km^{-1} sr^{-1}) are recorded below 1.5 km.

- On a seasonal basis, DD episodes are found to be more intense (up to 0.018 km^{-1} sr^{-1}) in spring, when dust is transported towards the central and eastern parts of the Mediterranean region.

At the last part of the present study, it is investigated how the desert dust outbreaks' vertical distribution can affect the level of agreement between columnar satellite AOD retrievals (MODIS) and ground PM_{10} concentrations. For this purpose four intense Mediterranean desert dust outbreaks of different geometrical characteristics that took place across the Mediterranean, namely in Spain (western), Sardinia (central) and Cyprus (eastern), are studied when satellite algorithm's outputs, ground PM_{10} concentrations and CALIOP-CALIPSO lidar profiles are available concurrently. Our analysis clearly shows that when a well-developed and compact dust layer is located in the lowest tropospheric levels, then the level of agreement between MODIS-PM_{10} is high. On the contrary, when the dust layer is aloft or its load is not equally distributed in vertical terms then a poor agreement between MODIS-PM_{10} is found.

This study attempts to highlight the importance of the synergistic use of satellite observations and the usage of surface-based measurements, targeting to the representation of the 3D structure of dust outbreaks and the description of their spatial and temporal features. For this reason, the further development of the satellite algorithm is an ongoing process by our group, aiming at extending the study domain from regional to global scale, considering the latest version of MODIS retrievals (Collection 006) as well as the Deep Blue Algorithm retrievals, available over the major dust sources of the planet.

Acknowledgements

The MDRAF project has received funding from the European Union's Seventh Framework Programme for research, technological development and demonstration under grant agreement no 622662. The Collection 051 MODIS-Terra and MODIS-Aqua data were obtained from NASA's Level 1 and Atmosphere Archive and Distribution System (LAADS) website (ftp://ladsweb.nascom.nasa.gov/). The Earth Probe (TOMS) and OMI aerosol climatology is available from the Mirador ftp server (http://mirador.gsfc.nasa.gov/). The CALIPSO retrievals have been derived from NASA's Earth Observing System Data and Information System (http://reverb.echo.nasa.gov/). We would like to thank the principal investigators maintaining the AERONET sites used in the present work. We would like to acknowledge the EMEP Programme and the public European databases Airbase and ACTRIS, which supplied PM10 data used in this study. J. Pey benefits from a Ramón y

Cajal Research Grant (RYC-2013-14159) from the Spanish Ministry of Economy and Competitiveness. S. Basart, O. Jorba, S. Gassó and J.M. Baldasano acknowledge the CICYT project CGL2013-46736 and Severo Ochoa (SEV-996 2011-00067) programme of the Spanish Government. The publication was supported by the European Union Seventh Framework Programme (FP-7-REGPOT-2012-2013-1), in the framework of the project BEYOND, under Grant Agreement No. 316210 (BEYOND – Building Capacity for a Centre of Excellence for EO-based monitoring of Natural Disasters. The figures 11, 12 and 13 have been produced with ccplot (http://ccplot.org/). This work is contributing to the Chemistry-Aerosol Mediterranean Experiment (ChArMEx) coordinated effort for the long-term Mediterranean aerosol characterization using available remote sensing datasets.

References

Adams, A. M., Prospero, J. M., and Zhang, C.: CALIPSO-derived three-dimensional structure of aerosol over the Atlantic Basin and adjacent continents, J. Climate, 25, 6862–6879, doi:10.1175/JCLI-D-11-00672.1, 2012.

Alados-Arboledas, A., Alcántara, A., Olmo, F. J., Martínez-Lozano, J. A., Estellés, V., Cachorro, V., Silva, A. M., Horvath, H., Gangl, A., Díaz, A., Pujadas, M., Lorente, J., Labajo, A., Sorribas, M., and Pavese, G.: Aerosol columnar properties retrieved from Cimel radiometers during VELETA 2002, Atmos. Environ., 42, 2630–2642, doi:10.1016/j.atmosenv.2007.10.006, 2008.

Alam, K., Trautmann, T., Blaschke, T., Subhan, F.: Changes in aerosol optical properties due to dust storms in the Middle East and Southwest Asia. Remote Sens. Environ. 143, 216–227, 2014.

Alpert, P., Kishcha, P., Shtivelman, A., Krichak, S.O., Joseph, J.H.: Vertical distribution of Saharan dust based on 2.5-year model predictions, Atmos. Res., 70, 109-130, 2004.

Amiridis, V., Kafatos, M., Pérez, C., Kazadzis, S., Gerasopoulos, E., Mamouri, R. E., Papayannis, A., Kokkalis, P., Giannakaki, E., Basart, S., Daglis, I., and Zerefos, C.: The potential of the synergistic use of passive and active remote sensing measurements for the validation of a regional dust model, Ann. Geophys., 27, 3155-3164, doi:10.5194/angeo-27-3155-2009, 2009.

Amiridis, V., Wandinger, U., Marinou, E., Giannakaki, E., Tsekeri, A., Basart, S., Kazadzis, S., Gkikas, A., Taylor, M., Baldasano, J. M., and Ansmann, A.: Optimizing CALIPSO Saharan dust retrievals, Atmos. Chem. Phys., 13, 12089-12106, doi:10.5194/acp-13-12089-2013, 2013.

Ångström, A.K.: On the atmospheric transmission of sun radiation and on the dust in the air, Geogr. Ann., 12, 130-159, 1929.

Balis, D., Amiridis, V., Kazadzis, S., Papayannis, A., Tsaknakis, G., Tzortzakis, S., Kalivitis, N., Vrekoussis, M., Kanakidou, M., Mihalopoulos, N., Chourdakis, G., Nickovic, S., Pérez, C., Baldasano, J. M., and Drakakis, M.: Optical characteristics of desert dust over the East Mediterranean during summer: a case study, Ann. Geophys., 24, 807-821, doi:10.5194/angeo-24-807-2006, 2006.

Balis, D.: Geometrical characteristics of desert dust layers over Thessaloniki estimated with backscatter/Raman lidar and the BSC/DREAM model, Remote Sensing Letters, 353-362, doi: 10.1080/01431161.2011.597793, 2012.

Barkan, J., Alpert, P., Kutiel, H., and Kishcha, P.: Synoptics of dust transportation days from Africa toward Italy and central Europe, J. Geophys. Res., 110, D07208, doi:10.1029/2004JD005222, 2005.

Barnaba, F. and Gobbi, G. P.: Aerosol seasonal variability over the Mediterranean region and relative impact of maritime, continental and Saharan dust particles over the basin from MODIS data in the year 2001, Atmos. Chem. Phys., 4, 2367-2391, doi:10.5194/acp-4-2367-2004, 2004.

Basart, S., Pérez, C., Cuevas, E., Baldasano, J. M., and Gobbi, G. P.: Aerosol characterization in Northern Africa, Northeastern Atlantic, Mediterranean Basin and Middle East from direct-sun AERONET observations, Atmos. Chem. Phys., 9, 8265-8282, doi:10.5194/acp-9-8265-2009, 2009.

Basart, S., Pay, M. T., Jorba, O., Pérez, C., Jiménez-Guerrero, P., Schulz, M., and Baldasano, J. M.: Aerosols in the CALIOPE air quality modelling system: evaluation and analysis of PM levels, optical depths and chemical composition over Europe, Atmos. Chem. Phys., 12, 3363-3392, doi:10.5194/acp-12-3363-2012, 2012.

Ben-Ami, Y., Koren, I., and Altaratz, O.: Patterns of North African dust transport over the Atlantic: winter vs. summer, based on CALIPSO first year data, Atmos. Chem. Phys., 9, 7867–7875, doi:10.5194/acp-9-7867-2009, 2009.

Ben-Ami, Y., Koren, I., Rudich, Y., Artaxo, P., Martin, S. T., and Andreae, M. O.: Transport of North African dust from the Bodélé depression to the Amazon Basin: a case study, Atmos. Chem. Phys., 10, 7533-7544, doi:10.5194/acp-10-7533-2010, 2010.

Bègue, N., Tulet, P., Chaboureau, J. P., Roberts, G., Gomes, L., and Mallet, M.: Long-range transport of Saharan dust over north-western Europe during EUCAARI 2008 campaign: Evolution of dust optical properties by scavenging, J. Geophys. Res., 117,D17201, doi:10.1029/2012JD017611, 2012.

Berthier, S., Chazette, P., Couvert, P., Pelon, J., Dulac, F., Thieuleux, F., Moulin, C., and Pain, T.: Desert dust aerosol columnar properties over ocean and continental Africa from Lidar in-Space Technology Experiment (LITE) and Meteosat synergy. J. Geophys. Res., 111, D21202, doi:10.1029/2005JD006999, 2006.

Bollasina, M. A., Ming, Y., and Ramaswamy, V.: Anthropogenic Aerosols and the Weakening of the South Asian Summer Monsoon, Science, 334, 502–505, 2011.

Bösenberg, J., Matthias, V., Amodeo, A., Amoiridis, V., Ansmann, A., Baldasano, J. M., Balin, I., Balis, D., Böckmann, C., Boselli, A., Carlsson, G., Chaikovsky, A., Chourdakis, G., Comerón, A., De Tomasi, F., Eixmann, R., Freudenthaler, V., Giehl, H., Grigorov, I., Hågård, A., Iarlori, M., Kirsche, A., Kolarov, G., Komguem, L., Kreipl, S., Kumpf, W., Larchevêque, G., Linné, H., Matthey, R., Mattis, I., Mekler, A., Mironova, I., Mitev, V., Mona, L., Müller, D., Music, S., Nickovic, S., Pandolfi,M., Papayannis, A., Pappalardo, G., Pelon, J., Pérez, C., Perrone, R. M., Persson, R., Resendes, D. P., Rizi, V., Rocadenbosch, F., Rodrigues, J. A., Sauvage, L., Schneidenbach, L., Schumacher, R., Shcherbakov, V., Simeonov, V., Sobolewski, P., Spinelli, N., Stachlewska, I., Stoyanov, D., Trickl, T., Tsaknakis, G., Vaughan, G., Wandinger, U., Wang, X., Wiegner, M., Zavrtanik, M. and Zerefos, C.: A European aerosol research lidar network to establish an aerosol climatology, MPI-Rep. 317, Max-Planck Inst. für Meteorol., Hamburg, Germany, 2003. http://www.mpimet.mpg.de/fileadmin/publikationen/Reports/max_scirep_348.pdf

Burton, S. P., Ferrare, R. A., Vaughan, M. A., Omar, A. H., Rogers, R. R., Hostetler, C. A., and Hair, J. W.: Aerosol classification from airborne HSRL and comparisons with the CALIPSO vertical feature mask, Atmos. Meas. Tech., 6, 1397-1412, doi:10.5194/amt-6-1397-2013, 2013.

Cachorro, V. E., Vergaz, R., de Frutos, A. M., Vilaplana, J. M., Henriques, D., Laulainen, N., and Toledano, C.: Study of desert dust events over the southwestern Iberian Peninsula in year 2000: two case studies, Ann. Geophys., 24, 1493-1510, doi:10.5194/angeo-24-1493-2006, 2006.

Cao, C. X., Zheng, S., and Singh, R. P.: Characteristics of aerosol optical properties and meteorological parameters during three major dust events (2005–2010) over Beijing, China, Atmos. Res., 150, 129–142, doi:10.1016/j.atmosres.2014.07.022, 2014.

Córdoba-Jabonero, C., Sorribas, M., Guerrero-Rascado, J. L., Adame, J. A., Hernández, Y., Lyamani, H., Cachorro, V., Gil, M., Alados-Arboledas, L., Cuevas, E., and de la Morena, B.: Synergetic monitoring of Saharan dust plumes and potential impact on surface: a case study of dust transport from Canary Islands to Iberian Peninsula, Atmos. Chem. Phys., 11, 3067-3091, doi:10.5194/acp-11-3067-2011, 2011.

Di Sarra, A., Di Iorio, T., Cacciani, M., Fiocco, G., and Fuà, D.: Saharan dust profiles measured by lidar at Lampedusa, J. Geophys. Res., 106, 10 335–10 348, 2001.

Díaz, J., Tobías A., and Linares, C.: Saharan dust and association between particulate matter and case-specific mortality: a case crossover analysis in Madrid (Spain), Environ. Health, doi:10.1186/1476-069X-11-11, 2012.

Draxler, R.R. and Rolph, G.D., 2015. HYSPLIT (HYbrid Single-Particle Lagrangian Integrated Trajectory) Model access via NOAA ARL READY Website (http://ready.arl.noaa.gov/HYSPLIT.php). NOAA Air Resources Laboratory, Silver Spring, MD.

Dubovik, O., Smirnov, A., Holben, B. N., King, M. D., Kaufman, Y. J., and Slutsker, I.: Accuracy assessments of aerosol optical properties retrieved from AERONET sun and sky radiance measurements, J. Geophys. Res., 105, 9791–9806, 2000.

Dubovik, O. and King, M. D.: A flexible inversion algorithm for retrieval of aerosol optical properties from Sun and sky radiance measurements, J. Geophys. Res., 105, 20673-20696, 2000.

Dulac, F., Moulin, C., Lambert, C.E., Guillard, F., Poitou, J., Guelle, W., Quetel, C.R., Schneider, X., Ezat, U., and Buat-Ménard, P.: Dry deposition of mineral aerosol particles in the atmosphere: Significance of the large size fraction, *in Precipitation Scavenging and Atmosphere-Surface Exchange*, edited by S. E. Schwartz and W.G. N. Slinn, pp. 841-854, Hemisphere. Richland, Wash., 1992.

Eck, T. F., Holben, B. N., Reid, J. S., Dubovik, O., Smirnov, A., O'Neill, N. T., Slutsker, I., and Kinne, S.: Wavelength dependence of optical depth of biomass burning, urban and desert dust aerosols, J. Geophys. Res., 104, 31333–31350, 1999.

Eguchi, K., Uno, I., Yumimoto, K., Takemura, T., Shimizu, A., Sugimoto, N., and Liu, Z.: Trans-pacific dust transport: integrated analysis of NASA/CALIPSO and a global aerosol transport model, Atmos. Chem. Phys., 9, 3137-3145, doi:10.5194/acp-9-3137-2009, 2009.

Escudero, M., Querol, X., Pey, J., Alastuey, A., Pérez, N., Ferreira, F., Alonso, S., Rodríguez, S., and Cuevas, E.: A methodology for the quantification of the net African dust load in air quality monitoring networks, Atmos. Environ., 41, 5516–5524, 2007.

Fotiadi, A., Hatzianastassiou, N., Drakakis, E., Matsoukas, C., Pavlakakis, K.G., Hatzidimitriou, D., Gerasopoulos, E., Mihalopoulos, N., and Vardavas, I.: Aerosol physical and optical properties in the Eastern Mediterranean Basin, Crete, from Aerosol Robotic Network data, Atmos. Chem. Phys., 6, 5399–5413, doi:10.5194/acp-6-5399-2006, 2006.

Ginoux, P., Prospero, J. M., Gill, T. E., Hsu, N. C., and Zhao, M.: Global-scale attribution of anthropogenic and natural dust sources and their emission rates based on MODIS Deep Blue aerosol products, Rev. Geophys., 50, RG3005, doi:10.1029/2012rg000388, 2012.

Gkikas, A., Hatzianastassiou, N., and Mihalopoulos, N.: Aerosol events in the broader Mediterranean basin based on 7-year (2000–2007) MODIS C005 data, Ann. Geophys., 27, 3509-3522, doi:10.5194/angeo-27-3509-2009, 2009.

Gkikas, A., Hatzianastassiou, N., Mihalopoulos, N., Katsoulis, V., Kazadzis, S., Pey, J., Querol, X., and Torres, O.: The regime of intense desert dust episodes in the Mediterranean based on contemporary satellite observations and ground measurements, Atmos. Chem. Phys., 13, 12135-12154, doi:10.5194/acp-13-12135-2013, 2013.

1301 Gkikas, A., Houssos, E. E., Lolis, C. J., Bartzokas, A., Mihalopoulos, N. and Hatzianastassiou, N.:
1302 Atmospheric circulation evolution related to desert-dust episodes over the Mediterranean. Q.J.R.
1303 Meteorol. Soc., 141: 1634–1645. doi: 10.1002/qj.2466, 2015.

1304 Gkikas, A., Houssos, E. E., Lolis, C. J., Bartzokas, A., Mihalopoulos, N. and Hatzianastassiou, N.:
1305 Atmospheric circulation evolution related to desert-dust episodes over the Mediterranean. Q.J.R.
1306 Meteorol. Soc., doi: 10.1002/qj.2466, 2014.

1307 Gobbi, G.P., Barnaba, F., Giorgi, R., Santacasa, A.: Altitude-resolved properties of a Saharan dust
1308 event over the Mediterranean, Atmos. Environ., 34, 5119-5127, 2000.

1309 Gobbi, G. P., Kaufman, Y. J., Koren, I., and Eck, T. F.: Classification of aerosol properties derived
1310 from AERONET direct sun data, Atmos. Chem. Phys., 7, 453-458, doi:10.5194/acp-7-453-2007, 2007.

1311 Gobbi, G. P., Angelini, F., Barnaba, F., Costabile, F., Baldasano, J. M., Basart, S., Sozzi, R., and
1312 Bolignano, A.: Changes in particulate matter physical properties during Saharan advections over Rome
1313 (Italy): a four-year study, 2001–2004, Atmos. Chem. Phys., 13, 7395–7404, doi:10.5194/acp-13-7395-
1314 2013, 2013.

1315 Hamonou, E., Chazette, P., Balis, D., Dulac, F., Schneider, X., Galani, E., Ancellet, G., and
1316 Papayannis, A.: Characterization of the vertical structure of Saharan dust export to the Mediterranean
1317 basin, J. Geophys. Res., 104, 22 257–22 270, 1999.

1318 Hara, Y., Yumimoto, K., Uno, I., Shimizu, A., Sugimoto, N., Liu, Z., and Winker, D. M.: Asian dust
1319 outflow in the PBL and free atmosphere retrieved by NASA CALIPSO and an assimilated dust
1320 transport model, Atmos. Chem. Phys., 9, 1227-1239, doi:10.5194/acp-9-1227-2009, 2009.

1321 Hatzianastassiou, N., Gkikas, A., Mihalopoulos, N., Torres, O., and Katsoulis, B. D.: Natural versus
1322 anthropogenic aerosols in the eastern Mediterranean basin derived from multiyear TOMS and MODIS
1323 satellite data, J. Geophys. Res., 114, D24202, doi:10.1029/2009JD011982, 2009.

1324 Heinold, B., Helmert, J., Hellmuth, O., Wolke, R., Ansmann, A., Marticorena, B., Laurent, B. and
1325 Tegen, I.: Regional modeling of Saharan dust events using LM-MUSCAT: Model description and case
1326 studies, J. Geophys. Res., 112, D11204, doi:10.1029/2006JD007443, 2007.

1327 Heinold, B., Tegen, I., Schepanski, K., and Hellmuth, O.: Dust Radiative feedback on Saharan
1328 boundary layer dynamics and dust mobilization. Geophys. Res. Lett., 35, L20817,
1329 doi:10.1029/2008GL035319, 2008.

1330 Herman, J. R., Bhartia, P. K., Torres, O., Hsu, N.C., Seftor, C. J., and Celarier E.: Global distribution of
1331 UV-absorbing aerosols from Nimbus-7/ TOMS data, J. Geophys. Res., 102, 16911– 16923, 1997.

1332 Holben, B. N., Eck, T. F., Slutsker, I., Tanré, D., Buis, J. P., Setzer, A., Vermote, E., Reagan, J. A.,
1333 Kaufman, Y. J., Nakajima, T., Lavenu, F., Jankowiak, I., and Smirnov, A.: AERONET – A federated
1334 instrument network and data archive for aerosol characterization, Remote Sens. Environ., 66, 1–16,
1335 1998.

1336 Huang, J., Minnis, P., Lin, B.,Wang, T.,Yi, Y.,Hu, Y., Sun-Mack, S. and Ayers, K.: Possible influences
1337 of Asian dust aerosols on cloud properties and radiative forcing observed from MODIS and CERES,
1338 Geophys. Res. Lett., 33, L06824, doi:10.1029/2005GL024724, 2006.

1339 Huang, J., Zhang, C., and Prospero, J. M.: African dust outbreaks: a satellite perspective of temporal
1340 and spatial variability over the tropical Atlantic Ocean, J. Geophys. Res., 115, D05202,
1341 doi:10.1029/2009JD012516, 2010.

1342 Hubanks, P. A., King, M. D., Platnick, S. A., and Pincus, R. A.: MODIS Atmosphere L3 Gridded
1343 Product Algorithm Theoretical Basis Document, MODIS Algorithm Theoretical Basis Document No.
1344 ATBD-MOD-30 for Level-3 Global Gridded Atmosphere Products (08 D3, 08 E3, 08M3), online:
1345 http://modis-atmos.gsfc.nasa.gov/ docs/L3 ATBD 2008 12 04.pdf, 2008.

1346 Hunt, W. H, Winker, D. M., Vaughan, M. A., Powell, K. A., Lucker, P. L., and Weimer, C.: CALIPSO
1347 Lidar Description and Performance Assessment, J. Atmos. Oceanic Technol., 26, 1214–1228,
1348 doi:10.1175/2009JTECHA1223.1, 2009.

1349 IPCC, 2013: Summary for Policymakers. In: Climate Change 2013: The Physical Science Basis.
1350 Contribution of Working Group I to the Fifth Assessment Report of the Intergovernmental Panel on
1351 Climate Change [Stocker, T.F., D. Qin, G.-K. Plattner, M. Tignor, S. K. Allen, J. Boschung, A. Nauels,
1352 Y. Xia, V. Bex and P.M. Midgley (eds.)]. Cambridge University Press, Cambridge, United Kingdom
1353 and New York, NY, USA.

1354 Kalivitis, N., Gerasopoulos, E., Vrekoussis, M., Kouvarakis, G., Kubilay, N.,Hatzianastassiou, N.,
1355 Vardavas, I., and Mihalopoulos, N.: Dust transport over the eastern Mediterranean derived from
1356 TOMS, AERONET and surface measurements, J. Geophys. Res., 112, D03202,
1357 doi:10.1029/2006JD007510, 2007.

Karanasiou, A., Moreno, N., Moreno, T., Viana, M., de Leeuw, F., Querol, X.: Health effects from Sahara dust episodes in Europe: literature review and research gaps, Environ. Int., 15, 107–114,doi:10.1016/j.envint.2012.06.012, 2012.

Karyampudi, V. M., Palm, S. P., Reagen, J. A., Fang, H., Grant, W. B., Hoff, R. M., Moulin, C., Pierce, H. F., Torres, O., Browell, E. V., and Melfi, S. H.: Validation of the Saharan dust plume conceptual model using lidar, Meteosat and ECMWF, B. Am. Meteorol. Soc., 80, 1045–1075, 1999.

Kaufman, Y. J., Tanré, D., Remer, L. A., Vermote, E. F., Chu, A., and Holben, B. N.: Operational remote sensing of tropospheric aerosol over land from EOS Moderate-resolution Imaging Spectroradiometer, J. Geophys. Res., 102, 17051–17065, 1997.

Kaufman, Y. J., Smirnov, A., Holben, B. N., and Dubovik, O.: Baseline maritime aerosol: methodology to derive the optical thickness and the scattering properties, Geophys. Res. Lett., 28, 3251– 3254, 2001.

Kaufman, Y. J., Tanre, D., Holben, B. N., Mattoo, S., Remer, L. A.,Eck, T. F., Vaughan, J., and Chatenet, B.: Aerosol radiative impact on spectral solar flux at the surface, derived from principal-plane sky measurements, J. Atmos. Sci., 59, 635–646, 2002.

Kazadzis, S., Bais, A., Amiridis, V., Balis, D., Meleti, C., Kouremeti, N., Zerefos, C. S., Rapsomanikis, S., Petrakakis, M., Kelesis, A., Tzoumaka, P., and Kelektsoglou, K.: Nine years of UV aerosol optical depth measurements at Thessaloniki, Greece, Atmos. Chem. Phys., 7, 2091-2101, doi:10.5194/acp-7-2091-2007, 2007.

Kishcha, P., Barnaba, F., Gobbi, G. P., Alpert, P., Shtivelman, A., Krichak, S. O., and Joseph, J. H.: Vertical distribution of Saharan dust over Rome (Italy): Comparison between 3-year model predictions and lidar soundings, J. Geophys. Res., 110, D06208, doi:10.1029/2004JD005480, 2005.

Klein, H., Nickovic, S., Haunold, W., Bundke, U., Nillius, B., Ebert, M., Weinbruch, S., Schuetz, L., Levin, Z., Barrie, L. A., and Bingemer, H.: Saharan dust and ice nuclei over Central Europe, Atmos. Chem. Phys., 10, 10211–10221, doi:10.5194/acp- 10-10211-2010, 2010.

Kubilay, N., Cokacar, T., and Oguz, T.: Optical properties of mineral dust outbreaks over the northeastern Mediterranean, J. Geophys. Res., 108, 4666, doi:10.1029/2003JD003798, 2003.

Lau, K. M., Kim, M. K., and Kim, K. M.: Asian summer monsoon anomalies induced by direct forcing: The role of the Tibetan plateau, Clim. Dynam., 26, 855–864, 2006.

1388 Levy, R. C., Remer, L. A., Tanré, D., Kaufman, Y. J., Ichoku, C., Holben, B. N., Livingston, J. M.,
1389 Russell, P. B., and Maring, H.: Evaluation of the Moderate-Resolution Imaging Spectroradiometer
1390 (MODIS) retrievals of dust aerosol over the ocean during PRIDE, J. Geophys. Res., 108, 8594,
1391 doi:10.1029/2002JD002460, 2003.

1392 Levy, R. C., Remer, L. A., Kleidman, R. G., Mattoo, S., Ichoku, C., Kahn, R., and Eck, T. F.: Global
1393 evaluation of the Collection 5 MODIS dark-target aerosol products over land, Atmos. Chem. Phys., 10,
1394 10399–10420, doi:10.5194/acp-10-10399-2010, 2010.

1395 Liu, D., Wang, Z., Liu, Z., Winker, D., and Trepte, C.: A height resolved global view of dust aerosols
1396 from the first year CALIPSO lidar measurements, J. Geophys. Res., 113, D16214,
1397 doi:10.1029/2007JD009776, 2008.

1398 Liu, Z., Vaughan, M., Winker, D., Kittaka, C., Getzewich, B., Kuehn, R., Omar, A., Powell, K., Trepte,
1399 C., and Hostetler, C.: The CALIPSO Lidar Cloud and Aerosol Discrimination: Version 2 Algorithm
1400 and Initial Assessment of Performance, J. Atmos. Ocean. Tech., 26, 1198–1213,
1401 doi:10.1175/2009jtecha1229.1, 2009.

1402 Luo, T., Wang, Z., Zhang, D., Liu, X., Wang, Y., and Yuan, R.: Global dust distribution from improved
1403 thin dust layer detection using A-train satellite lidar observations, Geophys. Res. Lett., 42,
1404 doi:10.1002/2014GL062111, 2015.

1405 Lyamani, H., Olmo, F. J., and Alados-Arboledas, L.: Saharan dust outbreak over southeastern Spain as
1406 detected by sun photometer, Atmos. Environ., 39, 7276–7284, 2005.

1407 Mallet, M., Tulet, P., Serça, D., Solmon, F., Dubovik, O., Pelon, J., Pont, V., and Thouron, O.: Impact
1408 of dust aerosols on the radiative budget, surface heat fluxes, heating rate profiles and convective
1409 activity over West Africa during March 2006, Atmos. Chem. Phys., 9, 7143-7160, doi:10.5194/acp-9-
1410 7143-2009, 2009.

1411 Mallet, M., Dubovik, O., Nabat, P., Dulac, F., Kahn, R., Sciare, J., Paronis, D., and Léon, J. F.:
1412 Absorption properties of Mediterranean aerosols obtained from multi-year ground-based remote
1413 sensing observations, Atmos. Chem. Phys., 13, 9195-9210, doi:10.5194/acp-13-9195-2013, 2013.

1414 Marrioti, A., Struglia, M.V., Zeng, N., Lau, K.-M.: The Hydrological Cycle in the Mediterranean
1415 Region and Implications for the Water Budget of the Mediterranean Sea, J. Clim., 15, 1674-1690,
1416 2002.

1417 Matthias, V., Balis, D., Bösenberg, J., Eixmann, R., Iarlori, M., Komguem, L., Mattis, I., Papayannis,
1418 A., Pappalardo, G., Perrone,M. R., and Wang, X.: Vertical aerosol distribution over Europe: Statistical
1419 analysis of Raman lidar data from 10 European Aerosol Research Lidar Network (EARLINET)
1420 stations, 109, D18201, doi:10.1029/2004JD004638, 2004.

1421 McGrath-Spangler, E. L. and Denning, A. S.: Global Seasonal Variations of Midday Planetary
1422 Boundary Layer Depth from CALIPSO Space-borne LIDAR, J. Geophys. Res. Atmos., 118, 1226–
1423 1233, 2013.

1424 Mehta, A. V. and Yang, S.: Precipitation climatology over Mediterranean Basin from ten years of
1425 TRMM measurements, Adv. Geosci., 17, 87-91, doi:10.5194/adgeo-17-87-2008, 2008.

1426 Meloni, D., di Sarra, A., Biavati, G., DeLuisi, J. J., Monteleone, F., Pace, G., Piacentino, S., and
1427 Sferlazzo, D. M.: Seasonal behavior of Saharan dust events at the Mediterranean island of Lampedusa
1428 in the period 1999–2005, Atmos. Environ., 41, 3041–3056, doi:10.1016/j.atmosenv.2006.12.001, 2007.
1429

1430 Meloni, D., di Sarra, A., Monteleone, F., Pace, G., Piacentino, S., and Sferlazzo, D. M.: Seasonal
1431 transport patterns of intense Saharan dust events at the Mediterranean island of Lampedusa, Atmos.
1432 Res., 88, 134–148, doi:10.1016/j.atmosres.2007.10.007, 2008.

1433 Middleton, N. J. and Goudie, A. S.: Saharan dust: sources and trajectories, Transactions of the Institute
1434 of British Geographers, 26, 165–181, 2001.

1435 Mielonen, T., Arola, A., Komppula, M., Kukkonen, J., Koskinen, J., de Leeuw, G., and Lehtinen, K. E.
1436 J.: Comparison of CALIOP level 2 aerosol subtypes to aerosol types derived from AERONET
1437 inversion data, Geophys. Res. Lett., 36, L18804, doi:10.1029/2009gl039609, 2009.

1438 Mona, L., Amodeo, A., Pandolfi, M. and Pappalardo, G.: Saharan dust intrusions in the Mediterranean
1439 area: Three years of Raman lidar measurements, J. Geophys. Res., 111, D16203,
1440 doi:10.1029/2005JD006569, 2006.

1441 Mona, L., Liu, Z., Müller, D., Omar, A., Papayannis, A., Pappalardo, G., Sugimoto, N., and
1442 Vaughan, M.: Lidar Measurements for Desert Dust Characterization: An Overview, Advances in
1443 Meteorology, 2012, 356265, doi:10.1155/2012/356265, 2012.

1444 Mona, L., Papagiannopoulos, N., Basart, S., Baldasano, J. M., Binietoglou, I., Cornacchia, C., and
1445 Pappalardo, G.: EARLINET dust observations vs. BSC-DREAM8b modeled profiles: 12-year-long

systematic comparison at Potenza, Italy, Atmos. Chem. Phys., 14, 8781-8793, doi:10.5194/acp-14-8781-2014, 2014.

Moulin, C., Lambert, C. E., Dulac, F., and Dayan, U.: Control of atmospheric export of dust from North Africa by the North Atlantic Oscillation, Nature, 387, 691–694, 1997.

Moulin, C., Lambert, C., Dayan, U., Masson, V., Ramonet, M., Bousquet, P., Legrand, M., Balkanski, Y., Guelle, W., Marticorena,B., Bergametti, G., and Dulac, F.: Satellite climatology of African dust transport in the Mediterranean atmosphere, J. Geophys. Res., 103, 13137–13144, 1998.

Nabat, P., Somot, S., Mallet, M., Chiapello, I., Morcrette, J. J., Solmon, F., Szopa, S., Dulac, F., Collins, W., Ghan, S., Horowitz, L. W., Lamarque, J. F., Lee, Y. H., Naik, V., Nagashima, T., Shindell, D., and Skeie, R.: A 4-D climatology (1979–2009) of the monthly tropospheric aerosol optical depth distribution over the Mediterranean region from a comparative evaluation and blending of remote sensing and model products, Atmos. Meas. Tech., 6, 1287–1314, doi:10.5194/amt-6-1287-2013, 2013.

Nowottnick, E. P., Colarco, P. R., Welton, E. J., and da Silva, A.: Use of the CALIOP vertical feature mask for evaluating global aerosol models, Atmos. Meas. Tech., 8, 3647-3669, doi:10.5194/amt-8-3647-2015, 2015.

Omar, A. H., Winker, D. M., Kittaka, C., Vaughan, M. A., Liu, Z. Y., Hu, Y. X., Trepte, C. R., 20 Rogers, R. R., Ferrare, R. A., Lee, K. P., Kuehn, R. E., and Hostetler, C. A.: The CALIPSO automated aerosol classification and lidar ratio selection algorithm, J. Atmos. Ocean. Tech., 26, 1994–2014, doi:10.1175/2009jtecha1231.1, 2009.

O'Neill, N. T., Eck, T. F., Smirnov, A., Holben, B. N., and Thulasiraman, S.: Spectral discrimination of coarse and fine mode optical depth, J. Geophys. Res.-Atmos., 108, 4559, doi:10.1029/2002JD002975, 2003.

Pace, G., di Sarra, A., Meloni, D., Piacentino, S., and Chamard, P.: Aerosol optical properties at Lampedusa (Central Mediterranean). 1. Influence of transport and identification of different aerosol types, Atmos. Chem. Phys., 6, 697-713, doi:10.5194/acp-6-697-2006, 2006.

Papadimas, C. D., Hatzianastassiou, N., Mihalopoulos, N., Querol, X., and Vardavas, I.: Spatial and temporal variability in aerosol properties over the Mediterranean basin based on 6-year (2000–2006) MODIS data, J. Geophys. Res., 113, D11205, doi:10.1029/2007JD009189, 2008.

Papadimas, C. D., Hatzianastassiou, N., Mihalopoulos, N., Kanakidou, M., Katsoulis, B. D., and Vardavas, I.: Assessment of the MODIS Collections C005 and C004 aerosol optical depth products over the Mediterranean basin, Atmos. Chem. Phys., 9, 2987– 2999, doi:10.5194/acp-9-2987-2009, 2009.

Papayannis, A., Balis, D., Amiridis, V., Chourdakis, G., Tsaknakis, G., Zerefos, C., Castanho, A.D.A., Nickovic, S., Kazadzis, S., and Grabowski, J.: Measurements of Saharan dust aerosols over the Eastern Mediterranean using elastic backscatter-Raman lidar, spectrophotometric and satellite observations in the frame of the EARLINET project, Atmos. Chem. Phys., 5, 2065–2079, doi:10.5194/acp-5-2065-2005, 2005.

Papayannis, A., Amiridis, V., Mona, L., Tsaknakis, G., Balis, D.,Bösenberg, J., Chaikovski, A., De Tomasi, F., Grigorov, I., Mattis,I., Mitev, V., Muller, D., Nickovic, S., Pérez, C., Pietruczuk, A., Pisani, G., Ravetta, F., Rizi, V., Sicard, M., Trickl, T., Wiegner, M., Gerding, M., Mamouri, R. E., D'Amico, G., and Pappalardo, G.: Systematic lidar observations of Saharan dust over Europe in the frame of EARLINET (2000–2002), J. Geophys. Res., 113, D10204, doi:10.1029/2007JD009028, 2008.

Papayannis, A., Mamouri, R. E., Amiridis, V., Kazadzis, S., Pérez, C., Tsaknakis, G., Kokkalis, P., and Baldasano, J. M.: Systematic lidar observations of Saharan dust layers over Athens, Greece in the frame of EARLINET project (2004–2006), Ann. Geophys., 27, 3611-3620, doi:10.5194/angeo-27-3611-2009, 2009.

Papayannis, A., Nicolaet, D., Kokkalis, P., Binietoglou, I., Talianu, C., Belegante, L., Tsaknakis, G., Cazacu, M.M., Vetres, I., Ilic, L.: Optical, size and mass properties of mixed type aerosols in Greece and Romania as observed by synergy of lidar and sunphotometers in combination with model simulations: A case study, Atmospheric Environment, Volumes: 500-501, 277-294, 2014.

Pereira, S. N., Wagner, F., and Silva, A. M.: Seven years of measurements of aerosol scattering properties, near the surface, in the southwestern Iberia Peninsula, Atmos. Chem. Phys., 11, 17-29, doi:10.5194/acp-11-17-2011, 2011.

Pérez, C., Nickovic, S., Pejanovic, G., Baldasano, J.M. and Özsoy, E.: Interactive dust-radiation modeling: A step to improve weather forecasts, J. Geophys. Res., 111, D16206, doi:10.1029/2005JD006717, 2006.

Pérez García-Pando, C., Stanton, M. C., Diggle, P. J., Trzaska, S., Miller, R. L., Perlwitz, J. P., Baldasano, J. M., Cuevas, E., Ceccato, P., Yaka, P., and Thomson, M. C.: Soil Dust Aerosols and Wind

as Predictors of Seasonal Meningitis Incidence in Niger, Environ. Health Perspect., 122, 679–686, doi:10.1289/ehp.1306640, 2014.

Pey, J., Querol, X., Alastuey, A., Forastiere, F., and Stafoggia, M.: African dust outbreaks over the Mediterranean Basin during 2001–2011: PM10 concentrations, phenomenology and trends, and its relation with synoptic and mesoscale meteorology, Atmos. Chem. Phys., 13, 1395–1410, doi: 10.5194/acp-13-1395-2013, 2013.

Pisani, G., Boselli, A., Spinelli, N., Wang, X.: Characterization of Saharan dust layers over Naples (Italy) during 2000–2003 EARLINET project, Atmos. Res. 102, 286 – 299, doi:10.1016/j.atmosres.2011.07.012, 2011.

Prospero, M. J., Ginoux, P., Torres, O., Nicholson, S. E., and Gill,T. E.: Environmental characterization of global sources of atmospheric soil dust identified with the Nimbus 7 Total Ozone Mapping Spectrometer (TOMS) absorbing aerosol product, Rev. Geophys., 40, 1002, doi:10.1029/2000RG000095, 2002.

Prospero, J. M. and Lamb, P. J.: African droughts and dust transport to the Caribbean: climate change mplications, Science, 302, 1024–1027,doi:10.1126/science.1089915, 2003.

Querol, X., Alastuey A., Lopez-Soler A., Plana F. Puicercus J.A, Mantilla E., Miro J.V.; Artiñano B.: Seasonal evolution of atmospheric suspended particles around a coal-fired power station: Particulate levels and sources, *Atmos. Environ.*, 32, 11, 1963-1978, 1998.

Querol, X., Alastuey, A., Pey, J., Cusack, M., Pérez, N., Mihalopoulos, N., Theodosi, C., Gerasopoulos, E., Kubilay, N., and Koçak, M.: Variability in regional background aerosols within the Mediterranean, Atmos. Chem. Phys., 9, 4575-4591, doi:10.5194/acp-9-4575-2009, 2009a.

Querol, X., Pey, J., Pandolfi, M., Alastuey, A., Cusack, M., Pérez, N., Moreno, T., Viana, N., Mihalopoulos, N., Kallos, G. and Kleanthous, S.: African dust contributions to mean ambient PM10 mass-levels across the Mediterranean basin, Atmos. Environ., 43, 4266–4277, doi:10.1016/j.atmosenv.2009.06.013, 2009b.

Redemann, J., Vaughan, M. A., Zhang, Q., Shinozuka, Y., Russell, P. B., Livingston, J. M., Kacenelenbogen, M., and Remer, L. A.: The comparison of MODIS-Aqua (C5) and CALIOP (V2 & V3) aerosol optical depth, Atmos. Chem. Phys., 12, 3025–3043, doi:10.5194/acp-12-3025-2012, 2012.

Remer, L. A., Tanré, D., Kaufman, Y. J., Ichoku, C., Mattoo, S., Levy, R., Chu, D. A., Holben, B., Dubovik, O., Smirnov, A., Martins, J. V., Li, R.-R., and Ahman, Z.: Validation of MODIS aerosol retrieval over ocean, Geophys. Res. Lett., 29, 8008, doi:10.1029/2001GL013204, 2002.

Remer, L. A., Kaufman, Y. J., Tanré, D., Mattoo, S., Chu, D. A., Martins, J. V., Li, R. R., Ichoku, C., Levy, R. C., Kleidman, R. G., Eck, T. F., Vermote, E., and Holben, B. N.: The MODIS aerosol algorithm, products and validation, J. Atmos. Sci., 62, 947–973, doi: http://dx.doi.org/10.1175/JAS3385.1, 2005.

Remer, L. A., Kleidman, R. G., Levy, R. C., Kaufman, Y. J., Tanré, D., Mattoo, S., Martins, J. V., Ichoku, C., Koren, I., Yu, H., and Holben, B. N.: Global aerosol climatology from the MODIS satellite sensors, J. Geophys. Res., 113, D14S07, doi:10.1029/2007JD009661, 2008.

Rodríguez, S., Querol, X., Alastuey, A., Kallos, G., Kakaliagou, O.: Saharan dust contributions to PM10 and TSP levels in Southern and Eastern Spain, *Atmos. Environ.*, 35, 2433–2447, 2001.

Salvador, P., Alonso-Pérez, S., Pey, J., Artíñano, B., de Bustos, J. J., Alastuey, A., and Querol, X.: African dust outbreaks over the western Mediterranean Basin: 11-year characterization of atmospheric circulation patterns and dust source areas, Atmos. Chem. Phys., 14, 6759-6775, doi:10.5194/acp-14-6759-2014, 2014.

Schepanski, K., Tegen, I., Todd, M. C., Heinold, B., Bönisch, G., Laurent, B., and Macke, A.: Meteorological processes forcing Saharan dust emission inferred from MSG-SEVIRI observations of subdaily dust source activation and numerical models, J. Geophys. Res., 114, D10201, doi:10.1029/2008jd010325, 2009.

Schuster, G. L., Vaughan, M., MacDonnell, D., Su, W., Winker, D., Dubovik, O., Lapyonok, T., and Trepte, C.: Comparison of CALIPSO aerosol optical depth retrievals to AERONET measurements, and a climatology for the lidar ratio of dust, Atmos. Chem. Phys., 12, 7431-7452, doi:10.5194/acp-12-7431-2012, 2012.

Smirnov, A., Holben, B. N., Eck, T. F., Dubovik, O. and Slutsker, I.: Cloud screening and quality control algorithms for the AERONET database, Remote Sens. Environ., 73, 337–349, 2000.

Solmon, F., Mallet, M., Elguindi, N., Giorgi, F., Zakey, A. and Konaré, A.: Dust aerosol impact on regional precipitation over western Africa, mechanisms and sensitivity to absorption properties, Geophys. Res. Lett., 35, L24705, doi:10.1029/2008GL035900, 2008.

Stephens, G. L., Vane, D. G., Boain, R. J., Mace, G. G., Sassen, K., Wang, Z., Illingworth, A. J., O'Conner, E. J., Rossow, W. G., Durden, S. L., Miller, S. D., Austin, R. T., Benedetti, A., and Mitrescu, C.: The CloudSat mission and the A-Train, Bull. Amer. Meteorol. Soc., 83, 1771–1790, 2002.

Tafuro, A.M., Barnaba, F., De Tomassi, F., Perrone, M.R., Gobbi, G.P.: Saharan dust particle properties over the Central Mediterranean, Atmos. Res., 81, 67-93, doi:10.1016/j.atmosres.2005.11.008, 2006.

Tanré, D., Kaufman, Y. J., Herman, M., and Mattoo, S.: Remote sensing of aerosol properties over oceans using the MODIS/EOS spectral radiances, J. Geophys. Res., 102, 16971–16988, 1997.

Tegen, I.: Modelling the mineral dust aerosol cycle in the climate system, Quat. Sci. Rev., 22, 1821–1834, 2003.

Toledano, C., Cachorro, V. E., de Frutos, A. M. Sorribas, M., Prats, N., and de la Morena, B. A.: Inventory of African desert dust events over the southwestern Iberian Peninsula in 2000–2005 with an AERONET Cimel Sun Photometer, J. Geophys. Res., 112, D21201, doi:10.1029/2006JD008307, 2007a.

Toledano, C., Cachorro, V.E., Sorribas, M., Berjón, A., de la Morena, B.A., de Frutos, A.M. and Gouloub, P.: Aerosol optical depth and Ångström exponent climatology at El Arenosillo AERONET site (Huelva, Spain), Q. J. R. Meteorol. Soc., 133, 795–807, doi:10.1002/qj.54, 2007b.

Torres, O., Bhartia, P.K., Herman, J.R., Ahmad, Z. and Gleason, J.: Derivation of aerosol properties from a satellite measurements of backscattered ultraviolet radiation: Theoretical basis, J. Geophys. Res., 103, 17099–17110, 1998.

Torres, O., Bhartia, P. K., Herman, J. R., Sinyuk A., Holben, B.: A long term record of aerosol optical thickness from TOMS observations and comparison to AERONET measurements, J. Atmos. Sci., 59398-413, 2002.

Torres, O., Bhartia, P.K., Sinyuk, A., Welton, E.J., and Holben, D.: Total Ozone Mapping Spectrometer measurements of aerosol absorption from space: Comparison to SAFARI 2000 ground-based observations, J. Geophys. Res., 110, D10S18, doi:10.1029/2004JD004611, 2005.

Torres, O., A. Tanskanen, B. Veihelman, C. Ahn, R. Braak, P. K. Bhartia, P. Veefkind, and P. Levelt, Aerosols and Surface UV Products from OMI Observations: An Overview, J. Geophys. Res., 112, D24S47, doi:10.1029/2007JD008809, 2007.

Trigo, I. F., Bigg, G. R., and Davies, T. D.: Climatology of cyclogenesis in the Mediterranean. Mon. Weather Rev., 130, 549–569, 2002.

Tsamalis, C., Chédin, A., Pelon, J., and Capelle, V.: The seasonal vertical distribution of the Saharan Air Layer and its modulation by the wind, Atmos. Chem. Phys., 13, 11235-11257, doi:10.5194/acp-13-11235-2013, 2013.

Varga, G., Ùjvári, G., Kovács, J.: Spatiotemporal patterns of Saharan dust outbreaks in the Mediterranean Basin, Aeolian Res., Vol. 15, 151-160, doi:10.1016/j.aeolia.2014.06.005, 2014.

Vaughan, M. A., Powell, K. A., Kuehn, R. E., Young, S. A., Winker, D. M., Hostetler, C. A., Hunt, W. H., Liu, Z. Y., McGill, M. J., and Getzewich, B. J.: Fully automated detection of cloud and aerosol layers in the CALIPSO lidar measurements, J. Atmos. Ocean. Tech., 26, 2034–2050, doi:10.1175/2009jtecha1228.1, 2009.

Winker, D., Vaughan, M., Omar, A., Hu, Y., Powell, K., Liu, Z., Hunt, W., and Young, S.: Overview of the CALIPSO mission and CALIOP data processing algorithm, J. Atmos. Ocean. Tech., 26, 2310–2323, doi: http://dx.doi.org/10.1175/2009JTECHA1281.1, 2009.

Winker, D. M., Tackett, J. L., Getzewich, B. J., Liu, Z., Vaughan, M. A., and Rogers, R. R.: The global 3-D distribution of tropospheric aerosols as characterized by CALIOP, Atmos. Chem. Phys., 13, 3345-3361, doi:10.5194/acp-13-3345-2013, 2013.

Yoon, J., von Hoyningen-Huene, W., Kokhanovsky, A. A., Vountas, M., and Burrows, J. P.: Trend analysis of aerosol optical thickness and Ångström exponent derived from the global AERONET spectral observations, Atmos. Meas. Tech., 5, 1271-1299, doi:10.5194/amt-5-1271-2012, 2012.

Zhang, J. L., Reid, J. S., and Holben, B. N.: An analysis of potential cloud artifacts in MODIS over ocean aerosol optical thickness products, Geophys. Res. Lett., 32, L15803, doi:10.1029/2005GL023254, 2005.

Zhang, L., Li, Q. B., Gu, Y., Liou, K. N., and Meland, B.: Dust vertical profile impact on global radiative forcing estimation using a coupled chemical-transport–radiative-transfer model, Atmos. Chem. Phys., 13, 7097-7114, doi:10.5194/acp-13-7097-2013, 2013.

Table 1: AERONET stations, depicted with cyan colors in Figure 4, which have been used for the identification of desert dust (DD) episodes based on ground retrievals.

Stations	Latitude	Longitude	Study period
Blida	N 36° 30′ 28″	E 02° 52′ 51″	7 Nov. 2003 – 18 Feb. 2012
El Arenosillo	N 37° 06′ 18″	W 06° 43′ 58″	1 Mar. 2000 – 21 Feb. 2010
Evora	N 38° 34′ 04″	W 07° 54′ 43″	4 Jul. 2003 – 28 Feb. 2013
FORTH CRETE	N 35° 19′ 58″	E 25° 16′ 55″	23 Jan. 2003 – 6 Aug. 2011
IMC Oristano	N 39° 54′ 36″	E 08° 30′ 00″	30 May 2000 – 28 Feb. 2003
IMS METU Erdemli	N 36° 33′ 54″	E 34° 15′ 18″	1 Mar. 2000 – 28 Feb. 2013
Nes Ziona	N 31° 55′ 19″	E 34° 47′ 20″	1 Feb. 2000 – 28 Feb. 2013

Table 2: Percentages of the satellite Ångström exponent, Fine fraction, Effective Radius and Aerosol Index retrievals satisfying the defined thresholds in the satellite algorithm for the identification of desert dust episodes.

Parameter	Valid	Invalid	Number of DD episodes
Ångström exponent	97.8%	2.2%	232
Fine fraction	98.7%	1.3%	232
Effective radius	94.5%	5.5%	117
Aerosol Index	86.9%	13.1%	206

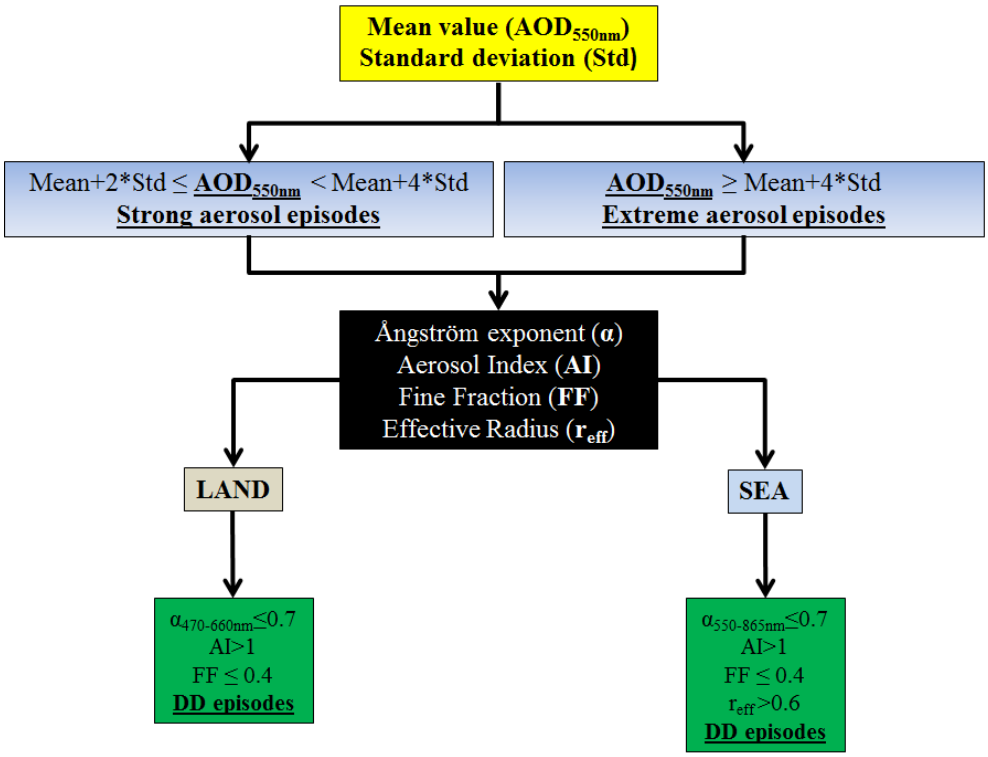

Figure 1: Methodology applied to each 1° x 1° grid cell for the identification of the intense Mediterranean desert dust outbreaks.

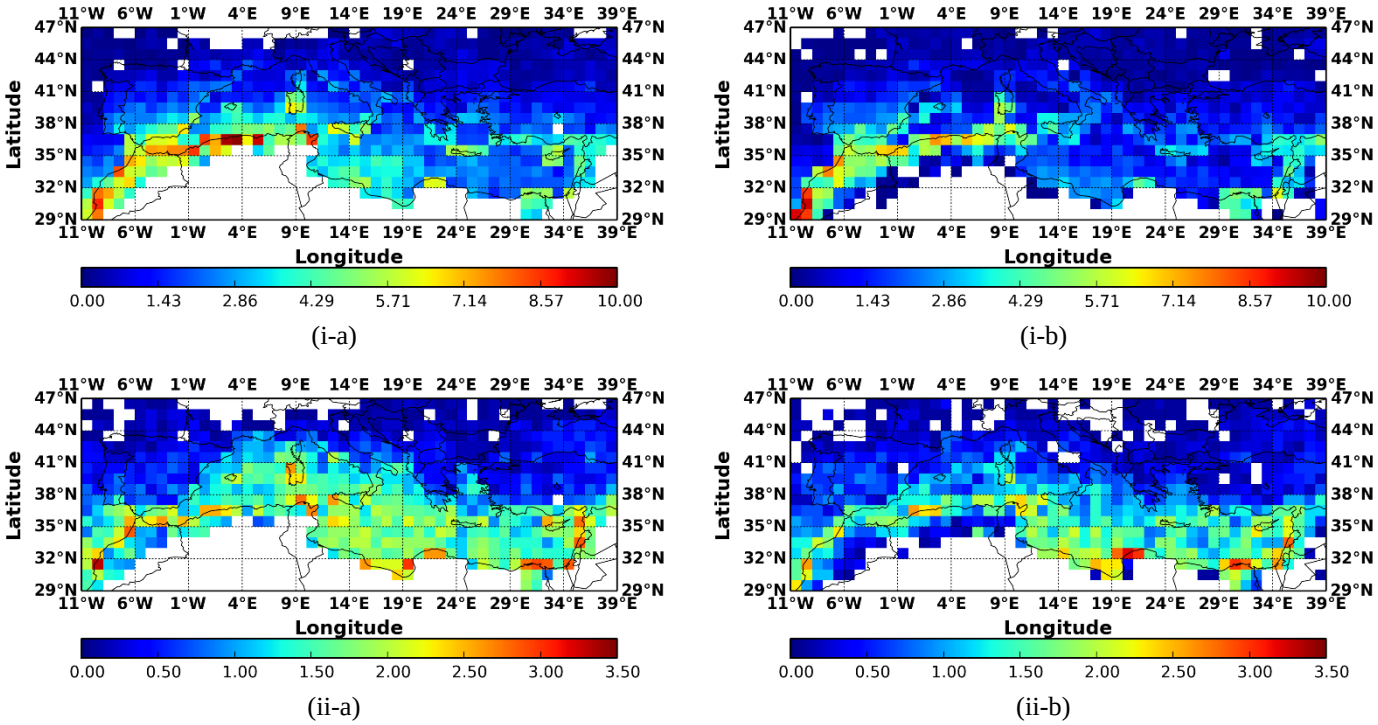

Figure 2: Geographical distributions of the occurrence frequency (episodes/year) of: (i) strong and (ii) extreme desert dust episodes, averaged for the periods: (a) Mar. 2000 – Feb. 2013 (MODIS-Terra) and (b) 2003 – 2012 (MODIS-Aqua), over the broader area of the Mediterranean basin.

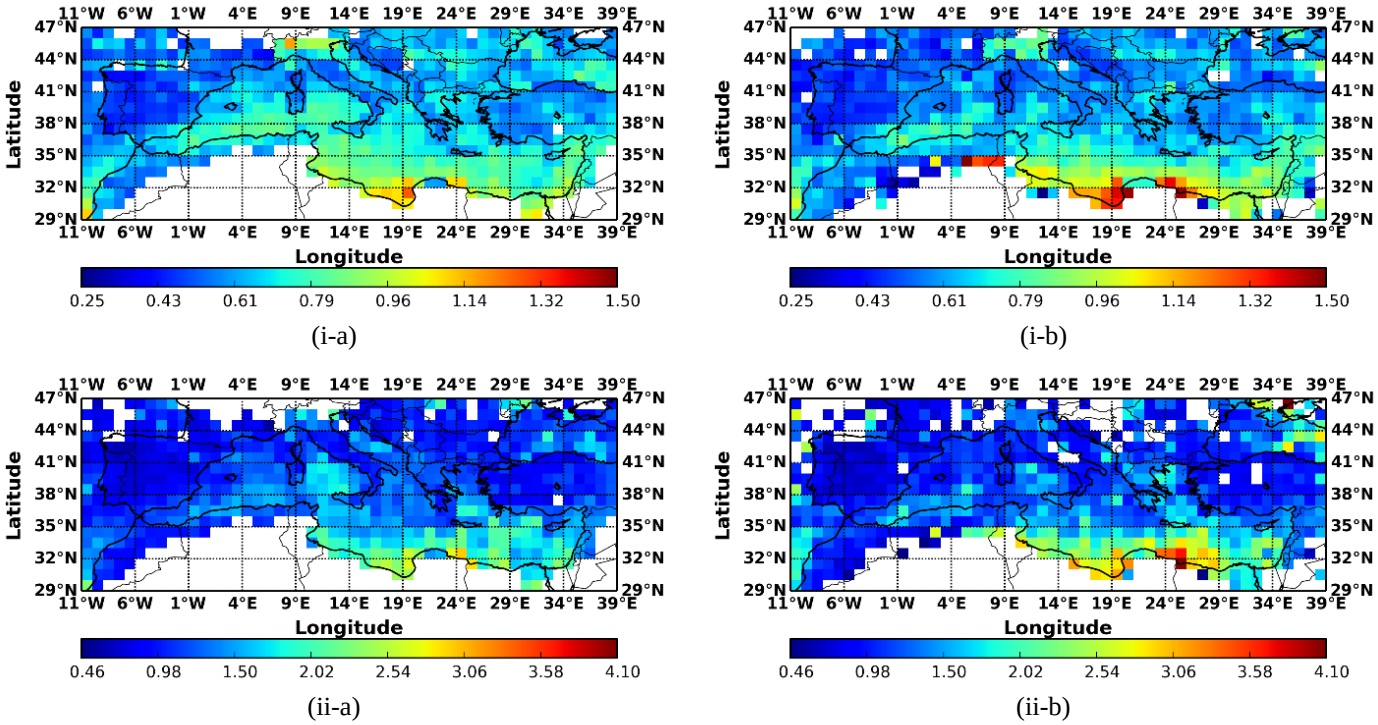

Figure 3: Geographical distributions of the intensity (in terms of AOD_{550nm}) of: (i) strong and (ii) extreme desert dust episodes, averaged for the periods: (a) 2000 – 2013 and (b) 2003 – 2012, over the broader area of the Mediterranean basin.

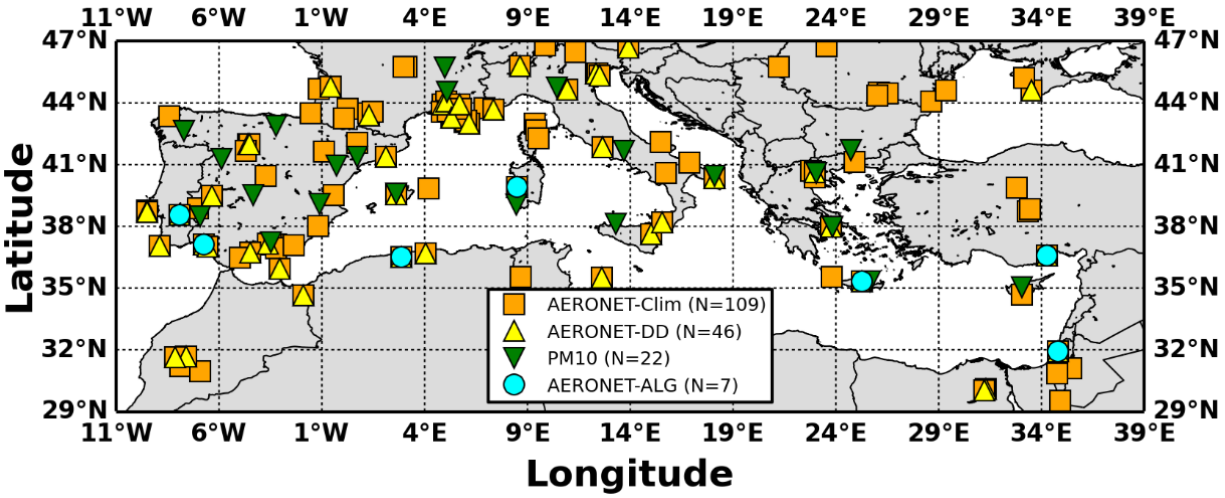

Figure 4: Locations of the AERONET and PM_{10} stations which have been used for the evaluation of the algorithm's outputs. More specifically, with orange squares are denoted the AERONET stations located into the study region, with the yellow triangles the AERONET stations with coincident satellite and ground retrievals under dust episodes conditions, with the cyan circles the AERONET stations which have been used for the evaluation of the defined algorithm thresholds and with the green triangles are depicted the PM_{10} stations.

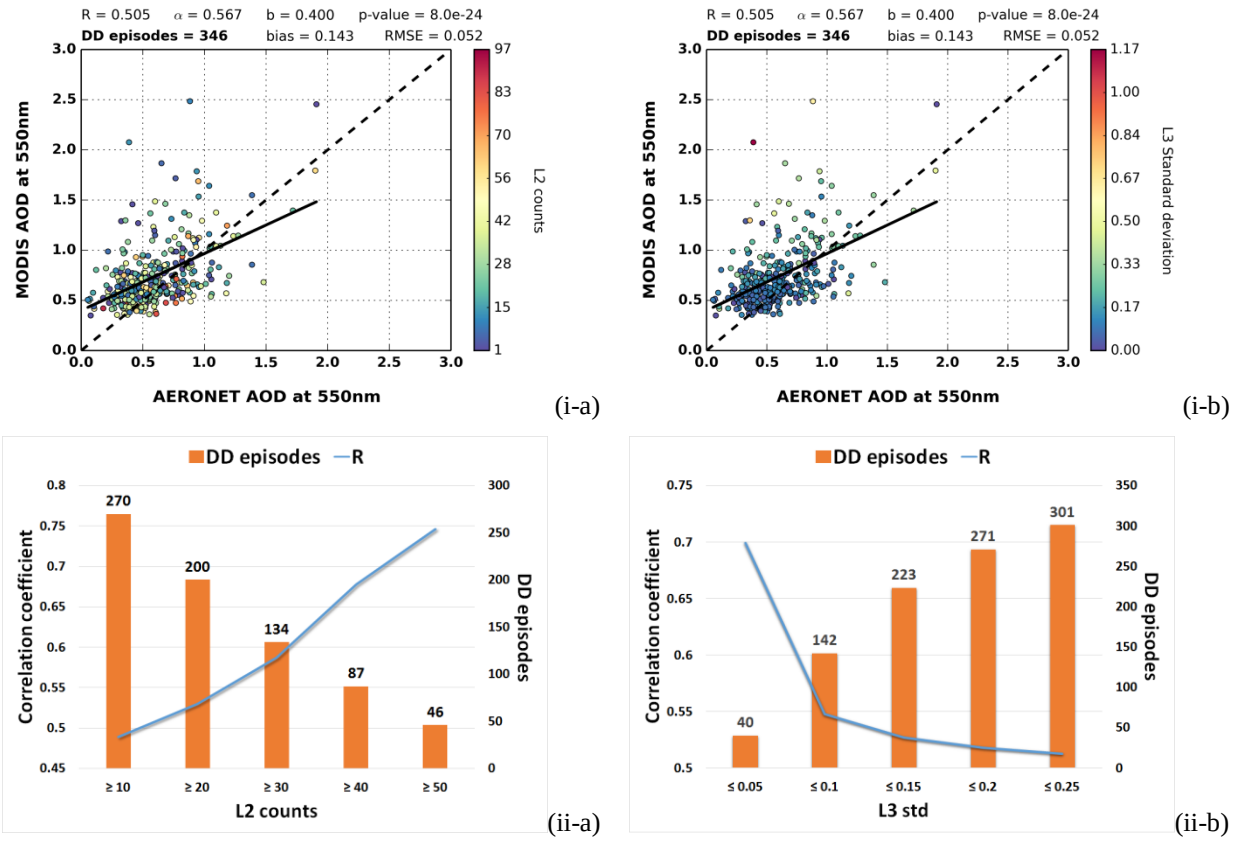

Figure 5: (i) Scatterplots between MODIS-Terra and AERONET aerosol optical depths at 550 nm under intense desert dust episodes conditions related to the: (a) number of level 2 counts which are used for the calculation of the level 3 retrievals and (b) spatial standard deviation inside the 1° x 1° grid cells (level 3 retrievals). (ii) Sensitivity analysis for the calculated correlation coefficients between satellite and ground *AODs*, depending on the: (a) number of level 2 retrievals and (b) sub-grid standard deviation of level 3 retrievals.

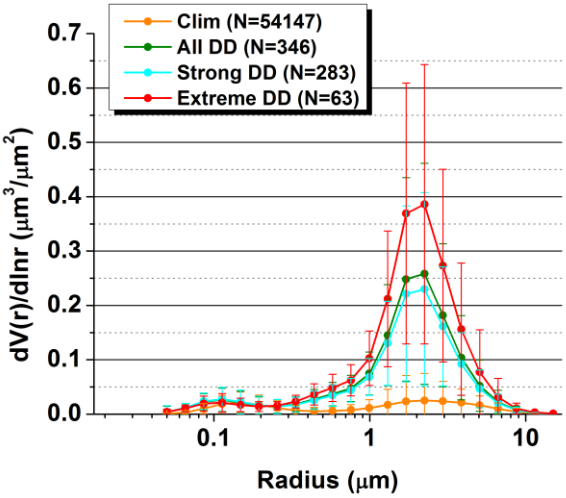

Figure 6: AERONET size distributions averaged for all available retrievals (orange curve) as well as for the total (green curve), strong (cyan curve) and extreme (red curve) desert dust episodes, occurred over the broader area of the Mediterranean basin, during the period Mar. 2000 – Feb. 2013. The error bars represent the calculated standard deviation.

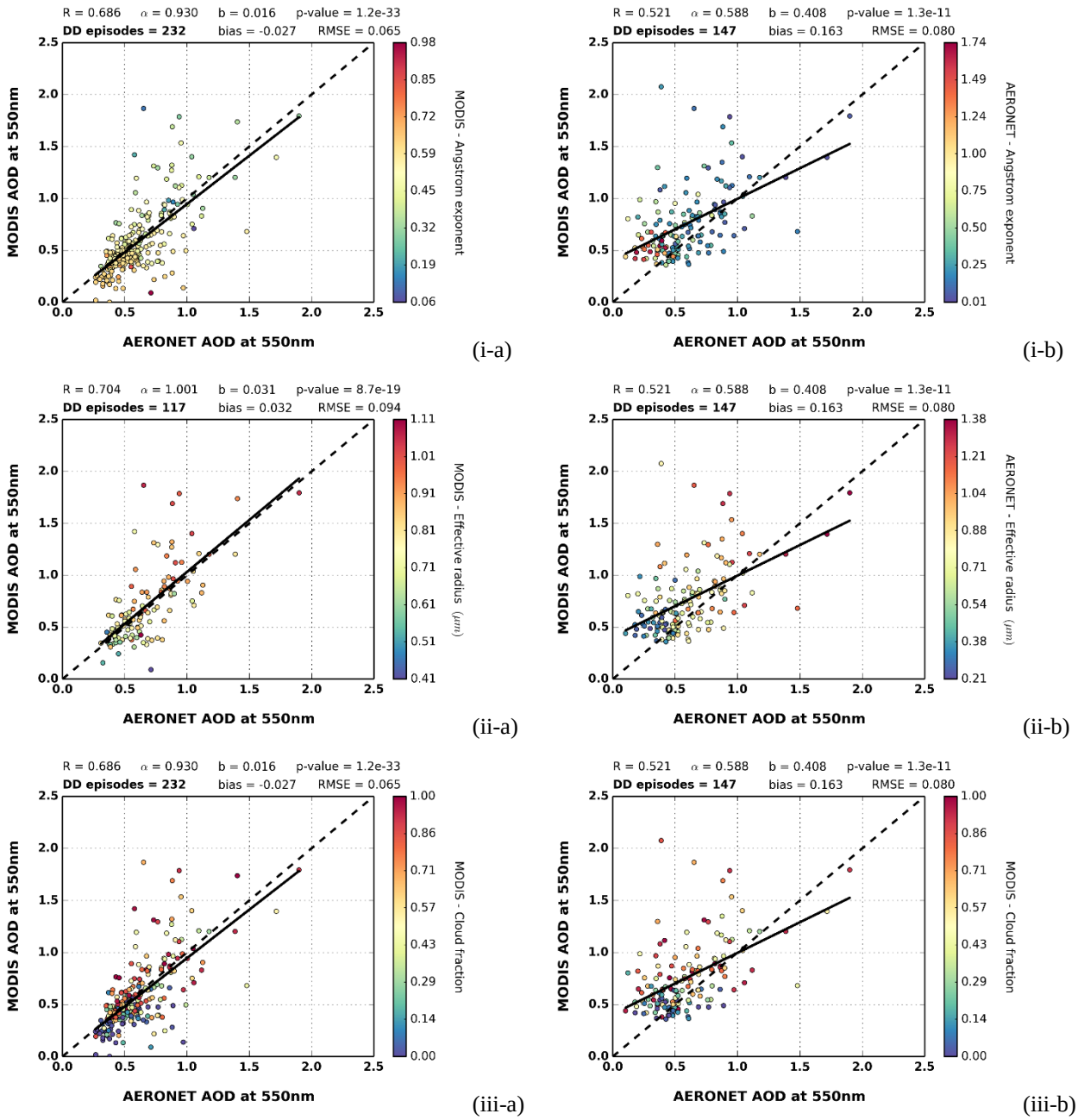

Figure 7: Scatterplots of MODIS-Terra and AERONET aerosol optical depths at 550 nm when intense dust episodes have been identified based on: (a) AERONET retrievals and (b) satellite algorithm, respectively. In the left column, colormaps indicate the corresponding values of: (i) Ångström exponent, (ii) Effective radius and (iii) Day cloud fraction derived by MODIS-Terra retrievals. In the right column, colormaps indicate the corresponding values of: (i) AERONET Ångström exponent, (ii) AERONET Effective radius and (iii) MODIS day cloud fraction retrievals. For each scatterplot, are provided the correlation coefficient (*R*), slope (α), intercept (*b*), p-value, number of DD episodes, bias and root mean square error (*RMSE*).

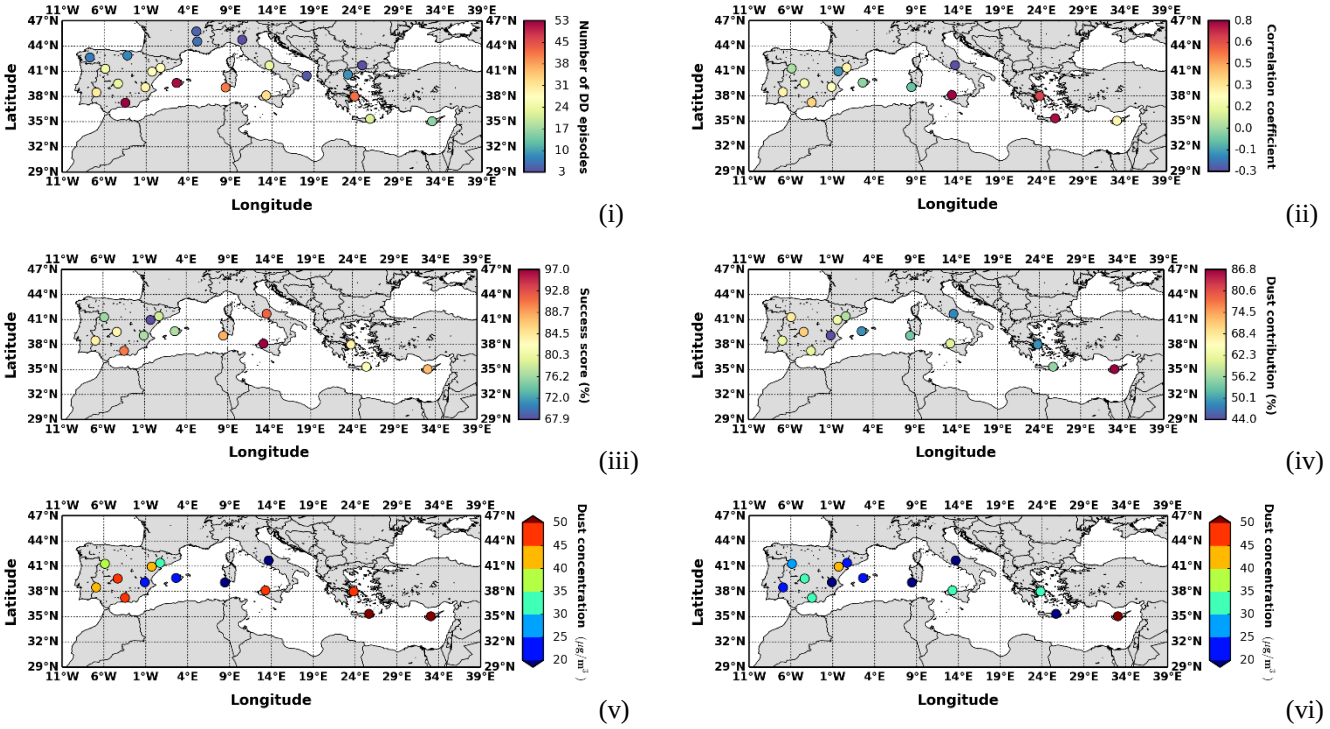

Figure 8: (i) Number of concurrent intense DD episodes where total PM_{10} concentrations and MODIS-Terra *AOD* retrievals are available, (ii) Computed correlation coefficient values between total PM_{10} concentrations and MODIS-Terra *AOD* retrievals in stations where at least 10 DD episodes have been recorded, (iii) Percentage of intense DD episodes where dust particles have been identified by the ground stations, (iv) Dust contribution percentages (%) to the total PM_{10} concentrations, (v) Calculated mean and (vi) median dust concentrations (μg m^{-3}), based on ground measurements for the identified intense DD episodes by the satellite algorithm.

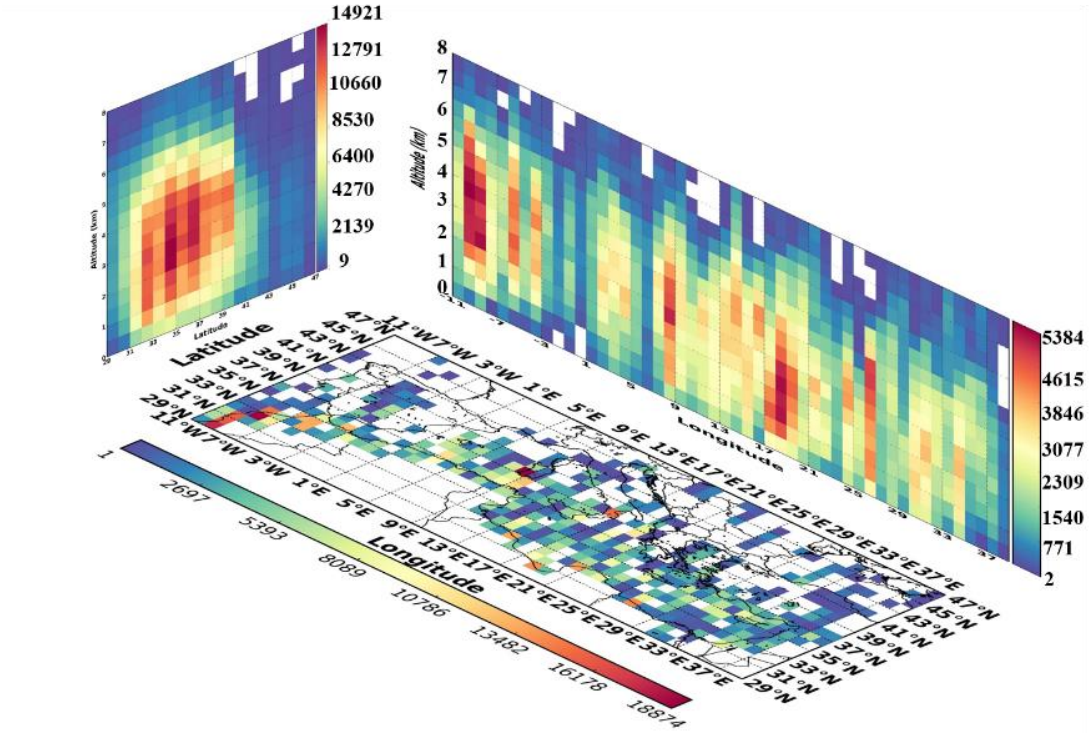

(i)

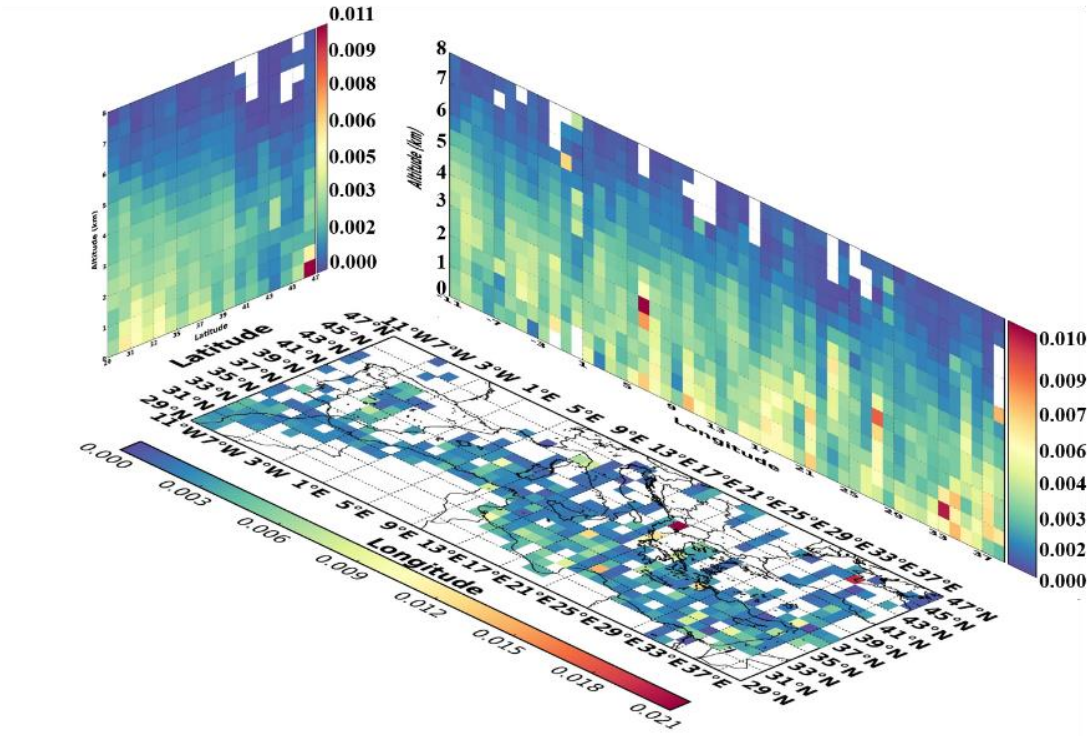

(ii)

1784 **Figure 9:** Three dimensional structure of the: (i) overall number of dust and polluted dust observations and (ii) total
1785 backscatter coefficient at 532 nm (in km^{-1} sr^{-1}), over the broader Mediterranean basin under DD episodes conditions, based
1786 on CALIOP-CALIPSO vertical resolved retrievals for the period Jun. 2006 – Feb. 2013.

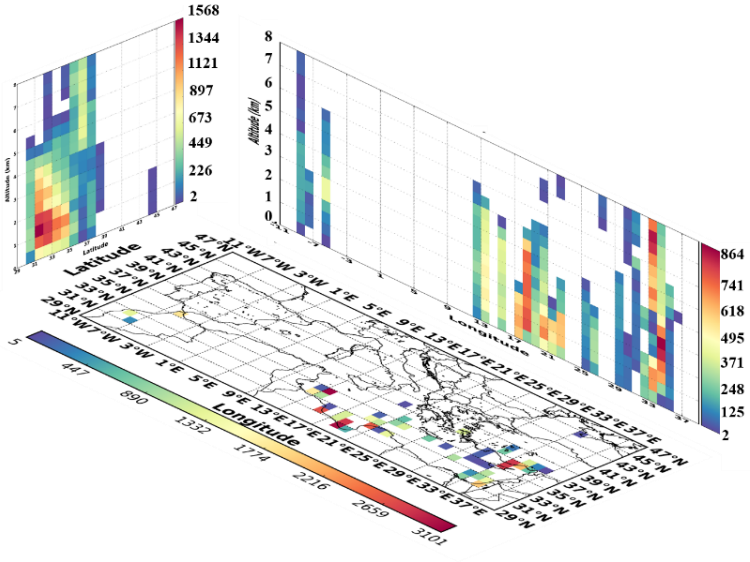
Latitude
Longitude
Altitude (km)
1568
1344
1121
897
673
449
226
2
864
741
618
495
371
248
125
2
447
890
1332
1774
2216
2659
3101

(i-a)

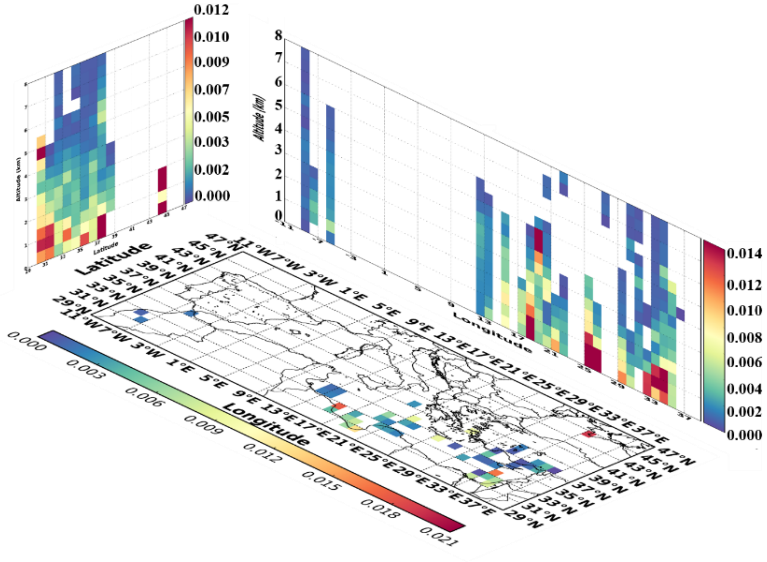
Latitude
Longitude
Altitude (km)
0.012
0.010
0.009
0.007
0.005
0.003
0.002
0.000
0.014
0.012
0.010
0.008
0.006
0.004
0.002
0.000
0.000
0.003
0.006
0.009
0.012
0.015
0.018
0.021

(i-b)

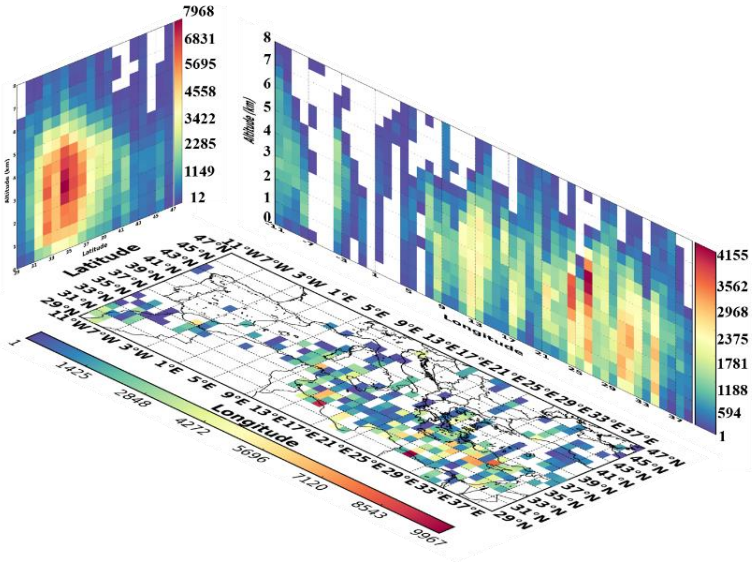
Latitude
Longitude
Altitude (km)
7968
6831
5695
4558
3422
2285
1149
12
4155
3562
2968
2375
1781
1188
594
1
1425
2848
4272
5696
7120
8543
9967

(ii-a)

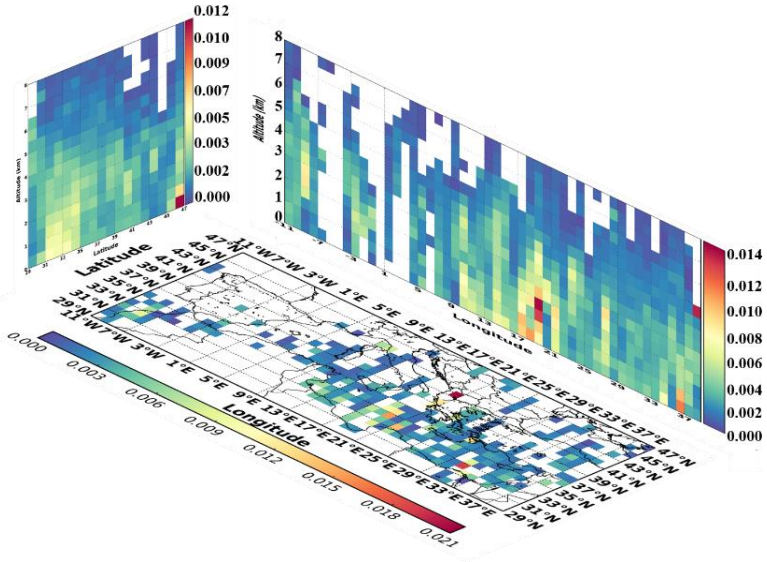
Latitude
Longitude
Altitude (km)
0.012
0.010
0.009
0.007
0.005
0.003
0.002
0.000
0.014
0.012
0.010
0.008
0.006
0.004
0.002
0.000
0.000
0.003
0.006
0.009
0.012
0.015
0.018
0.021

(ii-b)

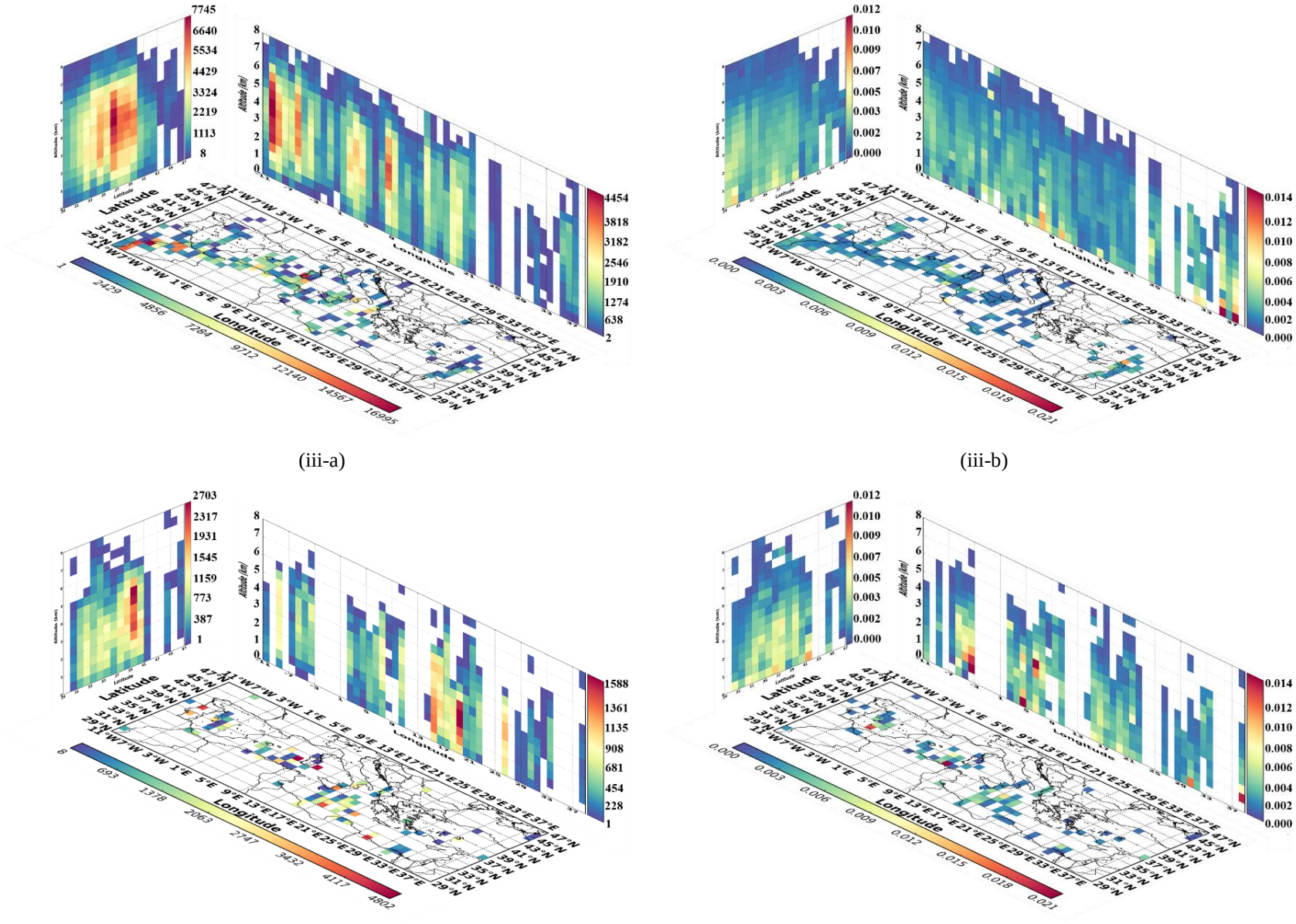

Figure 10: Three dimensional representation of the: (a) overall number of dust and polluted dust observations and (b) total backscatter coefficient at 532 nm (in km^{-1} sr^{-1}), over the broader Mediterranean basin, under DD episodes conditions, for: (i) winter, (ii) spring, (iii) summer and (iv) autumn based on CALIOP-CALIPSO vertical resolved retrievals, over the period Jun. 2006 – Feb. 2013.

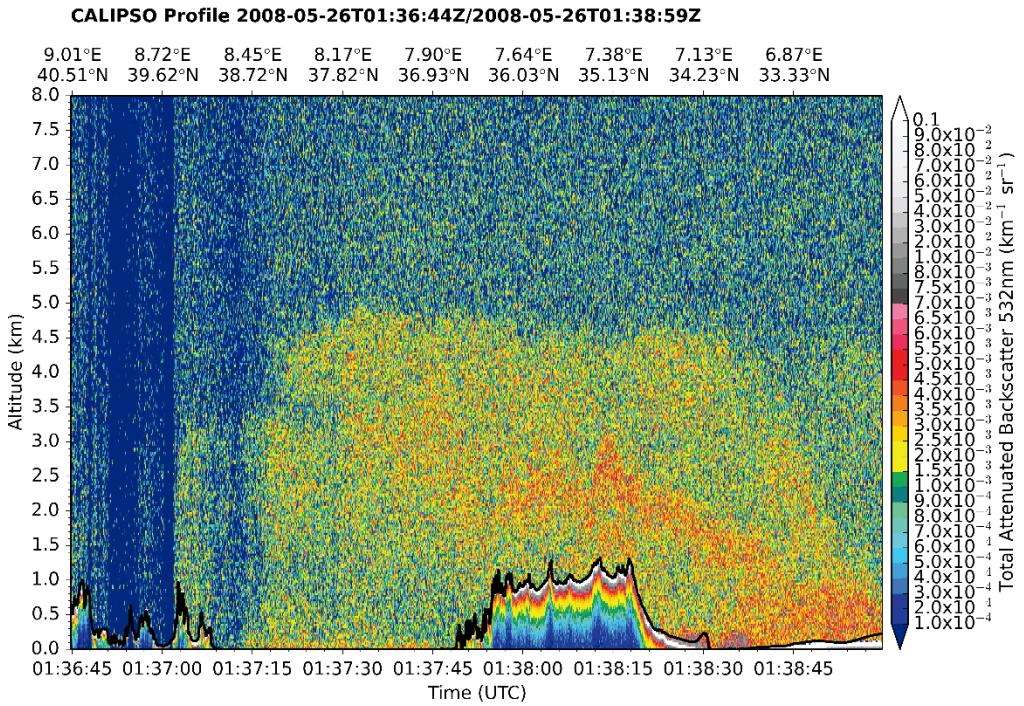

1790 (i)

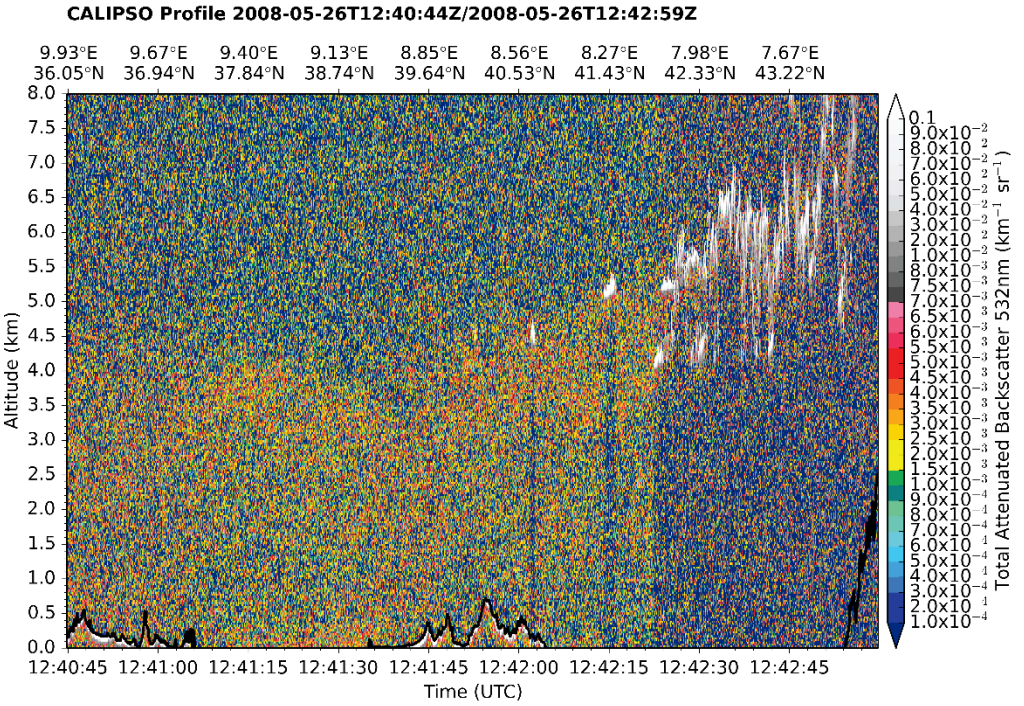

1791 (ii)

1792 **Figure 11:** Cross sections of the total backscatter coefficient at 532 nm (in km^{-1} sr^{-1}) vertical profiles along the CALIOP-
1793 CALIPSO track during: (i) nighttime and (ii) daytime, on 26th May 2008, over the station Censt (Lat: 39.064, Lon: 8.457).
1794 The black thick solid line represents the surface elevation.

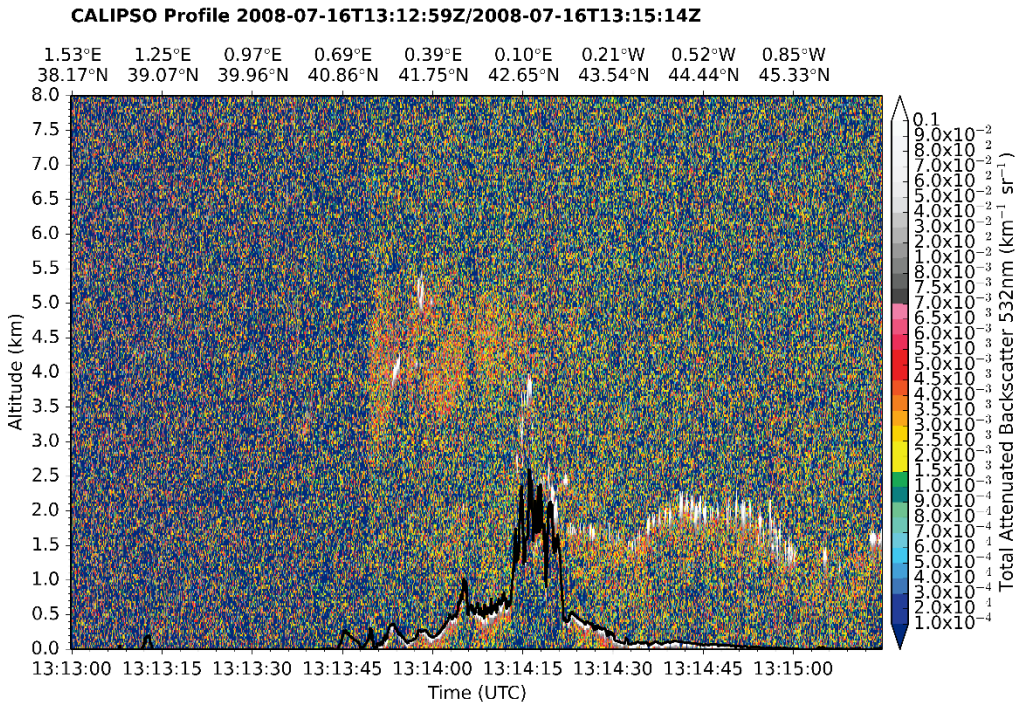

(i)

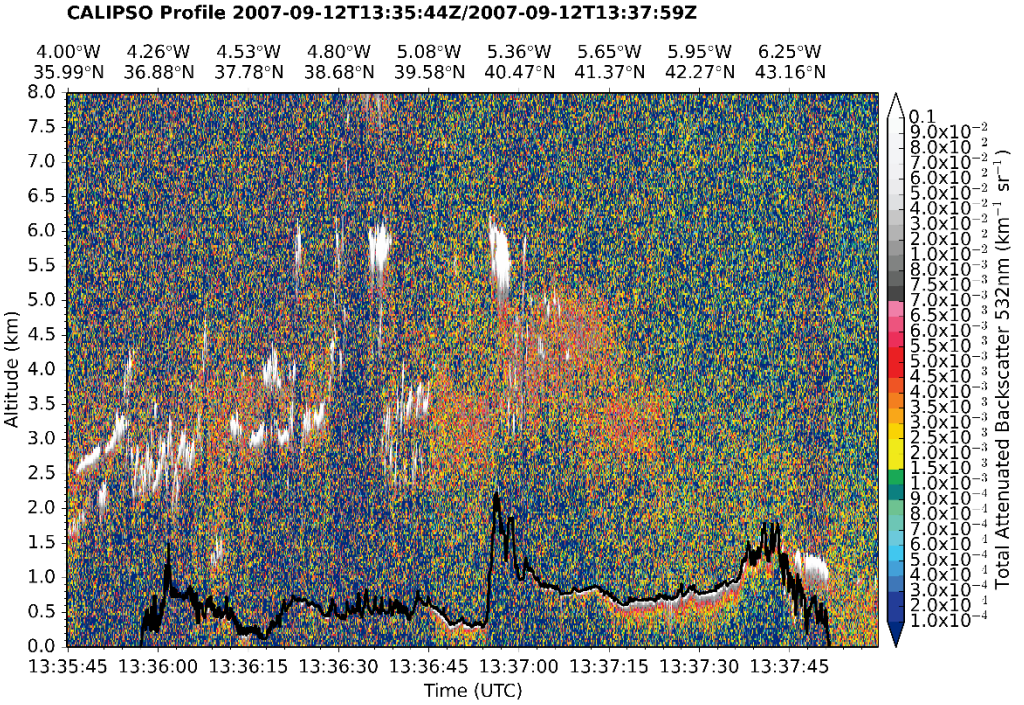

(ii)

Figure 12: Cross sections of the total backscatter coefficient at 532 nm (in km^{-1} sr^{-1}) vertical profiles along the CALIOP-CALIPSO track during daytime over the stations: (i) Els Torms (Lat: 41.395, Lon: 0.721) on 16th July 2008 and (ii) San Pablo (Lat: 39.525, Lon: -4.353) on 12th September 2007. The black thick solid line represents the surface elevation.

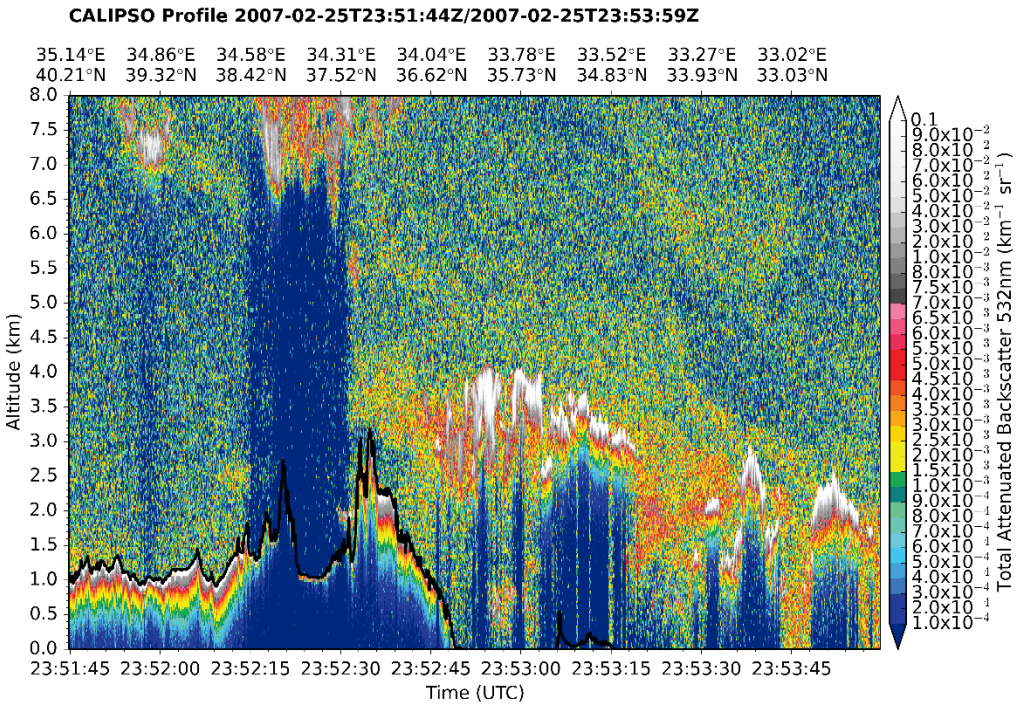

1800

1801 **Figure 13:** Cross section of the total backscatter coefficient at 532 nm (in km^{-1} sr^{-1}) vertical profiles along the CALIOP-
1802 CALIPSO track during daytime over the station Agia Marina (Lat: 35.039, Lon: 33.058) on 25th February 2007. The black
1803 thick solid line represents the surface elevation.

1804

1805

1806

1807

1808

1809

1810

1811